Determination of crystal structure and absolute configuration of thalidomide enantiomers

サリドマイド対掌体の結晶構造および絶対配置の決定

December, 2010

早稲田大学大学院　先進理工学研究科
生命医科学専攻　生物物性科学研究

Toshiya Suzuki

鈴木　俊哉

Preface

Crystals of the same molecule can be in multiple forms. Phenomena of polymorphism, solvate formation, and co-crystallization affect solubility, dissolution rate, and other physicochemical properties. Therefore, characterization and identification of multiple forms of crystals are one of the most popular topics in modern solid state chemistry.

Chirality is significant issue especially in pharmaceutical industry because many pharmaceutical compounds have chirality and several chiral drugs have different pharmacological effects between their enantiomers. In some cases, one enantiomer causes beneficial effect and yet the other harmful effect.

Thalidomide, one of chiral compounds, was marketed as a safe sedative and hypnotic drug in 1956. Before long, its side-effect of teratogenicity caused tragic drug disaster and thalidomide was withdrawn from market in 1962. Recently, however, its potential as a treatment for intractable diseases, such as erythema nodosum leplosum and multiple myeloma, has been revealed and thus thalidomide has attracted considerable attention again.

Although a number of researches have reported the bioactivity of thalidomide, only a few researches have reported its physicochemical properties. For instance, racemic thalidomide is known to exhibits lower solubility and higher melting point than the enantiomeric thalidomide. However, the origin of differences in these physicochemical properties between enantiomeric and racemic thalidomides has not been investigated. Although the knowledge about the crystal structure is essential for understanding these physicochemical properties, the crystal structure of enantiomeric thalidomide has not been published for about 40 years since that of racemic thalidomide was reported in 1971.

The objectives of this thesis are to evaluate methods for crystallization of thalidomide, to determine crystal structure and absolute configuration of enantiomeric thalidomide, and to investigate the origin of differences in physicochemical properties between enantiomeric and racemic thalidomides.

This thesis is composed of following five chapters.

Chapter 1 provides the general introduction of this thesis. As to crystal, chirality, and thalidomide, this chapter introduces the fundamental aspects such as definitions of terms, historical backgrounds, and significant properties.

Chapter 2 evaluates methods for crystallization of thalidomide. The crystallization methods are determined with consideration of possible multiple forms of thalidomide crystal and undesirable chiral inversion in crystallization of enantiomeric thalidomide.

Chapter 3 determines crystal structure of (*S*)-thalidomide with single crystal X-ray diffractometry. Hydrogen bonded dimers structure in unsolvate and infinite hydrogen bonded chains structure in solvate are investigated in detail.

Chapter 4 investigates the origin of differences in physicochemical properties between enantiomeric and racemic thalidomides. Crystal structures of (*S*)- and (*RS*)-thalidomides are compared and structural stabilities of dimers in each crystal are evaluated by theoretical calculations.

Chapter 5 concludes this thesis with future prospects.

Table of Contents

1. General introduction

1.1 Multiple forms of crystal

Crystal is a solid substance formed with orderly arranged units. These units generally consist of atoms or molecules. In the case of molecules, the crystals are especially called molecular crystals. Studies concerning crystal are called crystallography. The primary significance of the crystallography is investigations into crystal structures. The crystal structures are usually determined with X-ray diffractometry based on the property of orderly arrangements in crystals. Determinations of crystal structures provide valuable information of the substances. The principal information obtainable from X-ray diffractometry on molecular crystals is details of component molecules, such as those conformations and relative position to another molecule. Thus, determinations of crystal structures are useful for understanding the physicochemical properties of the substances.

Crystal structure is fundamental knowledge of a substance. However, crystal structure of a substance is not unique in a particular form. In other words, crystal structures of a substance obtained from various crystallization methods are not always correspond with each others. This phenomenon of the same component molecules being in different arrangements is called polymorphism (Figure 1.1). Polymorphic forms are generally distinguished by prefixes. Although the number of possible polymorphs is limited because crystalline solid is highly stable state, differences in crystal structures of polymorphs results in different physicochemical properties of each polymorph. Therefore, controlling polymorphism is a significant issue in crystal engineering.

Moreover, molecules of some compounds often crystallized with those of other compound. This phenomenon is called co-crystallization in the general meaning. In the case of crystallization from solution, solute molecules often form solvates: crystals including solvent molecules as guests. Solvates are often regarded as a particular case of co-crystals. Nevertheless, the discrimination of solvate and co-crystal has been in controversy. Physicochemical properties of solvates are also different from those of unsolvated polymorphs.

Thus, crystals of the same molecule can be in multiple forms. Phenomena of polymorphism, solvate formation, and co-crystallization affect solubility, dissolution rate, and other physicochemical properties. Therefore, characterization and identification of multiple forms of crystals are one of the most popular topics in modern solid state chemistry. [1-8]

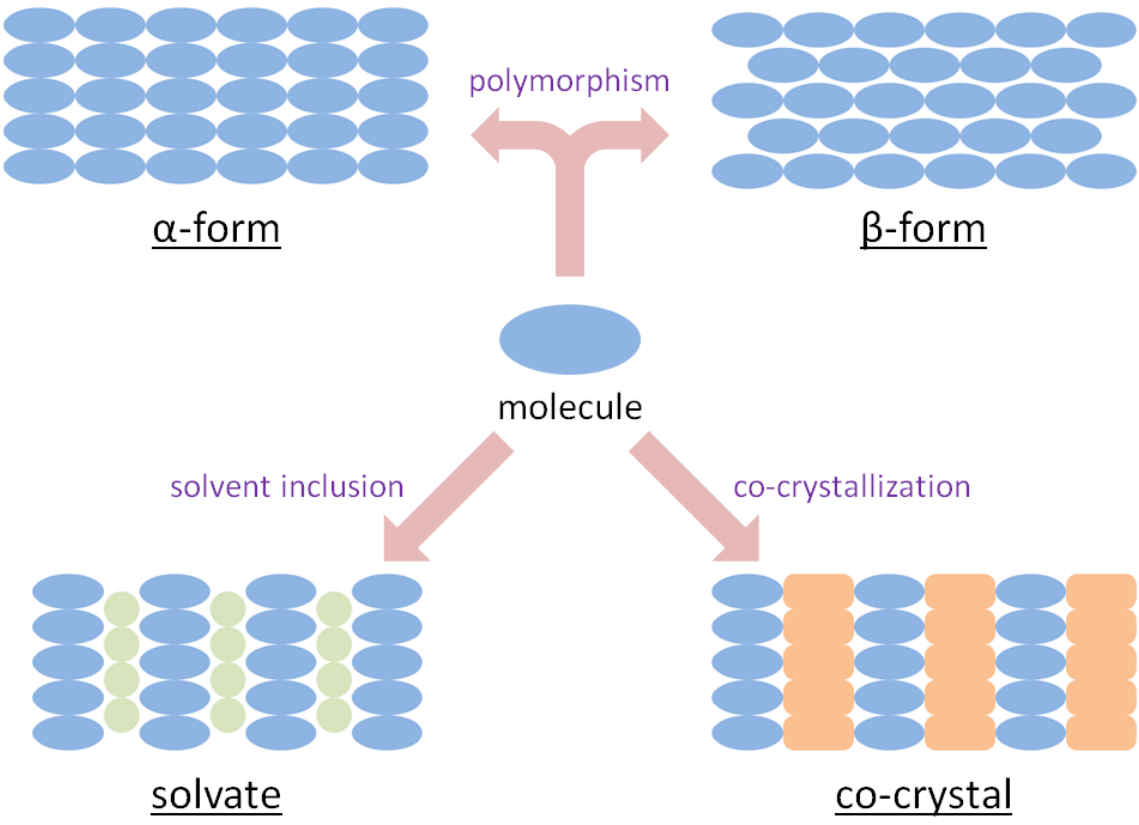

Figure 1.1 Multiple forms of molecular crystal.

1.2 Definition of chirality and trends in chiral drug development

Chirality is a property of an object to be non-superimposable on its mirror image, and the term "chiral" means having chirality. The term "achiral" means not chiral, i.e. being identical to its mirror image. Most universal example of chiral object is human hands: one hand is never superimposed on the other hand (Figure 1.2) [9, 10].

In the case of molecular structure, an atom with 4 different functional groups has chirality, and this is called molecular chirality (Figure 1.3). Two configurational isomers of chiral molecules are distinguished as (*R*)-isomer or (*S*)-isomer. Each of these two configurational isomers is called enantiomer. In chirality-independent physicochemical phenomena, one enantiomer exhibits same properties with the other. The mixture of enantiomers in same amount is called racemate. Generally, the term "racemate" is used in the same meaning with racemic mixture, which is different from racemic compound.

Figure 1.2 "human intelligence, a left and a right hand and two enantiomorphous tetrahedral" drawn by Hans Erni. This artwork was the commemorative gift to Vladimir Prelog, winner of the 1975 Novel Prize in chemistry for his research into the stereochemistry of organic molecules and reactions [9, 10].

The history of chirality started from two centuries ago. Jean-Baptiste Biot first observed the optical activity in 1815. The optical activity is a phenomenon based on molecular chirality that a solution of enantiomer rotates the plane of the incident polarized light. Louis Pasteur deduced that the origin of the optical activity is molecular structure. He achieved the mechanical separation of tartrate enantiomers in 1848. However, he coined the chiral structural arrangement in molecules as "dissymmetry". The term "chirality" itself originated from Lord Kelvin's coinage: "*I call any geometrical figure or group of points, chiral, and say that it has chirality, if its image in a plane mirror, ideally realized, cannot be brought to coincide with itself. Two equal and similar right hands are homochirally similar. Equal and similar right and left hands are heterochirally similar or allochirally similar (but heterochirally is better). These are also called enantiomorphs, after a usage introduced, I believe, by German writers. Any chiral object and its image in a plane mirror are heterochirally similar.*" [11].

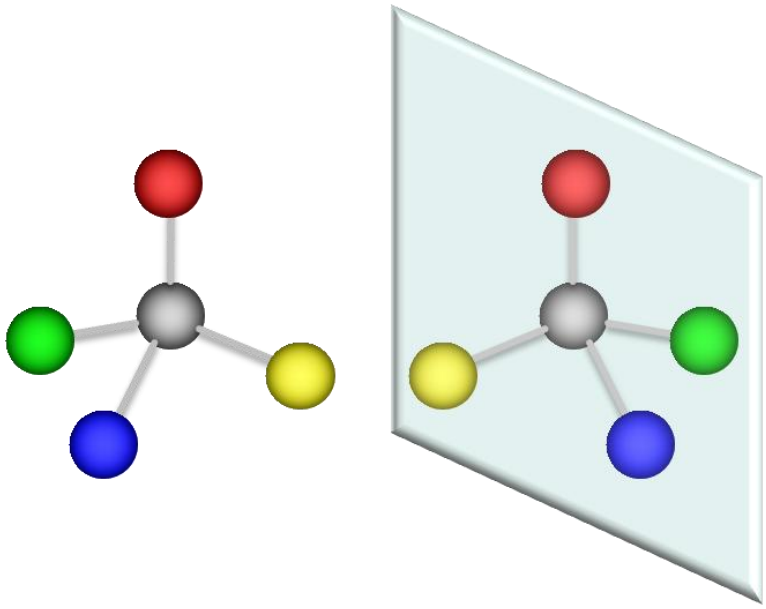

Figure 1.3 Configurational isomers of chiral molecule.

Chirality is significant issue especially in pharmaceutical industry because many pharmaceutical compounds have chirality and this fact cause undesirable problems. Several chiral drugs have different pharmacological effects between their enantiomers. In some cases, one enantiomer causes beneficial effect and yet the other harmful effect. This is mainly because protein, those receptor, homochirally consist of L-amino acids. Therefore, doses of chiral drug as racemate require careful attention.

In 1992, the US Food and Drug Administration (FDA) established the guideline for the development of chiral drugs [12]. Since then, the increasing number of chiral drugs has been developed as single enantiomer drugs. The distribution of worldwide-approved drugs concerning chirality is as follows: the ratio of single enantiomers is 39%, that of racemates is 23%, and that of achirals is 38%, respectively (Figure 1.4) [13].

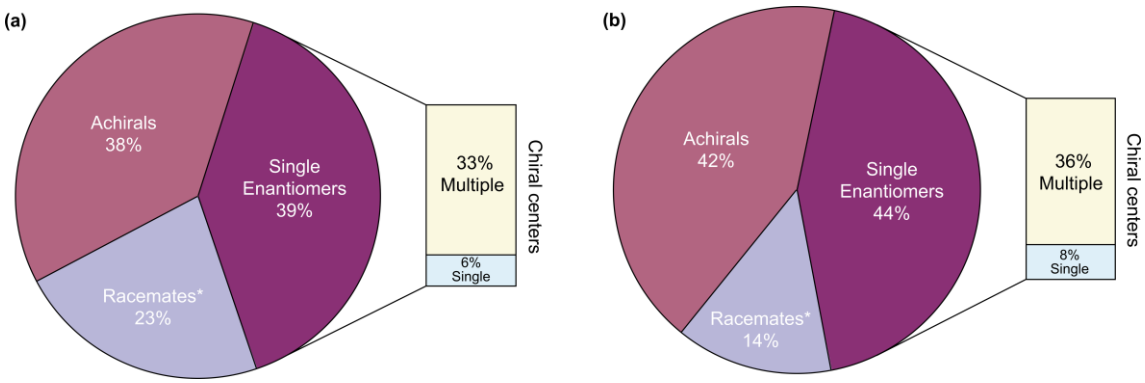

Figure 1.4 (a) Distribution of worldwide-approved drugs according to chirality character in the period 1983–2002 (b) Distribution of FDA approved drugs according to chirality character in the period 1991–2002 [13].

Determining absolute configurations [14] of chiral molecules are significant issues because of possible difference in physicochemical properties between enantiomers. There are two methods for non-empirically determining absolute configurations of chiral molecules. One is single crystal X-ray diffractometry with the Bijvoet method [15] and the other is circular dichroic exciton chirality method [16].

In the case of compounds of which single crystals are obtainable, single crystal X-ray diffractometry becomes the most established method. Bijvoet method in X-ray diffractometry is capable of determining absolute configurations of chiral molecules based on anomalous dispersion, a phenomenon of occurring dispersed X-ray by resonance. However, determining absolute configurations of molecules composed with only light atoms is difficult due to too small effect of this dispersion. Nevertheless, it has been becoming easier because technological progress has increased available intensity of X-ray and accuracy of diffraction data.

On the other hand, circular dichroic exciton chirality method requires no crystallization and has an advantage on compounds of which crystals are unobtainable or unstable. However, this method has difficulty in correctly understanding the results.

1.3 Historical background of thalidomide

3'-(N-phthalimide)glutarimide, thalidomide (Figure 1.5) is a chiral compound consisting of phthalimide ring and glutarimide ring. Thalidomide is most frequently mentioned as an example of chiral molecule because of its history. This section reviews the historical background of thalidomide in the following three subsections. Section 1.3.1 introduces the history of thalidomide, section 1.3.2 researches on the teratogenicity, section 1.3.3 undesirable property of chiral inversion.

1.3.1 Revival of dark remedy

Thalidomide was first synthesized by CIBA pharmaceutical company in 1953 and was first marketed as a safe sedative and hypnotic drug as the name of Contergan® by Chemie Grünenthal in 1956 [17]. Since then, the number of babies boned with limb defect had been increased. McBride, in 1961 [18], and Lenz, in 1962 [19], reported that this teratogenic effect is caused by pregnant women taking thalidomide, and then

thalidomide was withdrawn from market in 1962. This drug disaster caused by side-effect of thalidomide is called “thalidomide tragedy”. The number of worldwide victims is estimated to be over 10,000 [20].

However, anti-inflammatory effect of thalidomide was reported in 1965 [21], and thalidomide was approved as a treatment of erythema nodosum leprosum by the FDA and has been marketed as the name of THALOMID® by Celgene Corporation under the strict control since 1998. Furthermore, its potential of anti-angiogenesis activity was revealed in 1994 [22], and antitumor effect based on this activity was confirmed in 1999 [23]. Currently, thalidomide has been approved as a treatment of multiple myeloma in about 20 countries since the first approved in Australia in 2003 (Table 1.1) [24]. In Japan, thalidomide has been marketed as the name of THALED® Capsule 100 by Fujimoto Pharmaceutical Corporation since 2009. Other beneficial potentials of thalidomide for intractable diseases, such as behcet's disease, pyoderma gangrenosum, and rheumatologic arthritis, are also reported [25-28], and some of them are in clinical testing. The number of research papers concerning thalidomide is shown in Figure 1.6. This data were obtained by searching the word “thalidomide” through all type documents in each year using Web of Science®. Thus thalidomide has attracted considerable attention again.

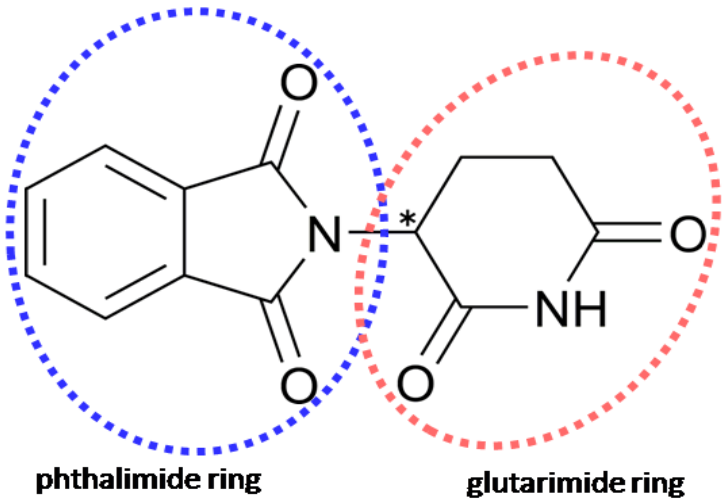

Figure 1.5 Structural formula of thalidomide (*: chiral center).

Table 1.1 The countries where thalidomide was approved as a treatment of multiple myeloma [24].

Approval Date	Country
2003/10	Australia
2003/12	New Zealand
2004/ 5	Turk
2004/ 8	Israel
2006/ 4	South Korea
2006/ 5	USA
2006/ 6	Thailand
2007/10	South Africa
2008/ 4	EU
2008/10	Japan

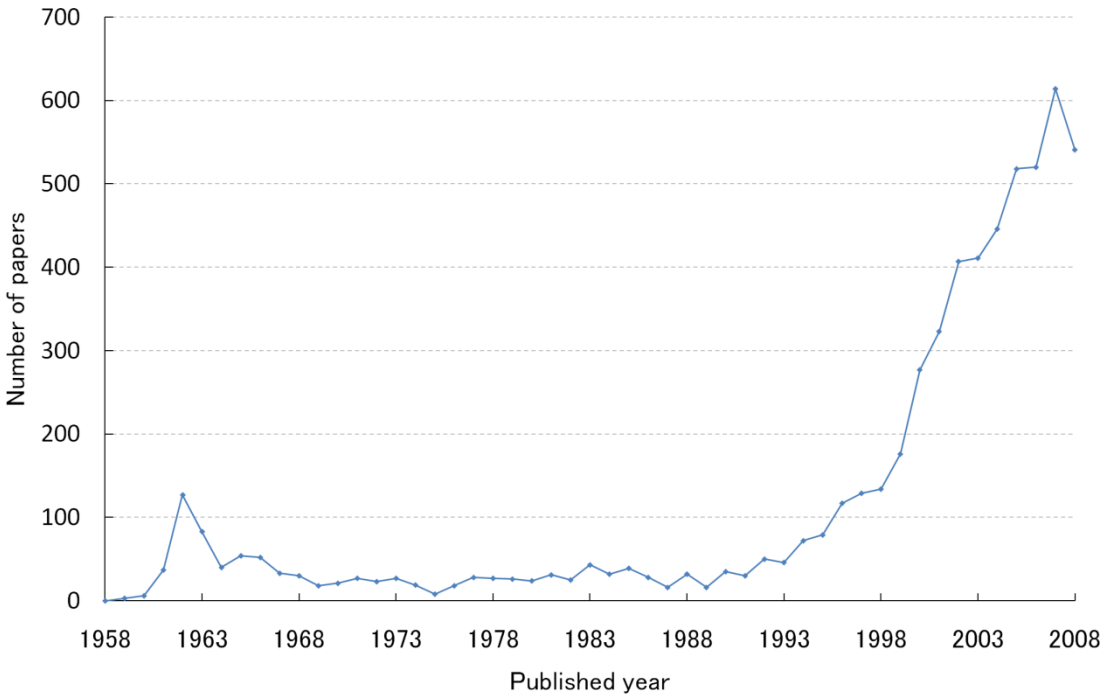

Figure 1.6 The number of research papers concerning thalidomide.

1.3.2 Controversy over teratogenicity

After the thalidomide tragedy, a number of researches, as a matter of course, have investigated the teratogenicity of thalidomide. However, the mechanism of its teratogenicity had been unclear for a long period, although influence of anti-angiogenesis activity [29, 30] and damage of DNA by oxidation [31] had been proposed as possible causes. Revelation of the mechanism of thalidomide teratogenicity is extremely difficult because metabolism and hydrolysis of thalidomide progressed in human body, and result in the existence of enormous number of products.

More recently, Handa *et al.* identified a protein cereblon as a primary target of thalidomide teratogenicity [32]. They immobilized thalidomide derivatives to ferrite-glycidyl methacrylate beads. These beads were incubated in human HeLa cell extracts. As a result, protein specifically interacted with these beads was identified as cereblon. Cereblon is revealed to be a subunit of a functional E3 ubiquitin ligase complex. Thalidomide teratogenicity was indicated to arise from inhibition of the function of this E3 ubiquitin ligase. However, as they mentioned, whether thalidomide or one of its metabolites is actually interacted with cereblon remain unclear. In addition, chirality of thalidomide was not described in their study. More specifically, whether or not there is difference in binding behavior with cereblon between enantiomers of thalidomide has been unclear.

Several researches focused on the difference in bioactivities between enantiomers of thalidomide. In 1979, Blaschke *et al.* reported that only (*S*)-thalidomide shows teratogenicity with the examinations of separately dosing enantiomers to rats and mice [33]. This report, as a matter of course, attracted considerable attention, and has been thought to trigger the present guideline for the development of chiral drugs as mentioned in section 1.2. However, this report has been doubted in several points. One of examples is employing rats and mice as the model animal because rats and mice strongly resist to teratogenicity. Furthermore, no difference was observed between enantiomers of thalidomide in a similar experiment to rabbits, showing sensitivity to teratogenicity [34].

On the contrary, Schmahl *et al.* examined on EM12, an analog of thalidomide with stronger teratogenicity, by dose of each enantiomer to marmoset monkeys [35]. As a result, the incidence rate of teratogenic effect in the case of (*S*)-EM12 was extremely higher than that of (*R*)-EM12. Although this results support the Blaschke's report, the

teratogenic effect was slightly observed in the case of (*R*)-EM12. To understand these results consistently, a phenomenon of "chiral inversion" is never negligible.

1.3.3 Chiral inversion: cause of the confusion

The chiral inversion is phenomenon that a chiral compound inverts its chirality, namely, one enantiomer turns into the other. Thalidomide is well-known to show this phenomenon of chiral inversion [36]. The chiral inversion mechanism of thalidomide is proposed as isomerization via base-catalyzed keto-enol tautomerism due to high acidity of the proton bonding to the chiral center, as shown in Figure 1.7 [37]. According to this mechanism, the chiral inversion will be avoidable in polar aprotic and nonpolar solvents. Nevertheless, thalidomide easily inverts its chirality in polar solution state. For instance, Hashimoto *et al.* reported that almost all enantiomers of thalidomide invert their chirality with incubation in water solution for 10 h at 37°C [38].

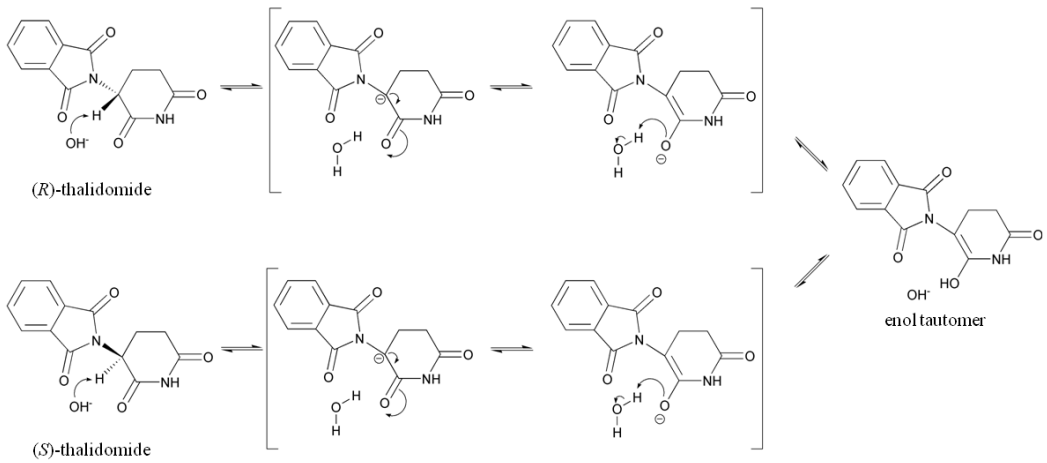

Figure 1.7 Chiral inversion via base-catalyzed keto-enol tautomerism.

Moreover, this chiral inversion of thalidomide is accelerated especially in human body. This is because albumin, hydroxyl ions, phosphate, and amino acids catalyze the chiral inversion [39]. Blaschke *et al.* also reported that chiral inversion of thalidomide in human citric plasma is extremely fast: 25% of enantiomers invert their chirality with incubation for 10 min at 37°C [40]. Therefore, experimentally confirming the differences in bioactivity between the enantiomers of thalidomide is extremely difficult. Furthermore, the unavoidable chiral inversion in human body of thalidomide is thought to one of the reasons why thalidomide has been approved for sale as the racemate against the recent trends in the development of chiral drugs.

1.4 Overall objectives

In the case of solution state, molecules play main roll in physicochemical phenomena. Thus, there is no difference in chirality-independent properties between an enantiomer and the racemate. Whereas in the case of solid state, major differences of chirality-independent properties are in between an enantiomer and the racemate, not the enantiomeric isomers. This is because crystal structures of enantiomeric and racemic compounds are essentially different. Therefore, the idea of comparison between an enantiomer and the racemate is significant for studies concerning crystals of chiral compounds, particularly for pharmaceutical compounds due to recent trends in the chiral drug development.

Although a number of studies have reported the bioactivity of thalidomide [20, 26-28, 31, 34, 41], only a few studies have reported its physicochemical properties. Racemic thalidomide is known to exhibit lower solubility and higher melting point than the enantiomers [34]. It is also known that the oral absorption of racemic thalidomide is slower than that of the enantiomers [27, 41]. However, the origin of differences in these physicochemical properties between enantiomeric and racemic thalidomides has not been investigated.

Crystal structures of racemic thalidomide have been investigated since 1971. Two polymorphs of α and β forms are known in racemic thalidomide. However, despite the renewed attention to thalidomide, crystal structures of enantiomeric thalidomide had not been reported.

There are a few possible reasons for this. First, thalidomide has not been regarded as focus of research, not only crystallography but also in other fields, due to the

disaster. This fact is reflected in Figure 1.6. The other reason may be in asymmetric synthesis of enantiomeric thalidomides. Until recently, practical asymmetric synthesis of the enantiomeric thalidomide had not been achieved. This is because the chiral inversion easily occurs under high temperature and high basicity conditions for creating the phthalimide and glutarimide rings of thalidomide. At long last, in 2001, the three-step synthesis of enantiomeric thalidomide from ornithine with 99% e.e. in good yield was achieved.

As to experimental difficulty, chiral inversion of thalidomide will be a problem in crystallization of enantiomeric thalidomides. This is because the enantiomeric isomers generated by chiral inversion are nothing but impurities in crystallization of enantiomeric thalidomides. Therefore, it requires proper consideration of crystallization method. Although chiral inversion of thalidomide has often been concerned, particularly in pharmacological study, mechanism of the chiral inversion has been referred in few studies.

In addition, even if enantiomeric crystals of thalidomide were successfully obtained, another problem may have been in determination of absolute configuration with single crystal X-ray diffractometry. This is because thalidomide is composed with only light atoms of carbon, nitrogen, oxygen, and hydrogen. Nevertheless, determining absolute configuration of light molecules is becoming easier because of recent progress in X-ray diffractometry.

On the above background, this study focuses on crystal structures of thalidomide. The objectives of this thesis are summarized as:

- Evaluation of methods for crystallization of thalidomide;
- Determination of crystal structure and absolute configuration of enantiomeric thalidomide;
- Investigation into the origin of differences in physicochemical properties between enantiomeric and racemic thalidomides.

The primary significance of this study is on the idea of comparison between an enantiomer and the racemate. In chapter 2, methods for crystallization of thalidomide are evaluated with consideration of possible multiple forms. In chapter 3, detail structure of (*S*)-thalidomide crystals obtained from different methods are investigated. In chapter 4, crystal structures of (*RS*)-thalidomide obtained from different methods are investigated and compared with those of (*S*)-thalidomide.

1.5 References

[1] D. Braga, F. Grepioni, and L. Maini, "The growing world of crystal forms", *Chem. Commun.*, 46 (2010), pp. 6232-6242, DOI: 10.1039/c0cc01195a.

[2] D. Braga, F. Grepioni, L. Maini, and M. Polito, "Crystal Polymorphism and Multiple Crystal Forms", *Struct. Bond.*, 132 (2009), pp. 25-50, DOI: 10.1007/430_2008_7.

[3] A. Llinas and J. M. Goodman, "Polymorph control: past, present and future", *Drug Discov. Today,* 13 (2008), pp. 198-210, DOI: 10.1016/j.drudis.2007.11.006.

[4] C. B. Aakeröy, N. R. Champness, and C. Janiak, "Recent advances in crystal engineering", *CrystEngComm,* 12 (2010), pp. 22-43, DOI: 10.1039/b919819a.

[5] I. Miroshnyk, S. Mirza, and N. Sandler, "Pharmaceutical co-crystals–an opportunity for drug product enhancement", *Expert. Opin. Drug. Del.*, 6 (2009), pp. 333-341, DOI: 10.1517/17425240902828304.

[6] A. V. Trask, "An Overview of Pharmaceutical Cocrystals as Intellectual Property", *Mol. Pharmaceutics,* 4 (2007), pp. 301-309, DOI: 10.1021/mp070001z.

[7] T. Friščić and W. Jones, "Recent Advances in Understanding the Mechanism of Cocrystal Formation via Grinding", *Cryst. Growth. Des.*, 9 (2009), pp. 1621-1637, DOI: 10.1021/cg800764n.

[8] D. Braga, L. Brammer, and N. R. Champness, "New trends in crystal engineering", *CrystEngComm,* 7 (2005), pp. 1-19, DOI: 10.1039/b417413e.

[9] V. Prelog, "Chirality in chemistry", *Science*, 193 (1976), pp. 17-24, DOI: 10.1126/science.935852.

[10] V. Prelog, "Chirality in Chemistry", *Nobel Lecture* (1975), http://nobelprize.org/nobel_prizes/chemistry/laureates/1975/prelog-lecture.html

[11] P. Cintas, "Tracing the origins and evolution of chirality and handedness in chemical language", *Angew. Chem. Int. Ed.*, 46 (2007), pp. 4016-4024, DOI: 10.1002/anie.200603714.

[12] U.S. Food and Drug Administration, "Development of New Stereoisomeric Drugs", http://www.fda.gov/Drugs/GuidanceComplianceRegulatoryInformation/Guidances/ucm122883.htm

[13] H. Caner, E. Groner, L. Levy, and I. Agranat, "Trends in the development of chiral drugs", *Drug Discov. Today,* 9 (2004), pp. 105-110, DOI:

10.1016/S1359-6446(03)02904-0.

[14] V. Prelog and G. Helmchen, "Basic Principles of the CIP-System and Proposals for a Revision", *Angew. Chem. Int. Ed. Engl.,* 21 (1982), pp. 567-583, DOI: 10.1002/anie.198205671.

[15] J. M. Bijvoet, A. F. Peerdeman, and A. J. van Bommel, "Determination of the Absolute Configuration of Optically Active Compounds by Means of X-Rays", *Nature*, 168 (1951), pp. 271-272, DOI: 10.1038/168271a0.

[16] N. Harada and K. Nakanishi, "Exciton chirality method and its application to configurational and conformational studies of natural products", *Acc. Chem. Res.*, 5 (1972), pp. 257-263, DOI: 10.1021/ar50056a001.

[17] Y. Hashimoto, "Structural development of biological response modifiers based on thalidomide", *Bioorg. Med. Chem.,* 10 (2002), pp. 461-479, DOI: 10.1016/S0968-0896(01)00308-X.

[18] W. Mcbride, "THALIDOMIDE AND CONGENITAL ABNORMALITIES", *The Lancet*, 278 (1961), 1358, DOI: 10.1016/S0140-6736(61)90927-8

[19] W. Lenz, "THALIDOMIDE AND CONGENITAL ABNORMALITIES", *The Lancet*, 279 (1962), pp. 45-46, DOI: 10.1016/S0140-6736(62)92665-X.

[20] M. E. Franks, G. R. Macpherson, and W. D. Figg, "Thalidomide", *The Lancet*, 363 (2004), pp. 1802-1811, DOI: 10.1016/S0140-6736(04)16308-3.

[21] J. Sheskin, "THALIDOMIDE IN TREATMENT OF LEPRA REACTIONS", *Clin. Pharmacol. Ther.*, 6 (1965), pp. 303-306.

[22] R. J. D'Amato, M. S. Loughnan, E. Flynn, and J. Folkman, "Thalidomide is an inhibitor of angiogenesis", *Proc. Natl. Acad. Sci. U.S.A.,* 91 (1994), pp. 4082-4085.

[23] S. Singhal, J. Mehta, R. Desikan, D. Ayers, P. Roberson, P. Eddlemon, N. Munshi, E. Anaissie, C. Wilson, M. Dhodapkar, J. Zeldis, B. Barlogie, D. Siegel, and J. Crowley, "Antitumor Activity of Thalidomide in Refractory Multiple Myeloma", *N. Engl. J. Med.*, 341 (1999), pp. 1565-1571, DOI: 10.1056/NEJM199911183412102

[24] http://www.mhlw.go.jp/shingi/2008/08/s0826-5.html

[25] U.S. National Library of Medicine, "Thalidomide: Potential Benefits and Risks (CBM 97-4)", (1997), http://www.nlm.nih.gov/archive/20040831/pubs/cbm/thalidomide.html

[26] M. Melchert and A. List, "The thalidomide saga", *Int. J. Biochem. Cell Biol.*, 39 (2007), pp. 1489-1499., DOI: 10.1016/j.biocel.2007.01.022

[27] T. Eriksson, S. Björkman, and P. Höglund, "Clinical pharmacology of thalidomide", *Eur. J. Clin. Pharmacol.*, 57 (2001), pp. 365-376., DOI: 10.1007/s002280100320

[28] S. Tseng, G. Pak, K. Washenik, M. K. Pomeranz, and J. L. Shupack, "Rediscovering thalidomide: A review of its mechanism of action, side effects, and potential uses", *J. Am. Acad. Dermatol.*, 35 (1996), pp. 969-979., DOI: 10.1016/S0190-9622(96)90122-X

[29] H. Ledford, "How thalidomide makes its mark ", *Nature* (2009), DOI: 10.1038/news.2009.462.

[30] C. Therapontos, L. Erskine, E. R. Gardner, W. D. Figg, and N. Vargesson, "Thalidomide induces limb defects by preventing angiogenic outgrowth during early limb formation", *Proc. Natl. Acad. Sci. U.S.A.*, 106 (2009), pp. 8573-8578, DOI: 10.1073/pnas.0901505106.

[31] T. D. Stephens, C. J. W. Bunde, and B. J. Fillmore, "Mechanism of action in thalidomide teratogenesis", *Biochemical Pharmacology,* 59 (2000), pp. 1489-1499, DOI: 10.1016/S0006-2952(99)00388-3.

[32] T. Ito, H. Ando, T. Suzuki, T. Ogura, K. Hotta, Y. Imamura, Y. Yamaguchi, and H. Handa, "Identification of a Primary Target of Thalidomide Teratogenicity", *Science,* 327 (2010), pp. 1345-1350, DOI: 10.1126/science.1177319.

[33] G. Blaschke, H. P. Kraft, K. Fickentscher, and F. Kohler, "Chromatographic separation of racemic thalidomide and teratogenic activity of its enantiomers", *Arzneimittelforschung,* 29 (1979), pp. 1640-1642.

[34] S. Fabro, R. L. Smith, and R. T. Williams, "Toxicity and Teratogenicity of Optical Isomers of Thalidomide", *Nature,* 215 (1967), 296, DOI: 10.1038/215296a0

[35] H. Schmahl, H. Nau, and D. Neubert, "The enantiomers of the teratogenic thalidomide analogue EM 12", *Arch.Toxicol.*, 62 (1988), pp. 200-204., DOI: 10.1007/BF00570140

[36] N. Shibata, T. Yamamoto, and T. Toru, "Synthesis of Thalidomide", *Bioactive Heterocycles II,* 8 (2007), pp. 73-97, DOI: 10.1007/7081_2007_057.

[37] G. Schoetz, O. Trapp, and V. Schurig, "Determination of the enantiomerization barrier of thalidomide by dynamic capillary electrokinetic chromatography", *Electrophoresis,* 22 (2001), pp. 3185-3190, DOI: 10.1002/1522-2683(200109).

[38] K. Nishimura, Y. Hashimoto, and S. Iwasaki, "(S)-form of alpha-methyl-N(alpha)-phthalimidoglutarimide, but not its (R)-form,enhanced

phorbol ester-induced tumor necrosis factor-alpha production by humanleukemia cell HL-60: implication of optical resolution of thalidomidal effects.", *Chem. Pharm. Bull.,* 42 (1994), pp. 1157-1159.

[39] M. Reist, P. Carrupt, E. Francotte, and B. Testa, "Chiral Inversion and Hydrolysis of Thalidomide: Mechanisms and Catalysis by Bases and Serum Albumin, and Chiral Stability of Teratogenic Metabolites", *Chem. Res. Toxicol.,* 11 (1998), pp. 1521-1528, DOI: 10.1021/tx9801817.

[40] B. Knoche and G. Blaschke, "Investigations on the in vitro racemization of thalidomide by high-performance liquid chromatography", *J. Chromatogr. A,* 666 (1994), pp. 235-240., DOI: 10.1016/0021-9673(94)80385-4

[41] T. Eriksson, S. Björkman, B. Roth, Å. Fyge, and P. Höglund, "Stereospecific determination, chiral inversion in vitro and pharmacokinetics in humans of the enantiomers of thalidomide", *Chirality,* 7 (1995), pp. 44-52, DOI: 10.1002/chir.530070109.

2. Evaluation of methods for crystallization of thalidomide

2.1 Introduction

Molecules of a compound are capable of forming different crystals depending on the crystallization method. This multiple formation is characterized as a phenomenon of polymorphism. Moreover, molecules of a compound are often crystallized with including solvent molecules in its crystal lattice. These crystals are called as solvates. This phenomenon of solvate formation also depends on the crystallization method. These phenomena of polymorphism and solvate formation greatly impact on solubility, dissolution rate, and other physicochemical properties, because of difference in crystal structure between polymorphs and solvates. Therefore, controlling polymorphism and solvate formation is significant issues, particularly in pharmaceutical industry for drug safety and bioavailability.

Controlling habits of crystal is also important issue, for instance application in pharmaceutical preparation, although its effects on physicochemical properties are less than polymorphs and solvates. In some case, the habits of isomorphic crystals are different from each other depending on the crystallization methods.

Thus, characterization and identification of multiple forms of crystals are one of the most popular topics in modern solid state chemistry. [1-8] However, absolutely controlling the phenomena of polymorphism and solvate formation with the present crystal engineering is impossible. Actually, a number of polymorphs and solvates were obtained as unpredictable results. Nevertheless, appropriate consideration on the crystallization method is capable of narrowing the possibilities for occurrences of these phenomena.

Crystal structures of racemic thalidomide have been investigated since 1971. [9] Two polymorphs of α and β forms are known in (*RS*)-thalidomide. [10] However, crystallographical studies on enantiomeric thalidomide have not been reported.

This study, in this chapter, evaluates methods for crystallization of thalidomide with consideration of possible multiple forms of thalidomide crystal and undesirable

chiral inversion in crystallization of enantiomeric thalidomide. The crystallization methods were determined on the basis of consideration for selection of solvent and technique for crystallization. Chiral inversions in determined methods were estimated with circular dichroism (CD) measurements. Habits of obtained crystals were observed with polarizing microscope. The possibilities of polymorphs or solvates were investigated with thermogravimetry-differential thermal analyses (TG-DTA).

2.2 Determination of crystallization methods

A method for crystallization is divided into two major factors: selection of solvent and technique for crystallization.

The solvent for crystallization is one of most crucial factor impacting on the phenomena of polymorphism and solvate formation. At an early phase in crystal growth from solution, crystal nuclei are grew from clusters which are assembling unit of solute molecules. The forms of these clusters critically depend on the polarity of solvent: high-polar cluster form is more favorable in high-polar solvent, contrastingly, low-polar cluster form in low-polar solvent. Thus, crystallizations in solvents with different polarity often cause the formation of polymorphs and solvates.

The most common technique for crystallization is solvent evaporation. The solvent evaporation technique is easy to control the condition and require no unconventional equipment. Therefore, solvent evaporation technique suits for the first attempt of crystallization.

Water is one of the most important polar solvent, particularly for crystallizing pharmaceutical compound because only hydrates of solvates may be of practical use as drugs. Therefore, crystallization from water solution should be attempted. However, in the case of thalidomide, large crystals enough to conduct X-ray diffractometry are difficult to be obtained by crystallization from water solution due to poor solubility of thalidomide in water. Actually, preliminary experiment of crystallization from water solution with solvent evaporation technique obtained only powder, whose quality is impossible to be identified.

Methanol is also common polar solvent. According to previous study on solubility of thalidomide, solubility of thalidomide in water is 0.238 mM at 32 °C, whereas that in methanol is 4.38 mM at 32 °C [11]. On this point, single crystals of more suitable size for X-ray diffractometry should be obtainable with crystallization with solvent

evaporation technique from methanol solution. Nevertheless, this solubility of methanol is relatively poor compared to other solvents such as after mentioned chloroform. Therefore, crystallization of thalidomide from methanol solution occurs just before complete evaporation of the solution. In addition, methanol has relatively low boiling point. Because of these properties, optimizing evaporation ratio of methanol solution for crystallization is difficult. In some cases, colored crystals, whose color is thought to arise from impurities, were obtained by completely evaporating the solution. Thus, preliminary experiments of crystallization from methanol solution with solvent evaporation technique failed to obtain crystals with proper size and quality.

In the case of crystallization from methanol solution, spending a long time on will be undesirable because racemization of thalidomide progress in methanol solution. Considering this point, preliminary experiments attempted to crystallize from methanol solution with solvent evaporation technique. this attempt because optimizing crystallization conditions is difficult due to poor solubility and low boiling point.
While water is easier to control evaporation ratio than methanol because of higher boiling point than methanol, methanol has advantage in solubility of thalidomide compared to water. Considering these points and the property of methanol being miscible with water, crystallization from mixed solution of methanol and water with solvent evaporation technique were attempted. In this case, complete evaporation of the solution should be easily avoided. To increase solubility of thalidomide in the mixed solvent, the ratio of methanol prefers to be as high as possible. As a result of observation for evaporation ratio with gradually changing the mixing ratio, the optimal ratio was determined as methanol:water = 5:3. Thus, methanol-water (5:3) was selected as a polar solvent for crystallization of thalidomide.

However, crystallizations of enantiomeric thalidomide from polar solutions require special attention because an undesirable reaction of racemization progress in polar protic solvents such as water and methanol. In crystallization of enantiomeric thalidomide, the enantiomeric isomers generated through racemization are nothing but impurities. Nevertheless, single crystals of enantiomeric thalidomide may be obtainable by crystallizing before the racemization has completely proceeded. The racemization mechanism of thalidomide is proposed as chiral inversion via base-catalyzed keto-enol tautomerism (Figure 2.1) [12]. According to this mechanism, the racemization of thalidomide will be avoidable in polar aprotic and nonpolar solvents.

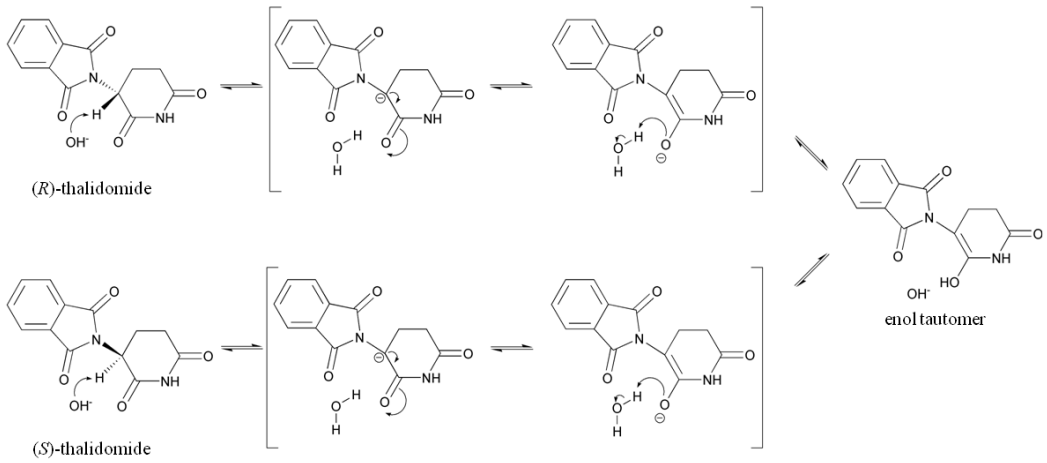

Figure 2.1 Chiral inversion via base-catalyzed keto-enol tautomerism.

Chloroform is one of common nonpolar solvents. According to the proposed mechanism, the chloroform solution of thalidomide should be suitably free from problem of racemization. In addition, (*R*)-thalidomide molecules in chloroform solution are indicated to exist in dynamic equilibrium of three isomeric dimers which differ in the hydrogen bonded ring moieties (Figure 2.2) [13]. With this indication, behavior of thalidomide molecules at cluster formation in nonpolar chloroform solution is expected to fundamentally different from that in polar methanol-water solution. Therefore, this study selected chloroform as a nonpolar solvent for crystallization.

In the case of crystallization from methanol-water solution, solubility of thalidomide in methanol-water is relatively poor. To increase the solubility, moderate heating is desired. Furthermore, spending long time will be unfavorable due to racemization. To appropriately increase the solubility and accelerate the evaporation of solvent, crystallization with solvent evaporation technique from methanol-water solution was attempted at temperatures around 50 °C.

In the case of crystallization from chloroform solution, chloroform has relatively high solubility of thalidomide at room temperature. Preliminary experiments demonstrate the solubilities of enantiomeric and racemic thalidomides in chloroform at room temperature are about 28.7 mM and 5.5 mM, respectively. These solubilities

appeared to be enough to attempt crystallization with vapor diffusion technique. The vapor diffusion technique requires the poor solvent of thalidomide with low boiling point and being miscible in chloroform. Diethyl ether is one of common nonpolar solvents and satisfies above requirements. Therefore, this study evaporated the chloroform solution at room temperature. Moreover, as a further experiment, crystallization with vapor diffusion technique, diffusing diethyl ether into chloroform solutions, was also attempted at room temperature.

On the basis of above consideration, this study attempted following three methods for crystallization of (*S*)- and (*RS*)-thalidomides:

- solvent evaporation technique from methanol-water solution;
- solvent evaporation technique from chloroform solution;
- vapor diffusion technique from chloroform solution.

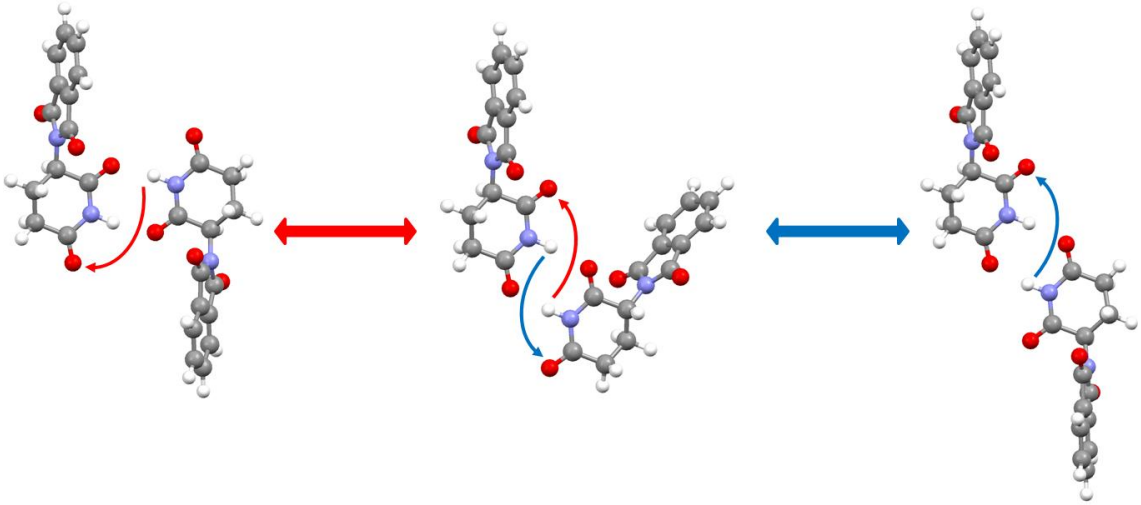

Figure 2.2 Dynamic equilibrium of three isomeric (*R*)-thalidomide dimers in chloroform solution [13]. Color code: C: gray, N: blue, O: red, H: white.

2.3 Estimation of chiral inversion with CD spectrometry

Although chiral inversion of thalidomide is unavoidable in methanol-water solution, single crystals of enantiomeric thalidomide are thought to be obtainable by crystallizing before the racemization has completely proceeded. While chiral HPLC is generally used for quantitative estimation of chiral inversion, CD measurement has advantage in minute observation of time course. Therefore, chiral inversions of (*S*)-thalidomide in crystallization conditions were estimated with CD measurements.

2.3.1 Basic theory of circular dichroism measurement

CD is an optical property that a substance shows different absorbance for left circularly polarized (LCP) and right circularly polarized (RCP) lights. Linearly polarized light is identified as a sum of LCP and RCP lights in the same amplitude. Therefore, CD turns the incident linearly polarized light into the elliptically polarized light with passing through the substance. The difference between absorbencies for LCP and RCP lights is expressed as

$$\Delta A = A_l - A_r, \tag{2.1}$$

where A_l and A_r represent the absorbance of LCP and RCP lights, respectively. Applying Beer–Lambert law into this equation leads the following equation:

$$\Delta A = (\varepsilon_l - \varepsilon_r)CL, \tag{2.2}$$

where ε_l and ε_r represent molar absorptivity for LCP and RCP lights, respectively. C is the molar concentration and L is the length of light path. The molar circular dichroism $\Delta\varepsilon$ is defined as

$$\Delta\varepsilon = \varepsilon_l - \varepsilon_r, \tag{2.3}$$

and then the molar ellipticity $[\theta]$ is expressed as

$$[\theta] = 100\left(\frac{\log_e 10}{4}\right)\left(\frac{180}{\pi}\right)\Delta\varepsilon. \tag{2.4}$$

Generally, this molar ellipticity is measured as the intensity of CD.

CD essentially originates from chirality of substances. Thus the CD experiments are widely applied to a number of researches on chiral substances. CD of one enantiomer has same amplitude and reverse sign of the other. Therefore, racemate, a mixture of enantiomers in equal amount, does not exhibit CD.

2.3.2 Materials

(*S*)-thalidomide was purchased from Sigma-Aldrich, Inc. Methanol, chloroform, diethyl ether, and acetonitrile were purchased from Wako Pure Chemical Industries, Ltd.

2.3.3 Experimental method

Measurement conditions were determined based on the crystallization conditions. To estimate the chiral inversion ratio in protic methanol-water solution, time course in CD spectra of 0.2 mM methanol-water solutions of (*S*)-thalidomide was measured at 50 °C for 10 hours. The mixture ratio of methanol-water is the same 5:3 as that of mixed solvent for crystallization. In addition, to confirm stability to chiral inversion in aprotic and nonpolar solutions, chloroform, diethyl ether, and acetonitrile solutions of (*S*)-thalidomide were conducted. Time course in CD spectra of 0.1 mM chloroform, 0.1 mM diethyl ether, and 0.1 mM acetonitrile solutions of (*S*)-thalidomides were measured at room temperature for 48 hours.

These measurements were immediately started after preparation of the solutions. However, chiral inversion during dissolution was not exactly considered in this estimation. Thus, it should be noted that these estimations are somewhat less quantitative in this point.

All CD measurement was conducted using JASCO J-820 spectrometer. A rectangular quartz cell of 10 mm light-path length was used. The measurement conditions were as follows: step scan measurement, 1 nm bandwidth, 2 sec response time, standard sensitivity, 1 nm wavelength resolution.

2.3.4 Result for protic methanol-water solution

CD spectra of 0.2 mM (*S*)-thalidomide methanol-water solution measured every 1 h at 50 °C are shown in Figure 2.3. The CD peak around 250 nm is obviously observable after 10 hours. This result supports that procession of racemization will be incomplete in 10 hours, although chiral inversion during dissolution was not exactly considered in this estimation as mentioned above. Therefore, single crystals of enantiomeric thalidomide will be obtainable from protic methanol-water solution by crystallizing in a few hours.

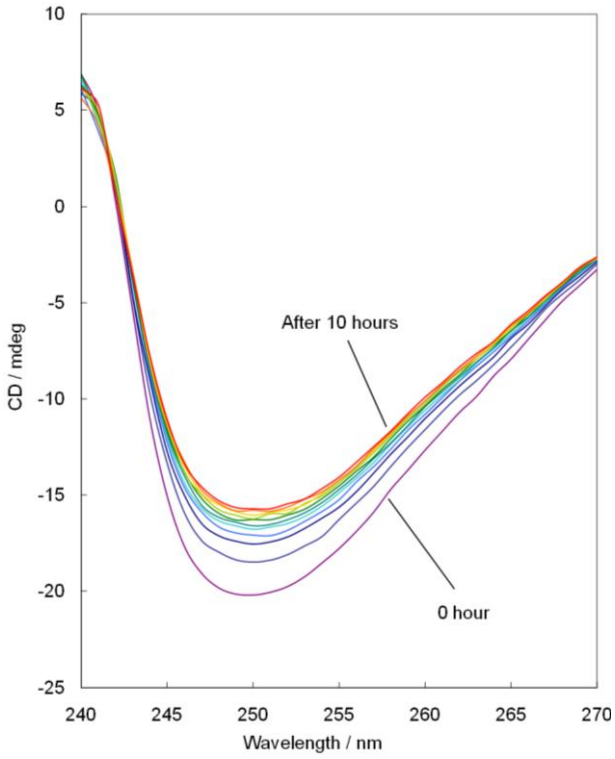

Figure 2.3 CD spectra of (*S*)-thalidomide methanol-water solution measured every 1 hour.

2.3.5 Result for polar aprotic and nonpolar solutions

To confirm stability to chiral inversion in polar aprotic and nonpolar solutions, CD spectra of 0.1 mM chloroform, diethyl ether, and acetonitrile solutions were measured at room temperature (Figure 2.4-2.6). In the results of chloroform and acetonitrile solutions, the CD peaks around 250 nm remain almost unchanged for 48 hours. Although the result of diethyl ether solution shows slight increase of the peak intensity, this should be caused by rise of the concentration due to high volatility of diethyl ether. Therefore, it is confirmed that chiral inversion of thalidomide is surely avoidable in polar aprotic and nonpolar solutions.

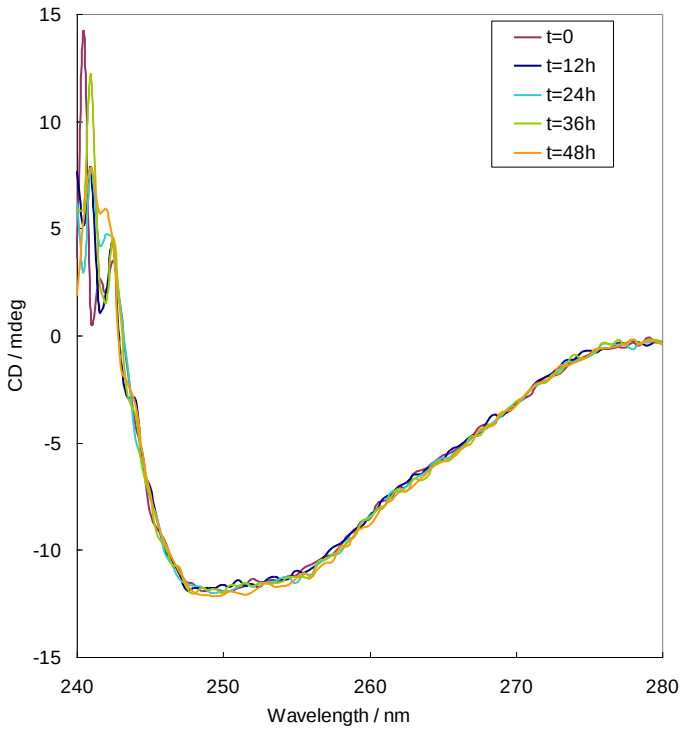

Figure 2.4 CD spectra of (*S*)-thalidomide chloroform solution measured every 12 hour.

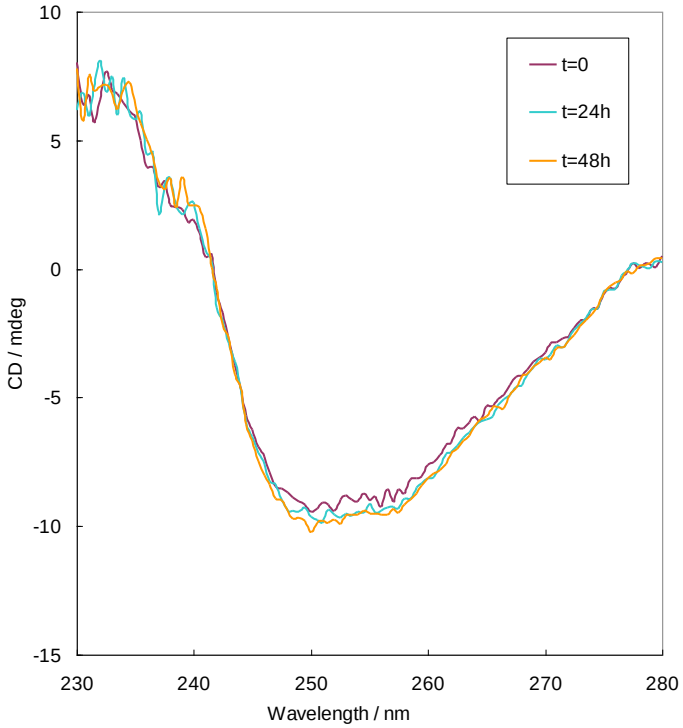

Figure 2.5 CD spectra of (*S*)-thalidomide diethyl ether solution measured every 24 hour.

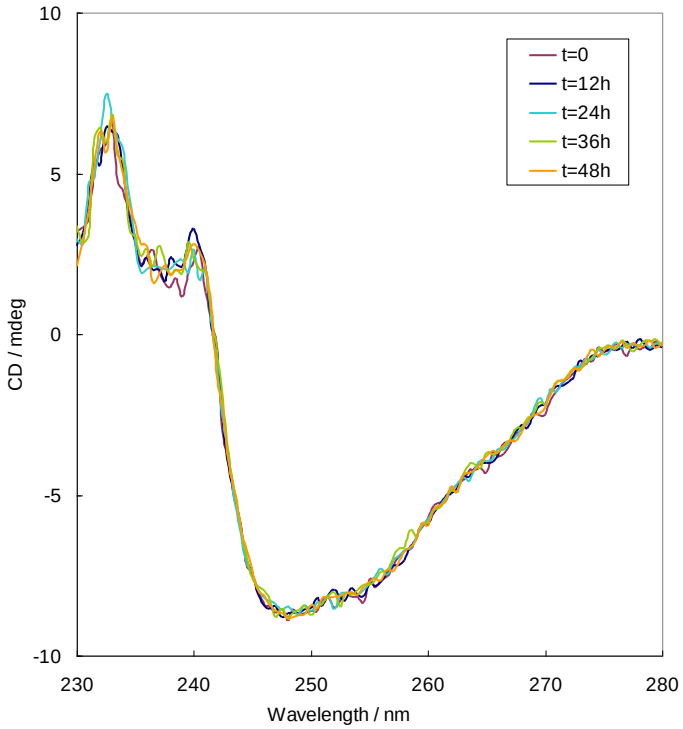

Figure 2.6 CD spectra of (*S*)-thalidomide acetonitrile solution measured every 12 hour.

2.4 Crystallization of (*S*)- and (*RS*)-thalidomides

2.4.1 Materials

(*S*)- and (*RS*)-thalidomides were purchased from Sigma-Aldrich, Inc. Methanol, chloroform, diethyl ether, and acetonitrile were purchased from Wako Pure Chemical Industries, Ltd.

2.4.2 Solvent evaporation technique from methanol-water solution

To avoid excess chiral inversion, (*S*)-thalidomide was crystallized in about 4 hours based on the result of CD measurement. In addition, to compare with the case of (*S*)-thalidomide, (*RS*)-thalidomide was also crystallized in about 4 hours.

Crystallization procedure of (*S*)-thalidomide with solvent evaporation technique from methanol-water solution was as follows:

(1) (*S*)-thalidomide powder (50 mg) was dissolved in 40 ml methanol-water (5:3).

(2) The solution was evaporated for about 4 h at 50 °C.

(3) The grown crystals floating on the solutions were filtered out.

Crystallization procedure of (*RS*)-thalidomide with solvent evaporation technique from methanol-water solution was as follows:

(1) (*RS*)-thalidomide powder (50 mg) was dissolved in 40 ml methanol-water (5:3).

(2) The solution was evaporated for about 4 h at 50 °C.

(3) The grown crystals floating on the solutions were filtered out.

2.4.3 Solvent evaporation technique from chloroform solution

Crystallization procedure of (*S*)-thalidomide with solvent evaporation technique from chloroform solution was as follows:

(1) (*S*)-thalidomide powder (77.3 mg) was dissolved in 14 ml chloroform.

(2) The solution was evaporated in a few days at room temperature.

(3) The grown crystals floating on the solutions were filtered out.

Crystallization procedure of (*RS*)-thalidomide with solvent evaporation technique from

chloroform solution was as follows:

(1) (*RS*)-thalidomide powder (6.28 mg) was dissolved in 4.8 ml chloroform.

(2) The solution was evaporated in a few days at room temperature.

(3) The grown crystals floating on the solutions were filtered out.

2.4.4 Vapor diffusion technique from chloroform solution

Crystallization procedure of (*S*)-thalidomide with vapor diffusion technique from chloroform solution was as follows:

(1) (*S*)-thalidomide powder (7.0 mg) was dissolved in 1 ml chloroform.

(2) The inner vial containing 1 ml of this chloroform solution was put in the outer beaker with about 20 ml of diethyl ether.

(3) This outer beaker was kept sealed for a few days at room temperature.

(4) The grown crystals were filtered out.

Crystallization procedure of (*RS*)-thalidomide with vapor diffusion technique from chloroform solution was as follows:

(1) (*RS*)-thalidomide powder (64.5 mg) was dissolved in 50 ml chloroform.

(2) The inner vial containing 50 ml of this chloroform solution was put in the outer beaker with about 80 ml of diethyl ether.

(3) This outer beaker was kept sealed for a few days at room temperature.

(4) The grown crystals were filtered out.

2.5 Polarizing microscope observation and thermal analysis

2.5.1 Experimental method

Habits of all crystals were observed with polarizing microscope. Furthermore, possibilities of polymorphs or solvates were investigated with TG-DTA. TG-DTA was conducted without grinding each crystal using Rigaku TG8120 with heating rate of 10.0 °C min^{-1}.

2.5.2 Crystals obtained with solvent evaporation technique from methanol-water solution

From the solution of (*S*)-thalidomide, needle shaped crystals (**I**) were obtained (Figure 2.7(A)). Similarly, from the solution of (*RS*)-thalidomide, needle shaped crystals (**II**) were obtained (Figure 2.7(B)). These results suggest that visually identifying the crystals of (*RS*)-thalidomide, which are generated by racemization of (*S*)-thalidomide, in the crystals obtained from solution of (*S*)-thalidomide will be impossible because the similar needle shaped crystals were obtained from solution of (*RS*)-thalidomide.

TG-DTA on 4.7 mg of **I** shows endothermic peaks around 240 °C and 270 °C (Figure 2.8(A)). The melting points of enantiomeric and racemic thalidomides are reported to be 241 °C and 271 °C, respectively [14]. According to this report, those two endothermic peaks indicates that **I** is mixture of (*S*)- and (*RS*)-thalidomides. TG-DTA on **I** also shows exothermic peak around 250 °C. This exothermic peak indicates possibility of polymorphic transformation of (*S*)-thalidomide because the weight is not increased. On the other hand, TG-DTA on 2.6 mg of **II** shows endothermic peaks around 270 °C (Figure 2.8(B)). This peak is reasonable because of consistency with known melting point of (*RS*)-thalidomide. TG-DTA on each of **I** and **II** shows the no weight reduction arising from solvent desorption. Therefore, both **I** and **II** are thought to be unsolvates.

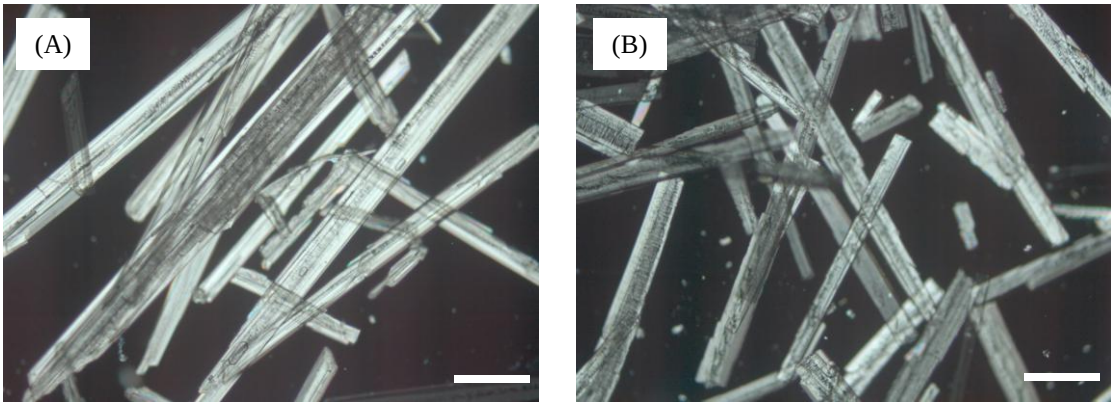

Figure 2.7 Polarizing microscopic images of needle shaped crystals of (A) (*S*)- and (B) (*RS*)-thalidomides crystallized with solvent evaporation technique from methanol water solutions. The scale bars represent 0.5 mm.

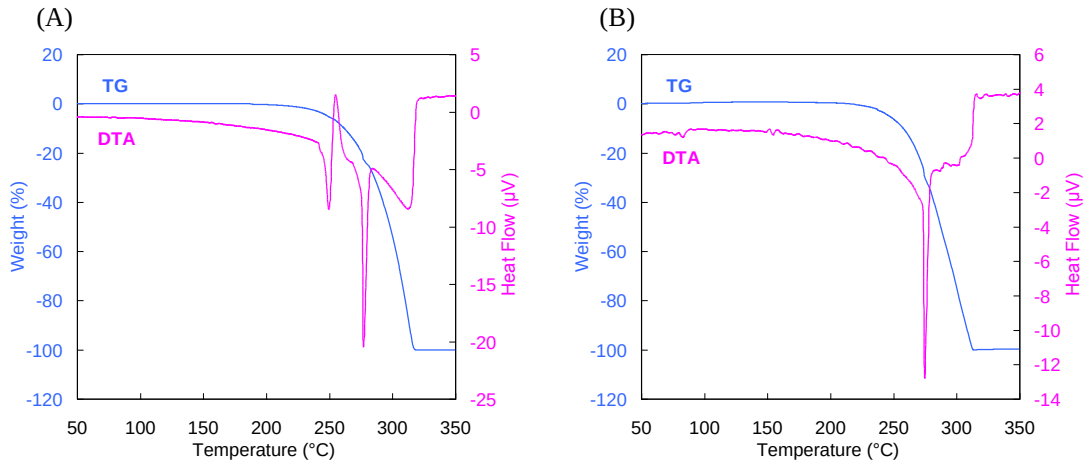

Figure 2.8 TG-DTA curves of (A) (*S*)-thalidomide crystals (**I**) and (B) (*RS*)-thalidomide crystals (**II**).

2.5.3 Crystals obtained with solvent evaporation technique from chloroform solution

From the solution of (*S*)-thalidomide, rod shaped crystals (**III**) were obtained (Figure 9(A)). Whereas, from the solution of (*RS*)-thalidomide, plate shaped crystals (**IV**) were obtained (Figure 9(B)). Comparing with the results of crystallization from methanol-water solution, crystal habits of both **III** and **IV** are different from those of **I** and **II**. This result suggests that those crystals are possibly polymorphs or solvates.

TG-DTA on 5.9 mg of **III** shows endothermic peak with weight reduction around 125 °C (Figure 2.10(A)). Therefore, **III** is thought to be solvates. In addition, no peaks around 270 °C support that racemization of thalidomide is not proceed in chloroform solution. TG-DTA on 2.2 mg of **IV** shows endothermic peaks around 270 °C (Figure 2.10(B)). This result on **IV** is almost similar to that on **II**. Therefore, **IV** may be isomorphic unsolvate with **II**, although those habits are significantly different.

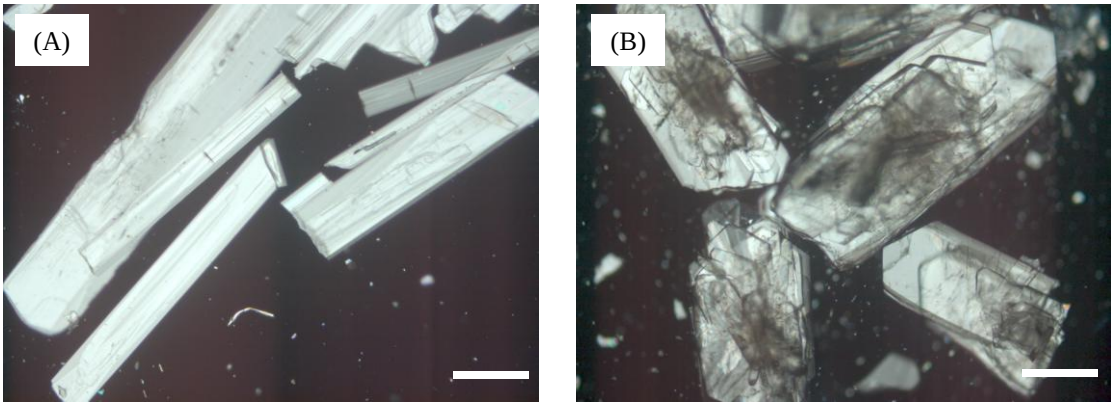

Figure 2.9 Polarizing microscopic images of (A) rod shaped crystals of (*S*)-thalidomide and (B) plate shaped crystals of (*RS*)-thalidomide crystallized with solvent evaporation technique from chloroform solutions. The scale bars represent 0.5 mm.

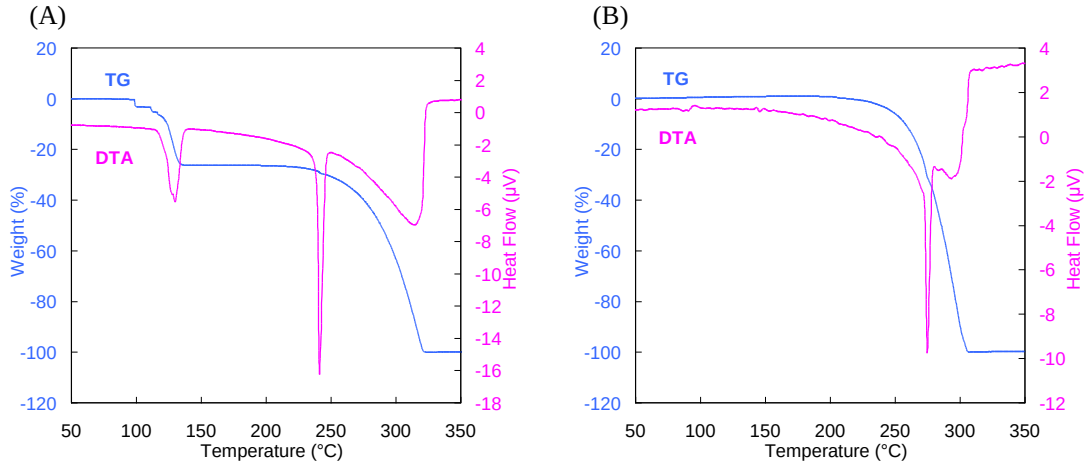

Figure 2.10 TG-DTA curves of (A) (*S*)-thalidomide crystals (**III)** and (B) (*RS*)-thalidomide crystals (**IV**).

2.5.4 Crystals obtained with vapor diffusion technique from chloroform solution

From the solution of (*S*)-thalidomide, rod shaped (**V**) and plate shaped (**VI**) crystals were concomitantly obtained (Figure 2.11(A)). These rod shaped crystals were almost similar to **III**. From the solution of (*RS*)-thalidomide, only plate shaped crystals (**VII**) were obtained (Figure 2.11(B)). These plate shaped crystals were almost similar to the plate shaped **VI**.

TG-DTA of **V** and **VI** were conducted on visually identified crystals from the mixture based on those different habits. Therefore, each of result may be negatively affected by the other. TG-DTA on 1.1 mg of **V** shows slightly noisy peaks because the amount of analyzed crystal was relatively small (Figure 2.12(A)). Similarly to **III**, the endothermic peak with weight reduction around 150 °C indicates that **V** is solvate. TG-DTA on 3.8 mg of **VI** shows marginal endothermic peaks with great weight reduction around 150 °C (Figure 2.12(B)). This weight reduction is too great to regard the cause as desorption of included solvent. Therefore, judging whether **VI** is solvate or unsolvate from this result is difficult. TG-DTA of **VII** was not conducted because the total amount of obtained crystals was not enough to appropriately conduct TG-DTA.

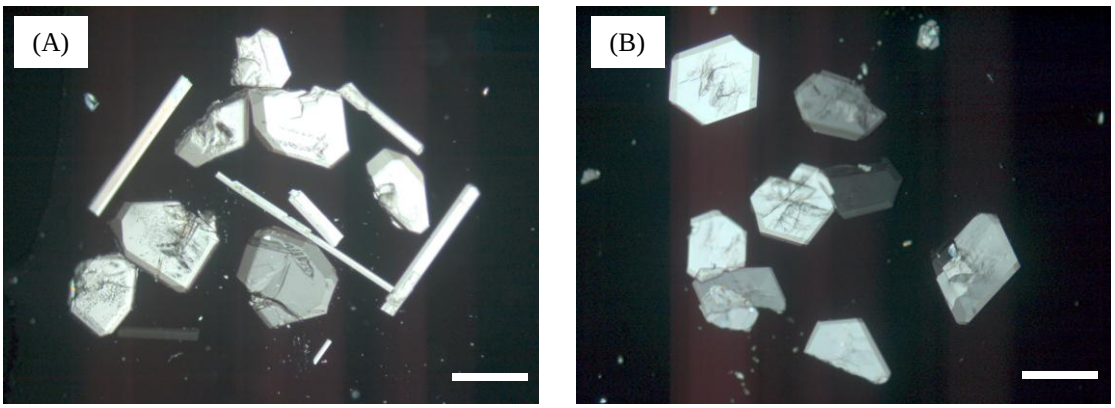

Figure 2.11 Polarizing microscopic images of (A) rod and plate shaped crystals of (*S*)-thalidomide and (B) plate shaped crystal of (*RS*)-thalidomide crystallized with vapor diffusion technique from chloroform solutions. The scale bars represent 0.5 mm.

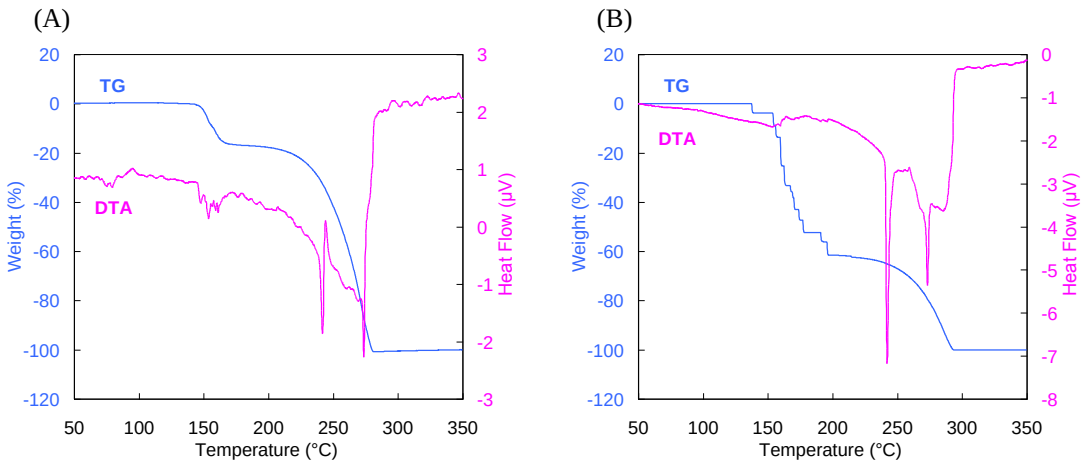

Figure 2.12 TG-DTA curves of (A) rod shaped (*S*)-thalidomide crystals (**V)** and (B) plate shaped (*S*)-thalidomide crystals (**VI**).

2.6 Conclusion

In this chapter, this study evaluates methods for crystallization of thalidomide. Considering possibilities of multiple forms, *i.e.* polymorphs or solvates, three different methods were determined in terms of selection of solvent and technique for crystallization. Undesirable chiral inversion in protic methanol-water solution and stability to chiral inversion in aprotic and nonpolar solutions were estimated with CD spectrometry. As summarized in Table 2.1, crystallizations with three different methods produced crystals with different habits. These results suggest that visually identifying the crystals of (*RS*)-thalidomide, which are generated by racemization of (*S*)-thalidomide, in the crystals obtained from solution of (*S*)-thalidomide will be impossible because the similar needle shaped crystals were obtained from solutions of both (*S*)- and (*RS*)-thalidomide. The results of TG-DTA suggested that **I**, **II**, and **IV** should be unsolvate and **III** and **V** should be solvate. On the basis of these results, all crystal structures of (*S*)- and (*RS*)-thalidomides are investigated in chapter 3 and 4, respectively.

As future works, possibility of polymorphic transformation of (*S*)-thalidomide, which is indicated by exothermic peak without weight increase around 250 °C in TG-DTA on **I**, and the cause of the excess weight reduction around 150 °C in TG-DTA on **VI**, should be investigated.

Table 2.1 Comparison of crystal habits between (*S*)- and (*RS*)-thalidomide crystals obtained with three different methods.

Solvent	Technique	Solute	
		(*S*)-thalidomide	(*RS*)-thalidomide
methanol-water	solvent evaporation	needle (**I**)	needle (**II**)
chloroform	solvent evaporation	rod (**III**)	plate (**IV**)
chloroform-diethyl ether	vapor diffusion	rod (**V**) / plate (**VI**)	plate (**VII**)

2.7 References

[1] D. Braga, F. Grepioni, and L. Maini, "The growing world of crystal forms", *Chem. Commun.*, 46 (2010), pp. 6232-6242, DOI: 10.1039/c0cc01195a.

[2] D. Braga, F. Grepioni, L. Maini, and M. Polito, "Crystal Polymorphism and Multiple Crystal Forms", *Struct. Bond.*, 132 (2009), pp. 25-50, DOI: 10.1007/430_2008_7.

[3] A. Llinas and J. M. Goodman, "Polymorph control: past, present and future", *Drug Discov. Today,* 13 (2008), pp. 198-210, DOI: 10.1016/j.drudis.2007.11.006.

[4] C. B. Aakeröy, N. R. Champness, and C. Janiak, "Recent advances in crystal engineering", *CrystEngComm,* 12 (2010), pp. 22-43, DOI: 10.1039/b919819a.

[5] I. Miroshnyk, S. Mirza, and N. Sandler, "Pharmaceutical co-crystals–an opportunity for drug product enhancement", *Expert. Opin. Drug. Del.,* 6 (2009), pp. 333-341, DOI: 10.1517/17425240902828304.

[6] A. V. Trask, "An Overview of Pharmaceutical Cocrystals as Intellectual Property", *Mol. Pharmaceutics,* 4 (2007), pp. 301-309, DOI: 10.1021/mp070001z.

[7] T. Friščić and W. Jones, "Recent Advances in Understanding the Mechanism of Cocrystal Formation via Grinding", *Cryst. Growth. Des.,* 9 (2009), pp. 1621-1637, DOI: 10.1021/cg800764n.

[8] D. Braga, L. Brammer, and N. R. Champness, "New trends in crystal engineering", *CrystEngComm,* 7 (2005), pp. 1-19, DOI: 10.1039/b417413e.

[9] F. H. Allen and J. Trotter, "Crystal and molecular structure of thalidomide, N-(α-glutarimido)-phthalimide", *J. Chem. Soc. B,* (1971), pp. 1073-1079, DOI: 10.1039/j29710001073.

[10] J. C. Reepmeyer, M. O. Rhodes, D. C. Cox, and J. V. Silverton, "Characterization and crystal structure of two polymorphic forms of racemic thalidomide", *J. Chem. Soc., Perkin Trans. 2,* (1994), pp. 2063-2067, DOI: 10.1039/p29940002063.

[11] C. Goosen, L. Timothy J., P. Jeanetta du, G. Theunis C., and F. Gordon L., "Physicochemical Characterization and Solubility Analysis of Thalidomide and Its N-Alkyl Analogs", *Pharm.Res.,* 19 (2002), pp. 13-19, DOI: 10.1023/A:1013643013244.

[12] G. Schoetz, O. Trapp, and V. Schurig, "Determination of the enantiomerization barrier of thalidomide by dynamic capillary electrokinetic chromatography", *Electrophoresis,* 22 (2001), pp. 3185-3190, DOI: 10.1002/1522-2683(200109).

[13] H. Izumi, S. Futamura, N. Tokita, and Y. Hamada, "Fliplike Motion in the Thalidomide Dimer: Conformational Analysis of (R)-Thalidomide Using Vibrational Circular Dichroism Spectroscopy", *J. Org. Chem.*, 72 (2007), pp. 277-279, DOI: 10.1021/jo061612q.

[14] S. Fabro, R. L. Smith, and R. T. Williams, "Toxicity and Teratogenicity of Optical Isomers of Thalidomide", *Nature*, 215 (1967), 296, DOI: 10.1038/215296a0

3. Determination of crystal structure and absolute configuration of (*S*)-thalidomide

3.1 Introduction

Crystal structures are fundamental knowledge of substances. Determinations of crystal structures provide detail information of component molecules, such as those conformations and relative position to another molecule. Physicochemical properties such as solubility and melting point are directly related with the structural stability of the crystal. In the case of chiral compounds, crystal structures of enantiomeric and racemic compounds are essentially different: enantiomeric crystals consist of either enantiomer, and racemic crystals consist of both enantiomeric isomers. Therefore, knowledge about structures of not only racemic crystal but also the enantiomeric crystal is significant for understanding the physicochemical properties of chiral compounds. Crystal structures of racemic thalidomide have been investigated since 1971 [1]. However, crystal structures of enantiomeric thalidomide have not been reported.

To determine crystal structure and absolute configuration of enantiomeric thalidomide, this study attempted to crystallize (*S*)-thalidomide. Considering chiral inversion of (*S*)-thalidomide and possibility for multiple forms, three different crystallization methods were attempted. All crystal structures were investigated with single crystal X-ray diffractometry.

3.2 Crystallization of (*S*)-thalidomide

3.2.1 Materials

(*S*)-thalidomides was purchased from Sigma-Aldrich, Inc. Methanol, chloroform, diethyl ether, and acetonitrile were purchased from Wako Pure Chemical Industries, Ltd.

3.2.2 Experimental method

On the basis of the evaluation in chapter 2, (*S*)-thalidomide crystals were obtained with following three different crystallization methods:

- solvent evaporation technique from methanol-water solution;
- solvent evaporation technique from chloroform solution;
- vapor diffusion technique from chloroform solution.

Detail procedures of crystallization are as follows.

Crystallization procedure of (*S*)-thalidomide with solvent evaporation technique from methanol-water solution was as follows:

(1) (*S*)-thalidomide powder (50 mg) was dissolved in 40 ml methanol-water (5:3).

(2) The solution was evaporated for about 4 h at 50 °C.

(3) The grown crystals floating on the solutions were filtered out.

Crystallization procedure of (*S*)-thalidomide with solvent evaporation technique from chloroform solution was as follows:

(1) (*S*)-thalidomide powder (77.3 mg) was dissolved in 14 ml chloroform.

(2) The solution was evaporated in a few days at room temperature.

(3) The grown crystals floating on the solutions were filtered out.

Crystallization procedure of (*S*)-thalidomide with vapor diffusion technique from chloroform solution was as follows:

(1) (*S*)-thalidomide powder (7.0 mg) was dissolved in 1 ml chloroform.

(2) The inner vial containing 1 ml of this chloroform solution was put in the outer beaker with about 20 ml of diethyl ether.

(3) This outer beaker was kept sealed for a few days at room temperature.

(4) The grown crystals were filtered out.

3.2.3 Results

Crystallization with solvent evaporation technique from methanol-water solution of (*S*)-thalidomide produced needle shaped crystals (**I**) (Figure 3.1(A)). To avoid excess chiral inversion, (*S*)-thalidomide was crystallized in about 4 hours at temperatures around 50 °C. In this case, (*RS*)-thalidomide crystals arising from the chiral inversion of (*S*)-thalidomide should be mixed with the crystals of (*S*)-thalidomide. However,

visually identifying the crystals of (*RS*)-thalidomide is impossible due to those almost same shapes. Therefore, (*S*)-thalidomide crystals were identified with repeated trials.

Crystallization with solvent evaporation technique from chloroform solution of (*S*)-thalidomide produced rod shaped crystals (**III**) (Figure 3.1(B)).Crystallization with vapor diffusion technique from chloroform solution of (*S*)-thalidomide concomitantly produced rod shaped (**V**) and plate shaped (**VI**) crystals (Figure 3.1(C)). As demonstrated in chapter 2, chloroform and diethyl ether solutions of enantiomeric thalidomide are free from chiral inversion. Therefore, crystals obtained from chloroform solutions were regarded without special attention to the chiral inversion.

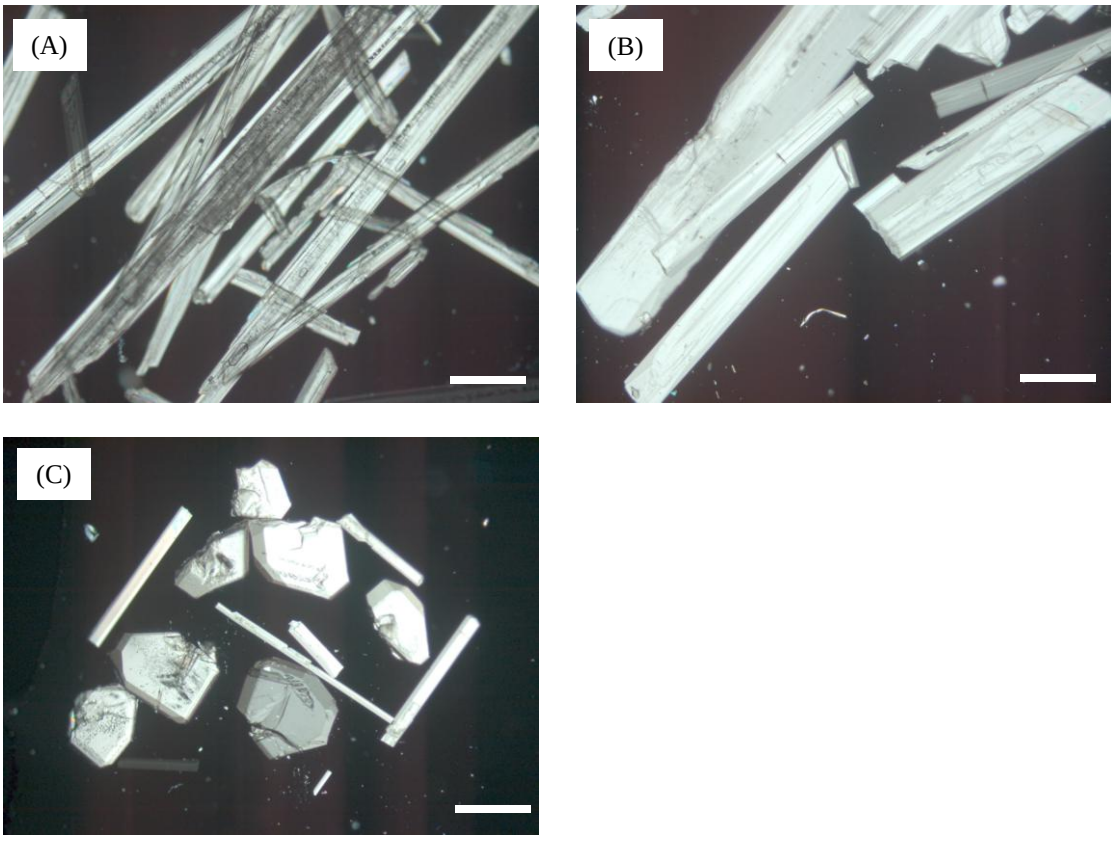

Figure 3.1 Polarizing microscopic images of (*S*)-thalidomide crystals obtained with (A) solvent evaporation technique from methanol-water solution (B) solvent evaporation technique from chloroform solution (C) vapor diffusion technique from chloroform solution. The scale bars represent 0.5 mm.

3.3 X-ray diffractometry on (*S*)-thalidomide crystals

3.3.1 Experimental method

Some points should be paid attention in selection of crystals for X-ray diffractometry. To minimize directional dependency in measurement, shape of the crystal is preferably similar to sphere. The least cracks on the crystal are desired due to its negative influence on diffraction. Moreover, particularly for film shaped crystal, possible existence of twined crystals, which appeared an isolated single crystal but is actually piled units of some single crystals with slight misalignments, should be cared. In this case, carefully observing extinction of transmitted light from crystal using polarizing microscope is important. Considering these points, crystals for X-ray diffractometry were selected.

X-ray diffraction data for all crystals (**I**, **III**, **V**, and **VI**) were collected using a Rigaku RAXIS RAPID imaging plate detector with graphite monochromated Cu-Kα radiation. Crystal structures were solved by direct methods and refined by full-matrix least-squares on F^2 [2]. Non-hydrogen atoms were refined with anisotropic displacement parameters, except for isotropically refined solvent molecules. Hydrogen atoms were refined using the riding model. Absolute configurations were determined based on Flack parameters.

3.3.2 Summary of results

As a result of single crystal X-ray diffractometry, **I** and **VI** are revealed to be unsolvate of (*S*)-thalidomide. **VI** is determined as the isomorphic form with **I**. On the other hand, **III** and **V** are revealed to be solvate of (*S*)-thalidomide. Crystal and structure refinement data are summarized in Table 3.1. Detail crystal structures of unsolvated and solvated (*S*)-thalidomide are discussed in Section 3.3.3 and Section 3.3.4, respectively.

R_{int} is the degree of agreement on equivalent reflections. R_1 and wR_2 are the unweighted and weighted degrees of agreement on structure factors based on calculated and observed reflections, respectively. Max Shift/Error is the indicator of convergence in the structure refinement, and is favorable to be almost equal to 0.

Goodness of fit represents the suitability of weighting, and is favorable to be almost equal to 1. Flack parameter is the indicator of absolute configuration. This parameter being almost equal to 0 means the absolute configuration is true.

To crystallographically determine the crystal structure, the result of single crystal X-ray diffractometry needs to fulfill the following requirements:

$R_{int} < 0.1$

$R_1 \leqq 0.1$

$wR_2 < 0.25$

$-0.01 <$ Max Shift/Error < 0.01

$0.8 \leqq$ Goodness of fit $\leqq 2.0$

According to these requirements, the crystal structure of **III** is crystallographically undetermined. Nevertheless, **III** is concluded to be chloroform solvate of (*S*)-thalidomide based on result of TG-DTA and comparison with **V** as described in section 3.3.3.

Table 3.1 Crystal and structure refinement data. The data for **III** is the final result of incomplete refinement, and the ratio of chloroform is assumed.

	I	**III**	**V**	**VI**
Empirical formula	$C_{13}H_{10}O_4N_2$	$C_{13.25}H_{10.25}N_2O_4Cl_{0.75}$	$C_{14.25}H_{12.75}Cl_{0.75}N_2O_{4.25}$	$C_{13}H_{10}O_4N_2$
M (g mol^{-1})	258.23	288.08	306.61	258.23
Temperature (K)	93(1)	223(1)	153(1)	263(1)
Crystal system	monoclinic	orthorhombic	orthorhombic	monoclinic
Space group	$P2_1$	$P2_12_12$	$P2_12_12$	$P2_1$
a (Å)	8.40187 (15)	13.4826(2)	13.2889(2)	8.3513(4)
b (Å)	10.02372 (18)	31.1367(5)	30.502(2)	10.1578(5)
c (Å)	14.4814 (7)	7.05915(10)	7.05698(10)	14.7613(7)
β (°)	103.4938 (8)	-	-	103.590(3)
V (Å^3)	1185.93 (7)	2963.46(8)	2860.5(2)	1217.16(10)
Z	4	8	8	4
D (g cm^{-3})	1.446	1.291	1.424	1.409
Reflection total/unique	13965/3822	32785/5331	33446/5162	12696/4236
R_{int}	0.025	0.136	0.033	0.063
R_1 [$I > 2\sigma(I)$]	0.0328	0.1223	0.0748	0.0392
wR_2 (all data)	0.0844	0.3558	0.2243	0.1084
Max Shift/Error	0.000	0.202	0.000	0.004
Goodness of fit	1.094	1.553	1.051	0.938
Flack Parameter	0.05(18)	0.10(11)	0.09(6)	0.0(2)

3.3.3 Crystal structures of unsolvated (*S*)-thalidomide

Both **I** and **VI** are revealed to be unsolvate of (*S*)-thalidomide. Although **VI** is determined as the isomorphic form with **I**, the result of structural refinement on **I** is better than that on **VI**. Therefore, this study focuses on **I** as the crystal structure of unsolvated (*S*)-thalidomide.

The crystal structure of unsolvated (*S*)-thalidomide is revealed to be formed with two conformational isomers, *i.e.* two (*S*)-thalidomide molecules with different conformation. To distinguish these two conformational isomers, they are hereafter designated as **S1** and **S2**, respectively. The unit-cell structure is shown in Figure 3.2. The packing structures are shown in Figure 3.3.

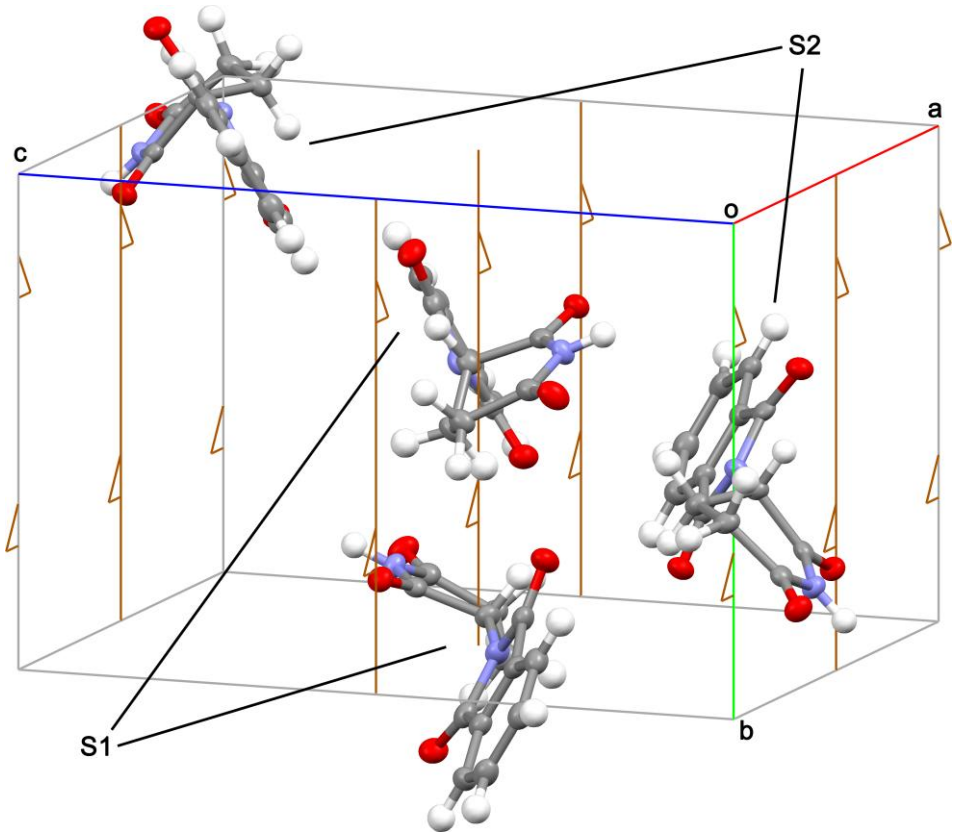

Figure 3.2 The unit-cell structure of (*S*)-thalidomide crystal drawn with thermal ellipsoids at 50% probability level. Brown axes represent 2-fold screw axes. Color code: C: gray, N: blue, O: red, H: white.

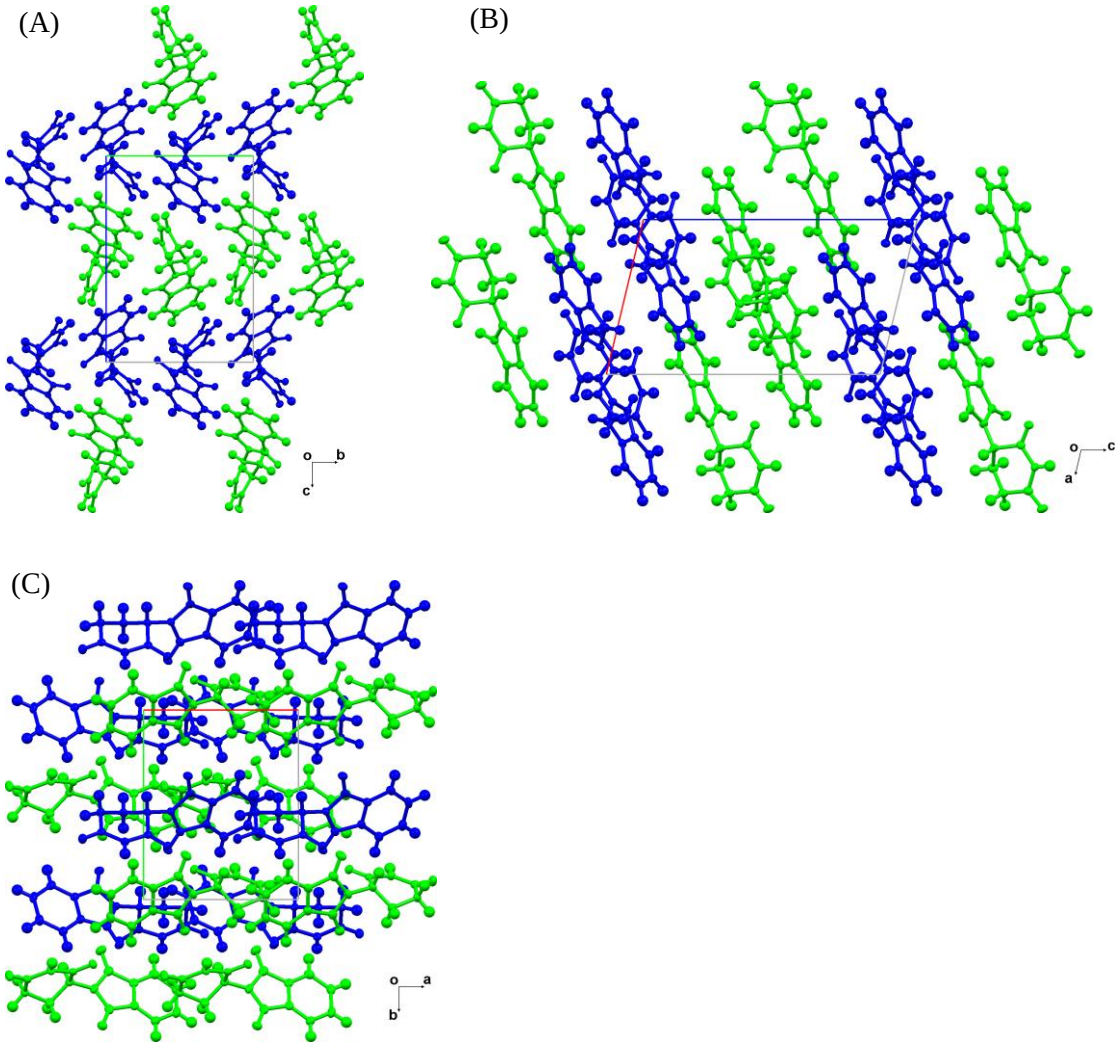

Figure 3.3 Packing structures of unsolvated (*S*)-thalidomide crystal drawn with thermal ellipsoids at 50% probability level: (A) along *a* axis, (B) along *b* axis, (C) along *c* axis. **S1** and **S2** are colored by symmetry equivalence as green and blue, respectively.

A thalidomide molecule consists of phthalimide ring (C1-C8, N1, O1, O2) and glutarimide ring (C9-C13, N2, O3, O4). The differences in corresponding bond length between **S1** and **S2** are tested with the following *t* value:

$$t = \frac{\left|\mathrm{L_{S1}} - \mathrm{L_{S2}}\right|}{\sqrt{\sigma^2(\mathrm{L_{S1}}) + \sigma^2(\mathrm{L_{S2}})}} \tag{3.1}$$

where

$t < 2$: the difference is not significant,

$2 \le t < 2.5$: the difference is probably significant,

$2.5 \le t$: the difference is significant.

Here $\mathrm{L_{S1}}$ and $\mathrm{L_{S2}}$ represent the length of particular bond in **S1** and **S2**, respectively. In addition, the differences in corresponding bond angle between **S1** and **S2** are analogically evaluated of the based above test. The all bond lengths are listed in Table 3.2. The bond angles of phthalimide and glutarimide rings are listed in Table 3.3 and Table 3.4, respectively.

As indicated in Figure 3.4, significant differences in corresponding bond length between **S1** and **S2** limitedly exist at N1-C8 and C6-C7 bonds in the phthalimide ring, and N2-C10 and C9-C13 bonds in the glutarimide ring. The differences in each of the corresponding bond lengths between **S1** and **S2** are 0.011(4) Å for N1-C8, 0.013(4) Å for C6-C7, 0.011(3) Å for N2-C10, and 0.010(4) Å for C9-C13, respectively, where values in the parentheses represent standard deviations. Such crystal structure formed with two conformational isomers is not unique for (*S*)-thalidomide but also shown in other compounds (*e.g.* L-leucine [3], L-valine [4, 5], L-cysteine [6]).

Table 3.2 The list of bond lengths in **S1** and **S2**. The values in the parentheses represent standard deviations. The *t* values over 2 are colored in orange.

Bond	L_{S1} / Å	L_{S2} / Å	$\|L_{S1}-L_{S2}\|$ / Å	*t*
O1-C1	1.205(2)	1.205(2)	0.000(3)	0.00
O2-C8	1.218(3)	1.214(2)	0.004(4)	1.11
N1-C1	1.413(3)	1.409(2)	0.004(4)	1.11
N1-C8	1.400(2)	1.411(3)	0.011(4)	3.05
C1-C2	1.492(2)	1.494(2)	0.002(3)	0.71
C2-C3	1.379(3)	1.371(3)	0.008(4)	1.89
C2-C7	1.385(3)	1.386(3)	0.001(4)	0.24
C3-C4	1.392(3)	1.398(3)	0.006(4)	1.41
C4-C5	1.395(3)	1.393(3)	0.002(4)	0.47
C5-C6	1.393(3)	1.393(3)	0.000(4)	0.00
C6-C7	1.380(3)	1.393(3)	0.013(4)	3.06
C7-C8	1.480(3)	1.482(2)	0.002(4)	0.55
N1-C9	1.453(2)	1.450(2)	0.003(3)	1.06
O3-C10	1.210(2)	1.213(2)	0.003(3)	1.06
O4-C11	1.223(2)	1.223(2)	0.000(3)	0.00
N2-C10	1.379(2)	1.390(2)	0.011(3)	3.89
N2-C11	1.382(3)	1.377(2)	0.005(4)	1.39
C9-C10	1.521(3)	1.514(3)	0.007(4)	1.65
C9-C13	1.518(3)	1.528(3)	0.010(4)	2.36
C11-C12	1.501(3)	1.502(3)	0.001(4)	0.24
C12-C13	1.524(3)	1.522(2)	0.002(4)	0.55

Table 3.3 The list of bond angles of phthalimide rings in **S1** and **S2**. A_{S1} and A_{S2} represent the angle of particular bond in **S1** and **S2**, respectively. The values in the parentheses represent standard deviations. The *t* values over 2 are colored in orange.

Bond	A_{S1} / deg	A_{S2} / deg	$\lvert A_{S1}-A_{S2}\rvert$ / deg	*t*
C1-N1-C8	111.26(17)	111.66(16)	0.40(23)	1.71
C1-N1-C9	125.14(18)	123.98(18)	1.16(25)	4.56
C8-N1-C9	121.0(2)	122.09(18)	1.09(27)	4.05
O1-C1-N1	125.2(2)	124.17(18)	1.03(27)	3.83
O1-C1-C2	129.5(2)	130.2(2)	0.7(3)	2.47
N1-C1-C2	105.35(19)	105.64(19)	0.29(27)	1.08
C1-C2-C3	130.0(2)	130.7(2)	0.7(3)	2.47
C1-C2-C7	108.2(2)	107.77(18)	0.43(27)	1.60
C3-C2-C7	121.82(19)	121.5(2)	0.32(28)	1.16
C2-C3-C4	116.7(2)	117.4(2)	0.7(3)	2.47
C3-C4-C5	121.7(2)	121.4(2)	0.3(3)	1.06
C4-C5-C6	120.8(2)	120.9(2)	0.1(3)	0.35
C5-C6-C7	117.1(2)	116.9(2)	0.2(3)	0.71
C2-C7-C6	121.8(2)	121.9(2)	0.1(3)	0.35
C2-C7-C8	108.55(18)	109.33(19)	0.78(26)	2.98
C6-C7-C8	129.6(2)	128.8(2)	0.8(3)	2.83
O2-C8-N1	124.13(19)	105.20(19)	0.41(26)	1.57
O2-C8-C7	129.8(2)	130.3(2)	0.5(3)	1.77
N1-C8-C7	106.0(2)	124.54(18)	0.8(28)	2.90

Table 3.4 The list of bond angles of glutarimide rings in **S1** and **S2**. A_{S1} and A_{S2} represent the angle of particular bond in **S1** and **S2**, respectively. The values in the parentheses represent standard deviations. The *t* values over 2 are colored in orange.

Bond	A_{S1} / deg	A_{S2} / deg	$\lvert A_{S1}-A_{S2} \rvert$ / deg	*t*
N1-C9-C10	109.57(19)	108.92(18)	0.65(26)	2.48
N1-C9-C13	115.0(2)	114.35(18)	0.65(27)	2.42
C10-C9-C13	111.46(18)	111.00(19)	0.46(26)	1.76
O3-C10-N2	121.8(2)	120.5(2)	1.3(3)	4.60
O3-C10-C9	122.80(18)	124.15(18)	1.35(25)	5.30
N2-C10-C9	115.30(19)	115.32(19)	0.02(27)	0.07
C10-N2-C11	127.2(2)	126.59(19)	0.61(28)	2.21
O4-C11-N2	119.5(2)	119.6(2)	0.1(3)	0.35
O4-C11-C12	123.3(2)	122.7(2)	0.6(3)	2.12
N2-C11-C12	117.22(18)	117.65(17)	0.43(25)	1.74
C11-C12-C13	113.9(2)	113.9(2)	0.0(3)	0.00
C9-C13-C12	108.9(2)	108.52(19)	0.38(28)	1.38

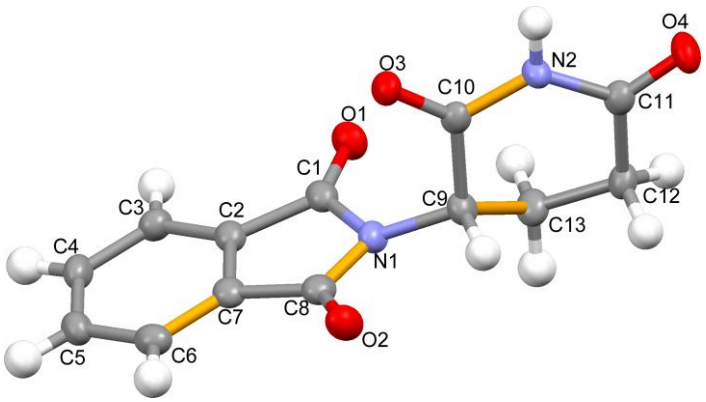

Figure 3.4 The conformation of **S1** drawn with thermal ellipsoids at 50% probability level. Bonds, of which lengths are significantly different between **S1** and **S2**, are represented in orange. Color code: C: gray, N: blue, O: red, H: white.

Furthermore, dimer formation by pairs of **S1** and **S2** molecules with hydrogen-bonded rings at each of the glutarimide rings is also revealed (Figure 3.5). Generally, hydrogen bond forming between atoms of X and A as X—H···A is judged by the distance between X and A is less than the sum of those Van der Waals radii. The strength of hydrogen bond is classified as Table 3.5. Nevertheless, the hydrogen-bonded ring in dimers formed by pairs of **S1** and **S2** molecules is unable to directly apply to this classification due to the hydrogen-bonded ring consisting of two hydrogen bonds. As shown in Figure 3.6, **S1** and **S2** form the dimers with each of the corresponding **S2** and **S1** in the adjacent unit cell. The lengths of these two intermolecular hydrogen-bonds are not significantly different: 2.912(3) Å for N2-O4' and 2.910(3) Å for O4-N2', respectively (the primed numbers represent atoms of **S2**). Similar hydrogen-bonded rings are often formed with such as amide units with dual capacity of donor and acceptor. A number of reports investigated in detail or systematically analyzed those hydrogen-bonded rings [7, 8].

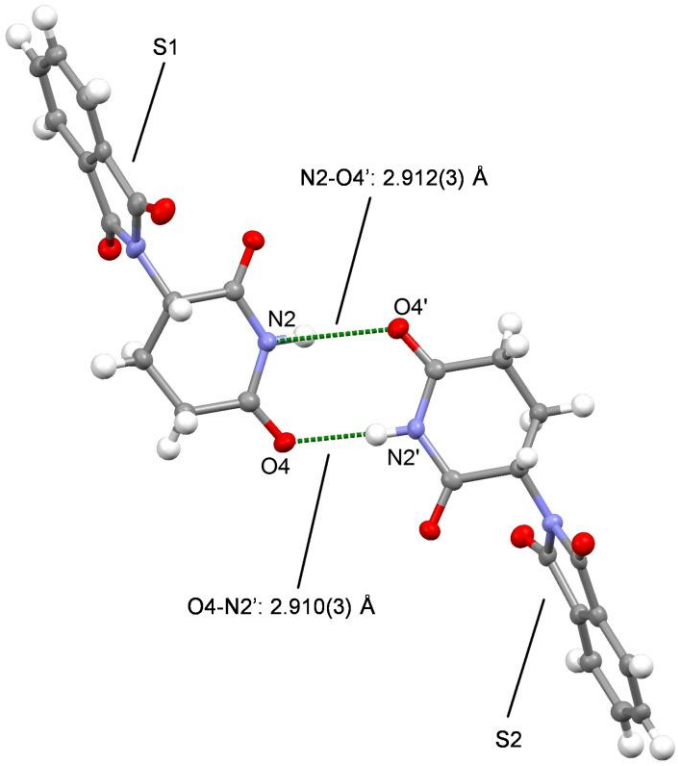

Figure 3.5 The dimer formation in (S)-thalidomide crystal drawn with thermal ellipsoids at 50% probability level. Green broken lines represent hydrogen bonds. Color code: C: gray, N: blue, O: red, H: white.

Table 3.5 The classification of strong, moderate, and weak hydrogen bonds.

	Strong	Moderate	Weak
interaction type	strongly covalent	mostly electrostatic	electrostatic / dispersion
H···A [Å]	1.2-1.5	1.5-2.2	>2.2
X—A [Å]	2.2-2.5	2.5-3.2	>3.2
X—H versus H···A	X—H≒H···A	X—H < H···A	X—H << H···A
lengthening of X—H [Å]	0.08-0.25	0.02-0.08	<0.02
directionality	strong	moderate	weak
bond angles [deg]	170-180	>130	>90

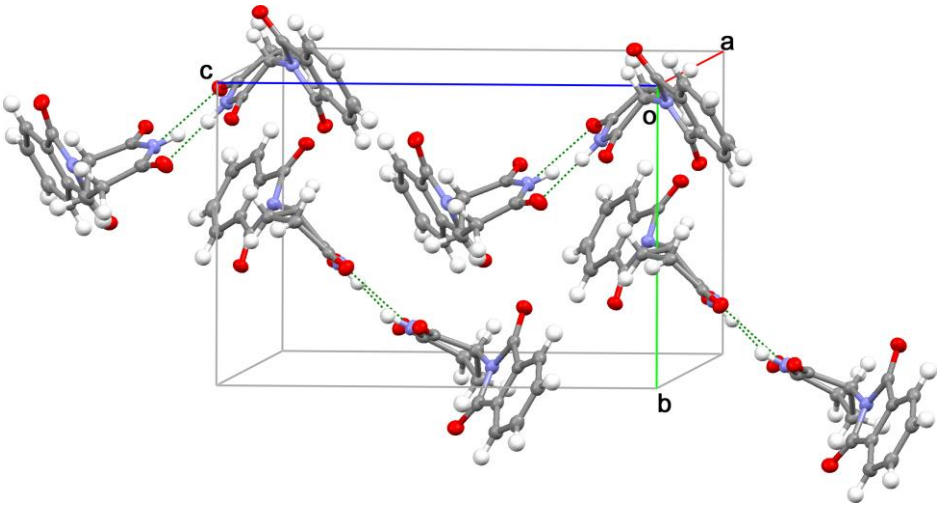

Figure 3.6 The packing structure and dimer formations by hydrogen-bonded rings.

In addition, (*R*)-thalidomide molecules in chloroform solution are suggested to exist in dynamic equilibrium of three isomeric dimers which differ in the hydrogen bonded ring moieties (Figure 3.7) [9]. Moreover, density functional theory calculation demonstrated that the most populated dimer is the lowest energy one (Table 3.6). The two hydrogen bonding moieties of dimers in (*S*)-thalidomide unsolvated crystal are the same as those of the most populated dimer of (*R*)-thalidomide in chloroform solution.

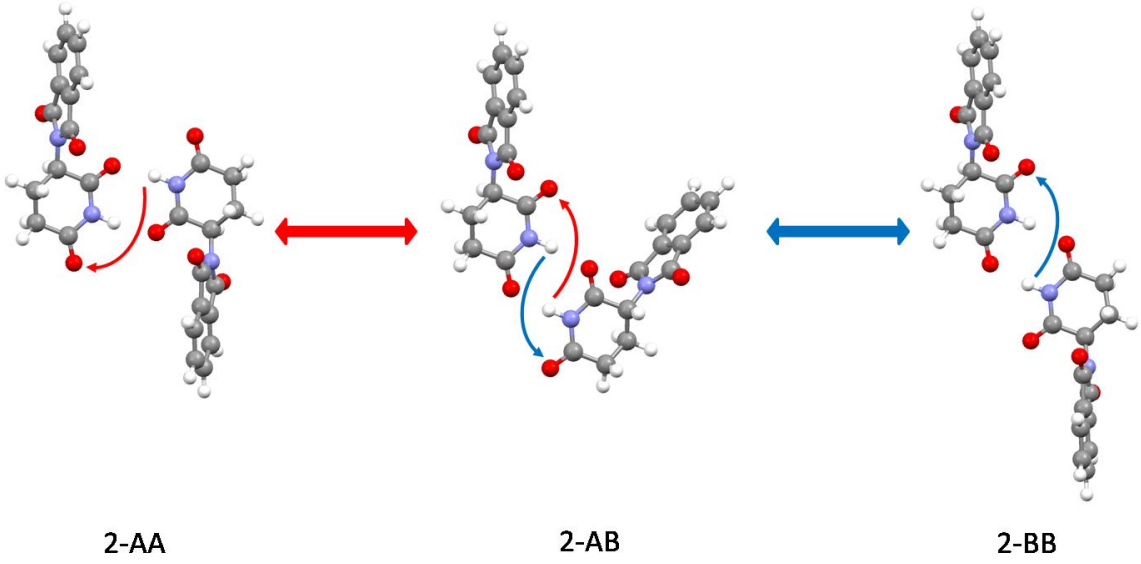

Figure 3.7 Dynamic equilibrium of three isomeric (*R*)-thalidomide dimers in chloroform solution [9]. Color code: C: gray, N: blue, O: red, H: white.

Table 3.6 Calculated Electronic energies (B3LYP/6-31G*) and populations of each dimers [9].

Dimer	Electronic energy [kcal/mol]	Population
2-AA	-1144431.463	0.235970024
2-AB	-1144431.613	0.335168207
2-BB	-1144431.674	0.428861769

3.3.4 Crystal structures of solvated (*S*)-thalidomide

As a result of single crystal X-ray diffractometry, both **III** and **V** are revealed to be solvate of (*S*)-thalidomide.

On one hand, the rod shaped **III** is concluded to be chloroform solvate of (*S*)-thalidomide. Although structure refinement is incomplete due to disordered chloroform molecules, the clathrate structure of host lattice formed with (*S*)-thalidomide molecules is almost determined (Figure 3.8). The final result of incomplete refinement is shown in Table 3.7. Disordered chloroform molecules appear to be confined into the channel spaces. The inclusion of chloroform molecules is also demonstrated in TG-DTA by the weight reduction at temperatures around 125 °C (Figure 3.9).

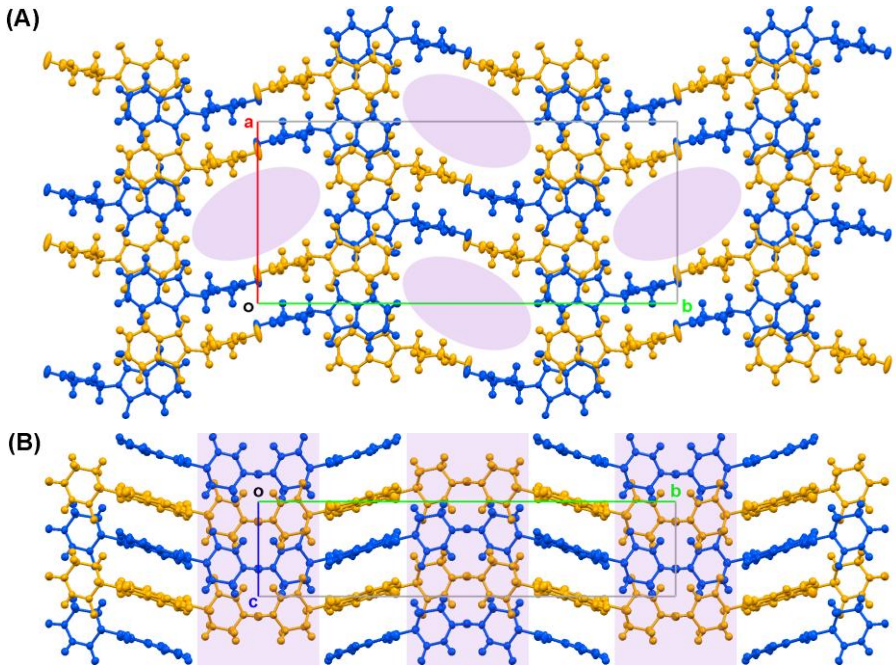

Figure 3.8 Packing arrangements of incompletely refined **III** colored by symmetry equivalence: (A) along *c* axis and (B) along *a* axis. Purple domains represent channel spaces where disordered chloroform molecules confined.

Table 3.7 The crystal data for **III**. The values are the final result of incomplete refinement, and the ratio of chloroform is assumed.

	III
Empirical formula	$C_{13.25}H_{10.25}N_2O_4Cl_{0.75}$
M (g mol^{-1})	288.08
Temperature (K)	223(1)
Crystal system	orthorhombic
Space group	$P2_12_12$
a (Å)	13.4826(2)
b (Å)	31.1367(5)
c (Å)	7.05915(10)
V (Å^3)	2963.46(8)
Z	8
D (g cm^{-3})	1.291

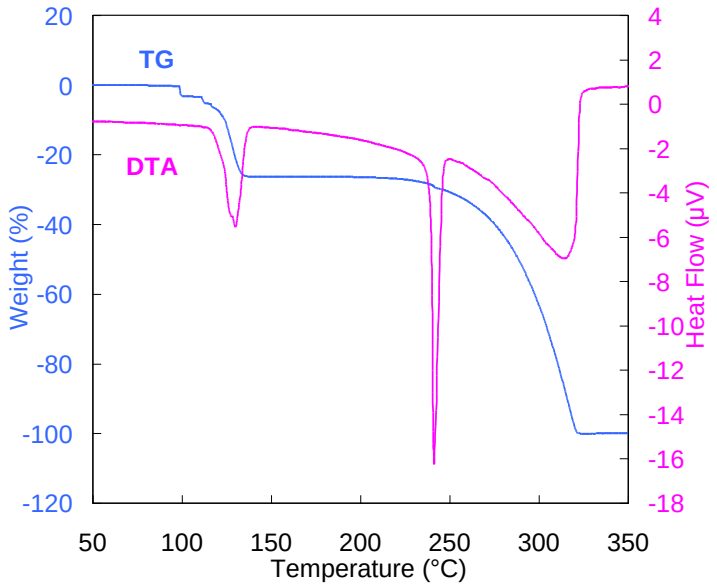

Figure 3.9 TG-DTA curves of **III**.

On the other hand, **V** is determined as chloroform and diethyl ether solvate of (*S*)-thalidomide. The composition ratio of **V** is (*S*)-thalidomide:chloroform:diethyl ether = 1:0.25:0.25. The packing arrangement of (*S*)-thalidomide molecules in **V** is determined as quite similar clathrate structure with **III** (Figure 3.10). This result indicates the crystallographically undetermined structure of **III** is almost isomorphic with the crystal structure of **V**. Disordered chloroform and diethyl ether molecules are confined into the channel spaces. According to the statistical study on the Cambridge Structural Database, each of chloroform and diethyl ether tends to form not only solvates but also heterosolvates, *i.e.* co-existing of two different solvent molecules in crystal. [10] Considering this tendency, the heterosolvate formation with chloroform and diethyl ether in **V** appear to be reasonable.

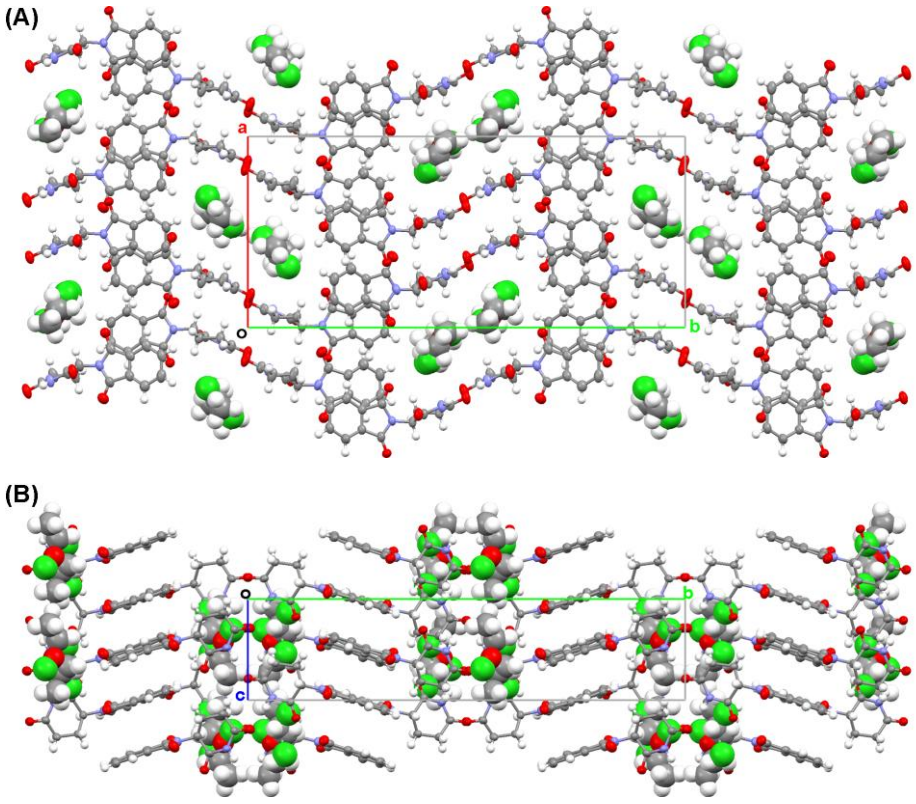

Figure 3.10 Packing arrangements of **V** drawn with thermal ellipsoids at 50% probability level: (A) along *c* axis and (B) along *a* axis. Disordered chloroform and diethyl ether molecules are overlaid with space filling model as 100% occupancy. Color code: C: gray, N: blue, O: red, H: white, Cl: green.

The crystal data for **V** is shown in Table 3.8. Both this non-stoichiometric inclusion of solvent molecules and the similarity between clathrate structures of **III** and **V** imply the capability for replacing solvent molecules at channel spaces with maintaining the host lattice of (*S*)-thalidomide, as demonstrated on a drug substance of FK041 [11, 12].

The crystal structure of **V** is revealed to be also formed with two conformational isomers, similarly to the unsolvated (*S*)-thalidomide crystals. To distinguish these two conformational isomers, they are designated as **S'1** and **S'2**, respectively. The unit-cell structure of **V** is shown in Figure 3.11. The all bond lengths are listed in Table 3.9. The bond angles of phthalimide and glutarimide rings are listed in Table 3.10 and Table 3.11, respectively. Significant differences in corresponding bond length between **S'1** and **S'2** exist at N1-C8 and C5-C6 bonds in the phthalimide ring, C9-C10 and C10-O3 bonds in the glutarimide ring, and N1-C9 bond of the connector for both rings (Figure 3.12). The differences in each of the corresponding bond lengths between **S'1** and **S'2** are 0.03(7) Å for N1-C8, 0.018(8) Å for C5-C6, 0.019(7) Å for C9-C10, 0.029(7) Å for C10-O3, and 0.018(6) Å for N1-C9, respectively.

Table 3.8 The crystal data for **V**.

	V
Empirical formula	$C_{14.25}H_{12.75}Cl_{0.75}N_2O_{4.25}$
M (g mol^{-1})	306.61
Temperature (K)	153(1)
Crystal system	orthorhombic
Space group	$P2_12_12$
a (Å)	13.2889(2)
b (Å)	30.502(2)
c (Å)	7.05698(10)
V (Å^3)	2860.5(2)
Z	8
D (g cm^{-3})	1.424

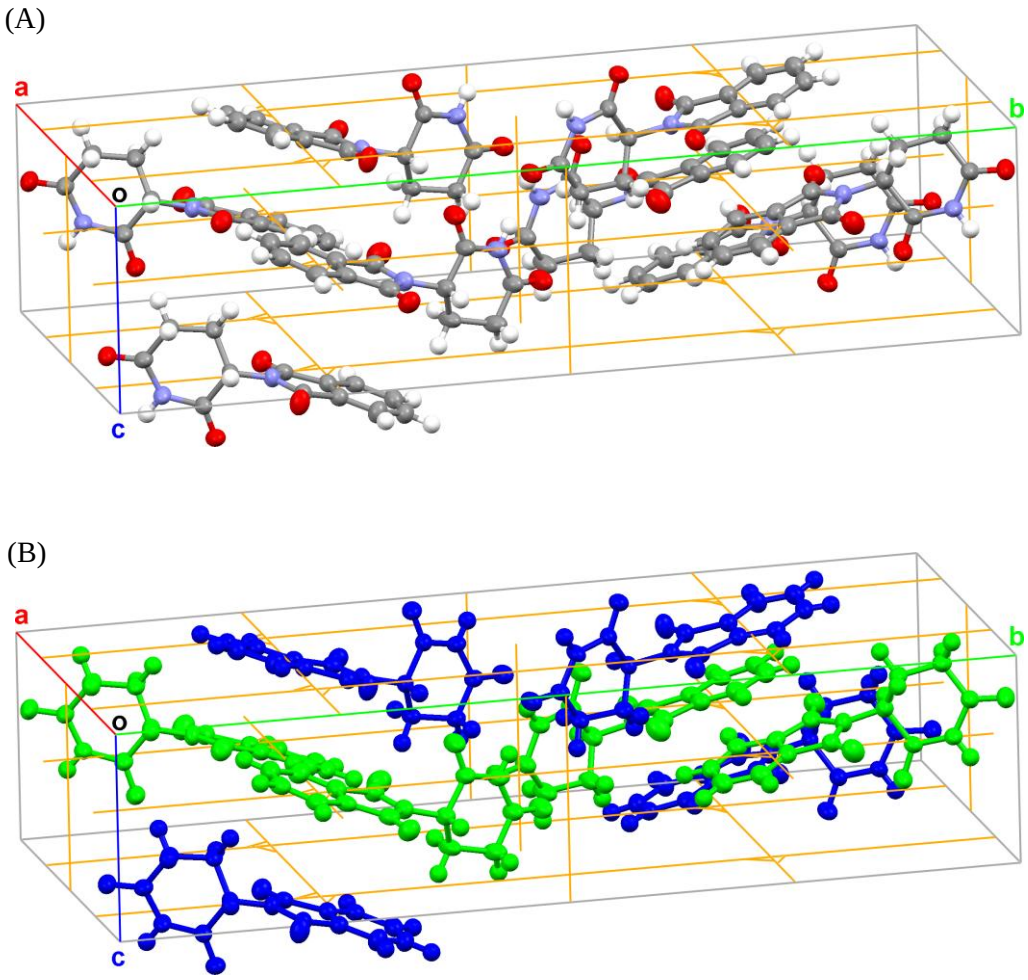

Figure 3.11 The unit-cell structure of **V** drawn with thermal ellipsoids at 50% probability level. Brown axes represent 2-fold screw axes. (A) Thalidomide molecules are colored by element as C: gray, N: blue, O: red, H: white. (B) **S'1** and **S'2** are colored by symmetry equivalence as green and blue, respectively.

Table 3.9 The list of bond lengths in **S'1** and **S'2**. The values in the parentheses represent standard deviations. The *t* values over 2 are colored in orange.

Bond	$L_{S'1}$ / Å	$L_{S'2}$ / Å	$\lvert L_{S'1}-L_{S'2}\rvert$ / Å	*t*
O1-C1	1.231(5)	1.219(4)	0.012(6)	1.87
O2-C8	1.203(5)	1.213(5)	0.01(7)	1.41
N1-C1	1.378(5)	1.385(4)	0.007(6)	1.09
N1-C8	1.417(5)	1.387(5)	0.03(7)	4.24
C1-C2	1.498(6)	1.493(5)	0.005(8)	0.64
C2-C3	1.355(6)	1.366(5)	0.011(8)	1.41
C2-C7	1.391(6)	1.401(5)	0.01(8)	1.28
C3-C4	1.396(6)	1.383(6)	0.013(8)	1.53
C4-C5	1.413(7)	1.400(6)	0.013(9)	1.41
C5-C6	1.361(6)	1.379(6)	0.018(8)	2.12
C6-C7	1.385(6)	1.379(6)	0.006(8)	0.71
C7-C8	1.480(6)	1.484(5)	0.004(8)	0.51
N1-C9	1.448(5)	1.466(4)	0.018(6)	2.81
O3-C10	1.216(5)	1.187(5)	0.029(7)	4.10
O4-C11	1.213(5)	1.217(5)	0.004(7)	0.57
N2-C10	1.385(5)	1.394(5)	0.009(7)	1.27
N2-C11	1.377(5)	1.381(5)	0.004(7)	0.57
C9-C10	1.521(5)	1.540(5)	0.019(7)	2.69
C9-C13	1.515(6)	1.519(5)	0.004(8)	0.51
C11-C12	1.497(6)	1.494(5)	0.003(8)	0.38
C12-C13	1.533(6)	1.518(5)	0.015(8)	1.92

Table 3.10 The list of bond angles of phthalimide rings in **S'1** and **S'2**. $A_{S'1}$ and $A_{S'2}$ represent the angle of particular bond in **S'1** and **S'2**, respectively. The values in the parentheses represent standard deviations. The *t* values over 2 are colored in orange.

Bond	$A_{S'1}$ / deg	$A_{S'2}$ / deg	$\lvert A_{S'1}-A_{S'2}\rvert$ / deg	*t*
C1-N1-C8	111.26(17)	111.66(16)	0.6	1.41
C1-N1-C9	125.14(18)	123.98(18)	1.9	4.48
C8-N1-C9	121.0(2)	122.09(18)	1.1	2.59
O1-C1-N1	125.2(2)	124.17(18)	0.3	0.53
O1-C1-C2	129.5(2)	130.2(2)	1.4	2.47
N1-C1-C2	105.35(19)	105.64(19)	1	2.36
C1-C2-C3	130.0(2)	130.7(2)	0.8	1.41
C1-C2-C7	108.2(2)	107.77(18)	1.6	3.77
C3-C2-C7	121.82(19)	121.5(2)	2.4	4.80
C2-C3-C4	116.7(2)	117.4(2)	0.9	1.59
C3-C4-C5	121.7(2)	121.4(2)	0.8	1.41
C4-C5-C6	120.8(2)	120.9(2)	0.5	0.88
C5-C6-C7	117.1(2)	116.9(2)	0.3	0.60
C2-C7-C6	121.8(2)	121.9(2)	1.6	3.20
C2-C7-C8	108.55(18)	109.33(19)	2.4	5.66
C6-C7-C8	129.6(2)	128.8(2)	0.7	1.40
O2-C8-N1	124.13(19)	105.20(19)	0.5	1.00
O2-C8-C7	129.8(2)	130.3(2)	1.8	3.60
N1-C8-C7	106.0(2)	124.54(18)	1.2	2.83

Table 3.11 The list of bond angles of glutarimide rings in **S'1** and **S'2**. $A_{S'1}$ and $A_{S'2}$ represent the angle of particular bond in **S'1** and **S'2**, respectively. The values in the parentheses represent standard deviations. The *t* values over 2 are colored in orange.

Bond	$A_{S'1}$ / deg	$A_{S'2}$ / deg	$\lvert A_{S'1}-A_{S'2}\rvert$ / deg	*t*
N1-C9-C10	109.57(19)	108.92(18)	1.2	2.83
N1-C9-C13	115.0(2)	114.35(18)	0.6	1.41
C10-C9-C13	111.46(18)	111.00(19)	0.4	0.94
O3-C10-N2	121.8(2)	120.5(2)	0.2	0.40
O3-C10-C9	122.80(18)	124.15(18)	0.1	0.20
N2-C10-C9	115.30(19)	115.32(19)	0.1	0.24
C10-N2-C11	127.2(2)	126.59(19)	0.3	0.71
O4-C11-N2	119.5(2)	119.6(2)	0.6	1.20
O4-C11-C12	123.3(2)	122.7(2)	0.2	0.40
N2-C11-C12	117.22(18)	117.65(17)	0.5	1.00
C11-C12-C13	113.9(2)	113.9(2)	2.5	5.00
C9-C13-C12	108.9(2)	108.52(19)	1.2	2.40

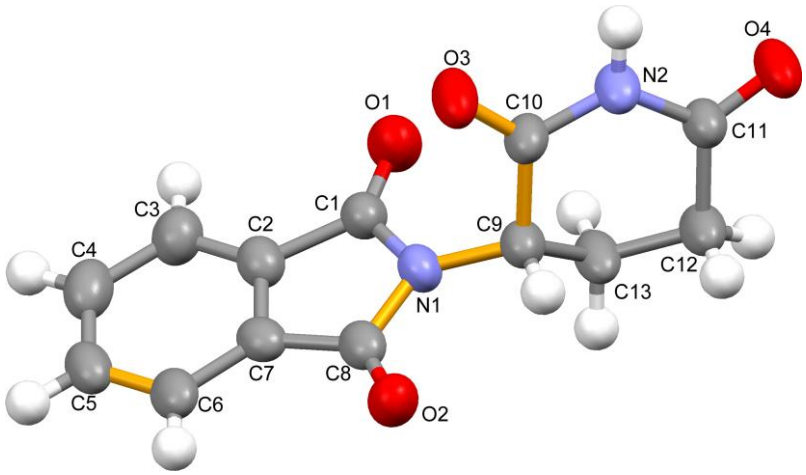

Figure 3.12 The conformation of **S'1** drawn with thermal ellipsoids at 50% probability level. Bonds, of which lengths are significantly different between **S'1** and **S'2**, are represented in orange. Color code: C: gray, N: blue, O: red, H: white.

Focusing on these conformational isomers, each of them is interacted with the other by hydrogen bonds. In the unsolvated crystal of (*S*)-thalidomide, pairs of conformational isomers forms dimers with the hydrogen bonded ring (Fig. 3.13(A)). Contrastingly, in the solvated crystal of (*S*)-thalidomide, alternate arrangement of conformational isomers forms infinite hydrogen bonded chain (Fig. 3.13(B)). Considering the fact that both unsolvated and solvated crystals were concomitantly obtained with the vapor diffusion technique, structural stabilities of each crystal appear to be close level.

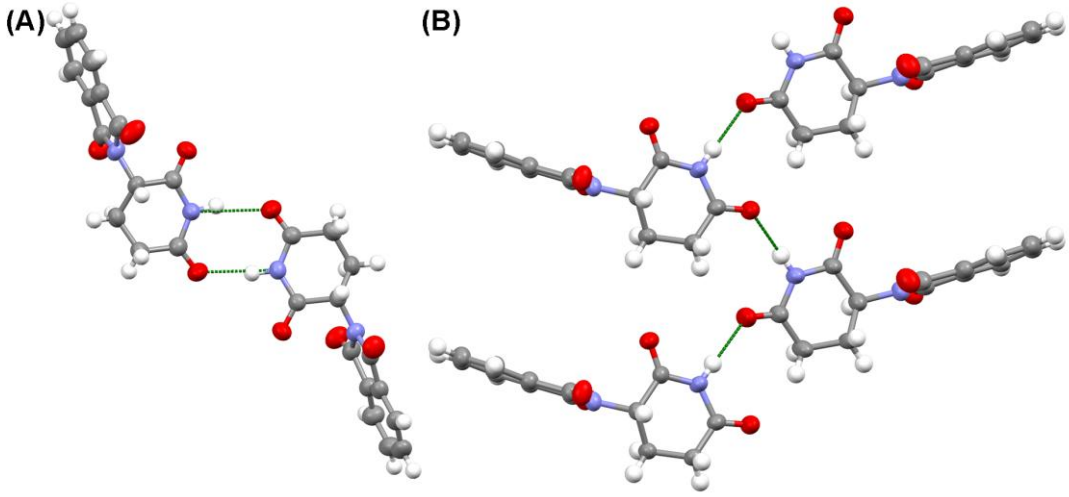

Figure 3.13 The structures of (A) hydrogen bonded dimer in unsolvated crystal of (*S*)-thalidomide and (B) hydrogen bonded chain in solvated crystal of (*S*)-thalidomide. Green broken lines represent hydrogen bonds. Color code: C: gray, N: blue, O: red, H: white, Cl: green.

3.4 Conclusion

In this chapter, crystal structure and absolute configuration of (*S*)-thalidomide was determined with single crystal X-ray diffractometry. Despite thalidomide has been attracting considerable attention again because of its wide-ranging bioactivity, the crystal structure of the enantiomeric thalidomide had not been published for about 40 years since that of racemic thalidomide was reported. This study revealed that crystallization from high polar methanol-water solution, in which hydrogen bonds are not generally formed, produces unsolvated (*S*)-thalidomide crystal and crystallization from nonpolar chloroform solution, in which thalidomide molecules exist in dynamic equilibrium of three isomeric dimers, produces solvated (*S*)-thalidomide crystal. Both unsolvated and solvated crystals are composed of two conformational isomers of (*S*)-thalidomide. The unsolvated crystals are formed with hydrogen bonded dimers consisting of pairs of these isomers, whereas the solvated crystals are formed with infinite hydrogen bonded chains consisting of alternately arranging conformational isomers.

As future works, the capability for replacing solvent molecules at channel spaces with maintaining the host lattice of the clathrate structure in the solvated (*S*)-thalidomide crystals should be investigated. Achieving this property of solvated crystals will be expected for pharmaceutical application, particularly with water because only hydrates may be of practical use as drugs.

3.5 References

[1] F. H. Allen and J. Trotter, "Crystal and molecular structure of thalidomide, N-(α-glutarimido)-phthalimide", *J. Chem. Soc. B,* (1971), pp. 1073-1079, DOI: 10.1039/j29710001073.

[2] G. M. Sheldrick, "A short history of SHELX", *Acta Crystallogr. A,* 64 (2008), pp. 112-122, DOI: 10.1107/S0108767307043930.

[3] M. M. Harding and R. M. Howieson, "L-Leucine", *Acta Cryst. B,* 32 (1976), pp. 633-634, DOI: 10.1107/S0567740876012405.

[4] F. Kaneko, K. Yagi-Watanabe, M. Tanaka, and K. Nakagawa, "Natural Circular Dichroism Spectra of Alanine and Valine Films in Vacuum Ultraviolet Region", *J. Phys. Soc. Jpn.,* 78 (2008), pp. 013001-013004, DOI: 10.1143/JPSJ.78.013001.

[5] K. Torii and Y. Iitaka, "The crystal structure of L-valine", *Acta Cryst. B,* 26 (1970), pp. 1317-1326, DOI: 10.1107/S0567740870004065.

[6] M. M. Harding and H. A. Long, "The crystal and molecular structure of L-cysteine", *Acta Cryst. B,* 24 (1968), pp. 1096-1102, DOI: 10.1107/S0567740868003742.

[7] T. Steiner, "The Hydrogen Bond in the Solid State", *Angew. Chem. Int. Ed.,* 41 (2002), pp. 48-76, DOI: 10.1002/1521-3773(20020104)41:1<48::AID-ANIE48>3.0.CO;2-U.

[8] F. H. Allen, W. D. Samuel Motherwell, P. R. Raithby, G. P. Shields, and R. Taylor, "Systematic analysis of the probabilities of formation of bimolecular hydrogen-bonded ring motifs in organic crystal structures", *New J. Chem.,* 23 (1999), pp. 25-34, DOI: 10.1039/a807212d.

[9] H. Izumi, S. Futamura, N. Tokita, and Y. Hamada, "Fliplike Motion in the Thalidomide Dimer: Conformational Analysis of (R)-Thalidomide Using Vibrational Circular Dichroism Spectroscopy", *J. Org. Chem.,* 72 (2007), pp. 277-279, DOI: 10.1021/jo061612q.

[10] C. H. Görbitz and H. Hersleth, "On the inclusion of solvent molecules in the crystal structures of organic compounds", *Acta Crystallogr. B,* 56 (2000), pp. 526-534, DOI: 10.1107/S0108768100000501.

[11] H. Mimura, S. Kitamura, T. Kitagawa, and S. Kohda, "Characterization of the non-stoichiometric and isomorphic hydration and solvation in FK041 clathrate", *Colloid. Surface B,* 26 (2002), pp. 397-406, DOI:

10.1016/S0927-7765(02)00026-7.

[12] H. Mimura, K. Gato, S. Kitamura, T. Kitagawa, and S. Kohda, "Effect of Water Content on the Solid-State Stability in Two Isomorphic Clathrates of Cephalosporin: Cefazolin Sodium Pentahydrate (α Form) and FK041 Hydrate", *Chem. Pharm. Bull.*, 50 (2002), pp. 766-770, DOI: 10.1248/cpb.50.766.

4. Investigation into the origin of differences in physicochemical properties between enantiomeric and racemic thalidomides

4.1 Introduction

Although a number of studies have reported bioactivities of thalidomide [1-8], only a few researches have reported its physicochemical properties. Racemic thalidomide is known to exhibit lower solubility and higher melting point than the enantiomers [1]. It is also known that the oral absorption of racemic thalidomide is slower than that of the enantiomers [2, 3]. However, the origin of differences in these physicochemical properties between enantiomeric and racemic thalidomides has not been investigated.

As to chiral compounds, crystal structures of enantiomeric and racemic compounds are essentially different. Therefore, the idea of comparing crystal structures between an enantiomer and the racemate is significant for understanding differences in such physicochemical properties between them.

Crystal structures of racemic thalidomide have been investigated since 1971 [9].Two polymorphs of α and β forms are known in (*RS*)-thalidomide [10]. However, crystal structures between enantiomeric and racemic thalidomides have not been compared because even crystal structures of enantiomeric thalidomide have not been reported.

To investigate the origin of differences in such physicochemical properties between (*S*)- and (*RS*)-thalidomides, this study, in this chapter, focuses on comparison of crystal structures between (*S*)- and (*RS*)-thalidomides. Crystallizations of (*S*)- and (*RS*)-thalidomide were performed with three different methods. The structures of (*S*)-thalidomide crystals investigated in chapter 3 are adopted for comparison with those of (*RS*)-thalidomide. The structures of (*RS*)-thalidomide crystals were investigated with X-ray diffractometry. Furthermore, structural stabilities of those crystals were evaluated with energy calculations.

4.2 Crystallization of (*RS*)-thalidomides

4.2.1 Materials

(*RS*)-thalidomides was purchased from Sigma-Aldrich, Inc. Methanol, chloroform, diethyl ether, and acetonitrile were purchased from Wako Pure Chemical Industries, Ltd.

4.2.2 Experimental method

As in the case of (*S*)-thalidomide, (*RS*)-thalidomide crystals were obtained with following three different crystallization methods:

- solvent evaporation technique from methanol-water solution;
- solvent evaporation technique from chloroform solution;
- vapor diffusion technique from chloroform solution.

Detail procedures of crystallization are as follows.

Crystallization procedure of (*RS*)-thalidomide with solvent evaporation technique from methanol-water solution was as follows:

(1) (*RS*)-thalidomide powder (50 mg) was dissolved in 40 ml methanol-water (5:3).
(2) The solution was evaporated for about 4 h at 50 °C.
(3) The grown crystals floating on the solutions were filtered out.

Crystallization procedure of (*RS*)-thalidomide with solvent evaporation technique from chloroform solution was as follows:

(1) (*RS*)-thalidomide powder (6.28 mg) was dissolved in 4.8 ml chloroform.
(2) The solution was evaporated in a few days at room temperature.
(3) The grown crystals floating on the solutions were filtered out.

Crystallization procedure of (*RS*)-thalidomide with vapor diffusion technique from chloroform solution was as follows:

(1) (*RS*)-thalidomide powder (64.5 mg) was dissolved in 50 ml chloroform.
(2) The inner vial containing 50 ml of this chloroform solution was put in the outer beaker with about 80 ml of diethyl ether.
(3) This outer beaker was kept sealed for a few days at room temperature.
(4) The grown crystals were filtered out.

4.2.3 Results

Crystallization with solvent evaporation technique from methanol-water solution produced needle shaped crystals (**II**) (Figure 4.1(A)). To appropriately realize the same crystallization condition with (*S*)-thalidomide, (*RS*)-thalidomide was also crystallized in about 4 hours at temperatures around 50 °C. Crystallization with solvent evaporation technique from chloroform solution produced plate shaped crystals (**IV**) (Figure 4.1(B)). Similarly, crystallization with vapor diffusion technique from chloroform solution also produced plate shaped crystals (**VII**) (Figure 4.1(C)).

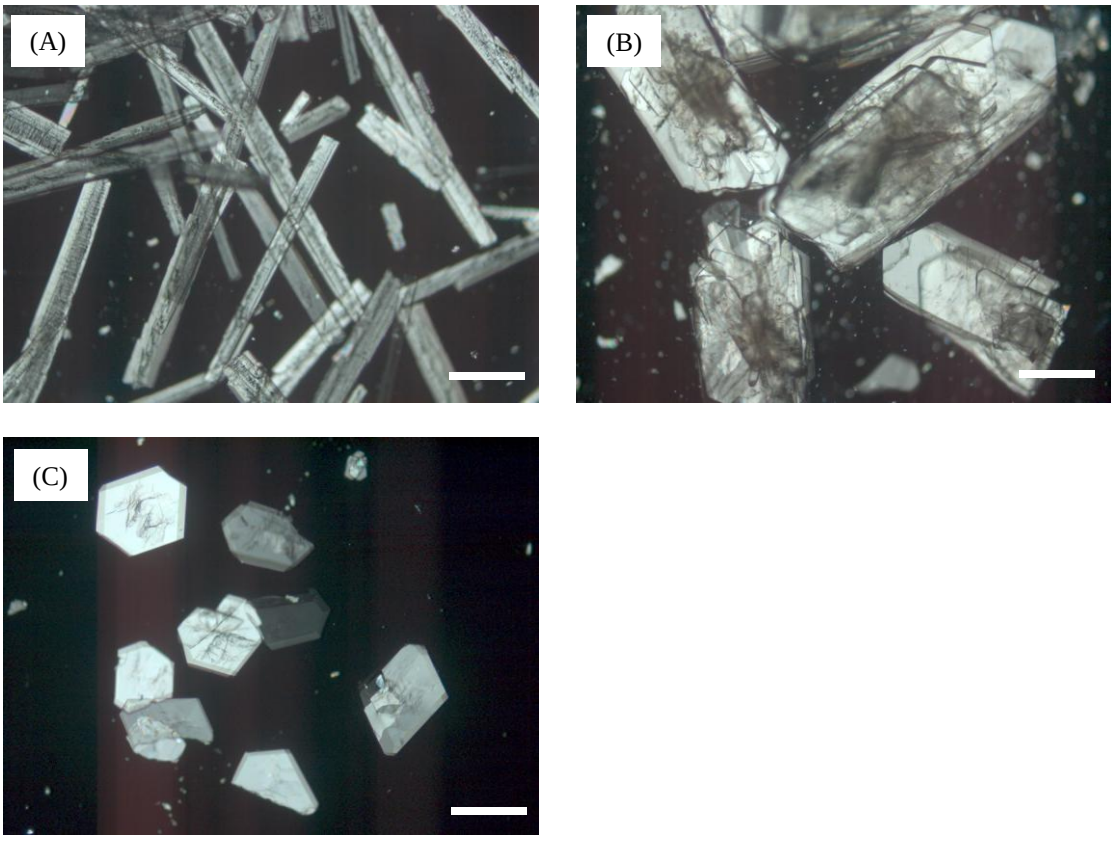

Figure 4.1 Polarizing microscopic images of (*RS*)-thalidomide crystals obtained with (A) solvent evaporation technique from methanol-water solution (B) solvent evaporation technique from chloroform solution (C) vapor diffusion technique from chloroform solution. The scale bars represent 0.5 mm.

4.3 X-ray diffractometry on (*RS*)-thalidomide crystals

4.3.1 Experimental method

Crystals for X-ray diffractometry were carefully selected considering the points as mentioned in Section 3.3.1. X-ray diffraction data for all crystals (**II**, **IV**, and **VII**) were collected using a Rigaku RAXIS RAPID imaging plate detector with graphite monochromated Cu-Kα radiation. Crystal structures were solved by direct methods and refined by full-matrix least-squares on F^2 [11]. Non-hydrogen atoms were refined with anisotropic displacement parameters, except for isotropically refined solvent molecules. Hydrogen atoms were refined using the riding model.

4.3.2 Summary of results

Crystal and structure refinement data combined with previous reports on α and β forms of (*RS*)-thalidomide are summarized in Table 4.1. To crystallographically determine the crystal structure, the result of single crystal X-ray diffractometry needs to fulfill the following requirements:

$R_{int} < 0.1$
$R_1 \leqq 0.1$
$wR_2 < 0.25$
$-0.01 <$ Max Shift/Error < 0.01
$0.8 \leqq$ Goodness of fit $\leqq 2.0$

According to these requirements, crystal strictures of **II**, **IV**, and **VII** were crystallographically determined and completely refined.

As a result of single crystal X-ray diffractometry, all of **II**, **IV**, and **VII** were determined as the isomorphic form with the previously reported α form of (*RS*)-thalidomide. Contrary to the case of (*S*)-thalidomide, all of **II**, **IV**, and **VII** are revealed to be unsolvated crystals of (*RS*)-thalidomide. To appropriately compare with the unsolvated (*S*)-thalidomide of **I**, this study focuses on **II**, which are crystallized with the corresponding method with **I**, as the crystal structure of α-(*RS*)-thalidomide.

Table 4.1 Crystal and structure refinement data for **II**, **IV**, and **VII** combined with those of previous reports on α and β forms of (*RS*)-thalidomide.

	Previous report				
	α-form [9]	β-form [10]	**II**	**IV**	**VII**
Empirical formula	$C_{13}H_{10}O_4N_2$	$C_{13}H_{10}O_4N_2$	$C_{13}H_{10}O_4N_2$	$C_{13}H_{10}O_4N_2$	$C_{13}H_{10}O_4N_2$
M (g mol^{-1})	258.23	258.23	258.23	258.23	258.23
Temperature (K)	NA	296(1)	93(1)	223(1)	173(1)
Crystal system	monoclinic	monoclinic	monoclinic	monoclinic	monoclinic
Space group	$P2_1/n$	$C2/c$	$P2_1/n$	$P2_1/n$	$P2_1/n$
a (Å)	8.233(1)	20.741(2)	8.3156(3)	8.2668(3)	8.2855(3)
b (Å)	10.070(2)	8.072(1)	9.9732(4)	10.0175(3)	10.0184(3)
c (Å)	14.865(2)	14.216(1)	14.5740(5)	14.7749(5)	14.6698(5)
β (°)	102.53(2)	102.78(1)	102.762(2)	102.603(2)	102.6511(19)
V (Å^3)	1203.0	2321. 1	1178.81(7)	1194.07(7)	1188.13(6)
Z	4	8	4	4	4
D (g cm^{-3})	1.426	1.48	1.455	1.436	1.444
Reflection total/unique	NA	NA/2350	12229/2122	13090/2170	11767/2139
R_{int}	NA	NA	0.064	0.038	0.089
R_1 [$I > 2\sigma(I)$]	0.053	0.057	0.0467	0.0447	0.0734
wR_2 (all data)	NA	0.081	0.1212	0.1333	0.0830
Max Shift/Error	NA	NA	0.000	0.000	0.000
Goodness of fit	NA	NA	0.999	1.013	0.977

4.3.3 Crystal structures of (*RS*)-thalidomide

The unit-cell structure of α-(*RS*)-thalidomide (**II**) is shown in Figure 4.2. The crystal structure of (*RS*)-thalidomide is formed with (*R*)- and (*S*)-thalidomide molecules in mirror conformation. In the α-(*RS*)-thalidomide crystal, pairs of (*R*)- and (*S*)-thalidomide molecules form the heterochiral dimers (Figure 4.3). Whereas, in the β-(*RS*)-thalidomide crystal, alternately arranged (*R*)- and (*S*)-thalidomide molecules form the infinite chain structure (Figure 4.4).

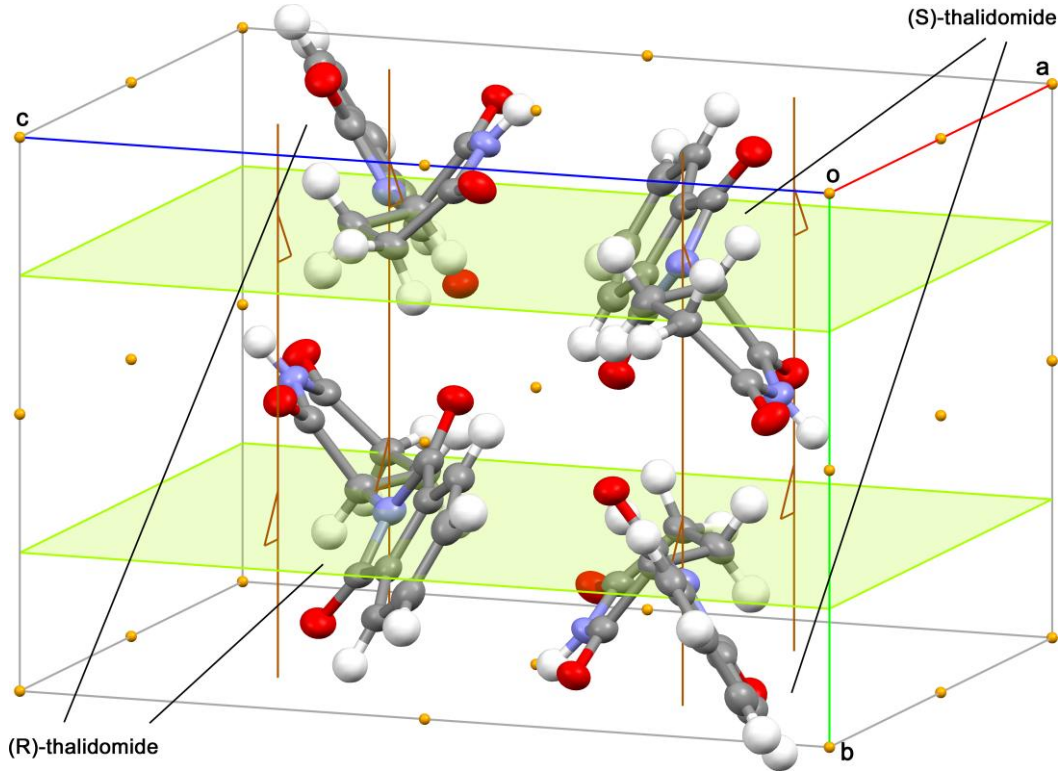

Figure 4.2 The unit-cell structure of (*RS*)-thalidomide crystal drawn with thermal ellipsoids at 50% probability level. Brown axes, green plane, and orange sphere represent 2-fold screw axes, mirror plane, and symmetry center, respectively. Color code: C: gray, N: blue, O: red, H: white.

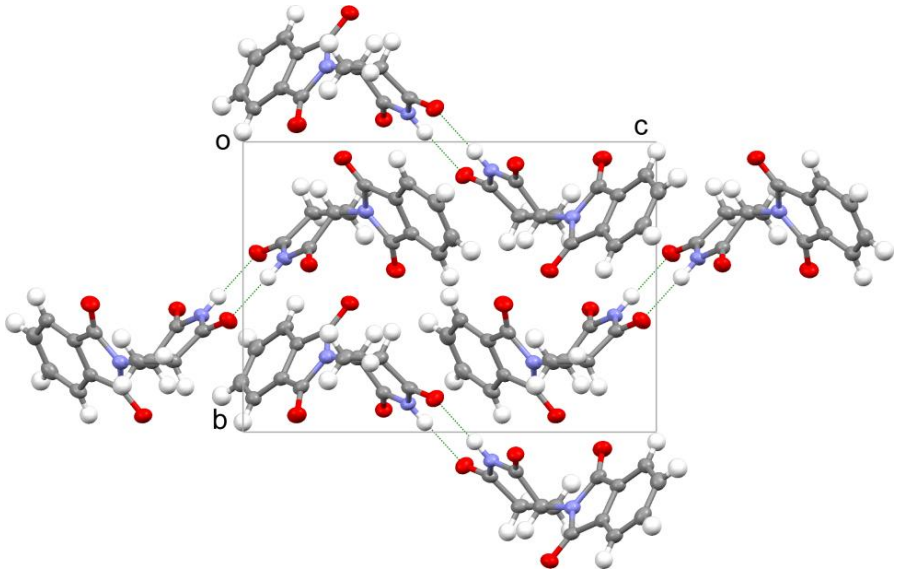

Figure 4.3 Packing structure of the α-(*RS*)-thalidomide crystal along *a* axis. Green broken lines represent hydrogen bonds. Color code: C: gray, N: blue, O: red, H: white.

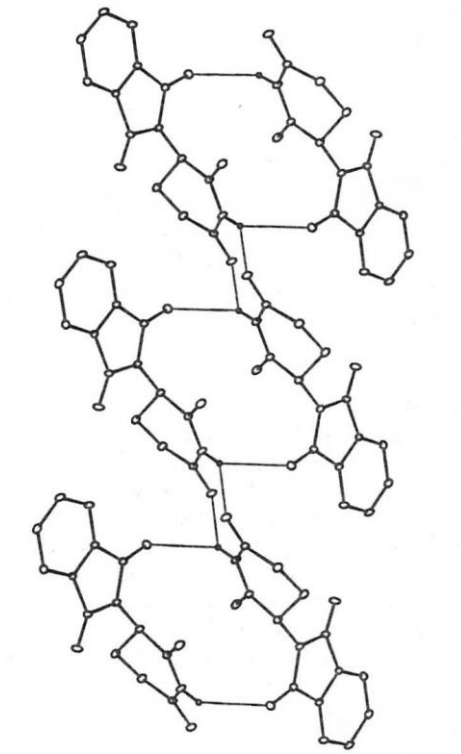

Figure 4.4 Packing structure of the β-(*RS*)-thalidomide crystal along *b* axis [10].

4.3.4 Comparison of crystal structures between (*S*)- and (*RS*)-thalidomides

The crystal structures of unsolvated (*S*)-thalidomide (**I**) and α-(*RS*)-thalidomide (**II**) were compared in detail. Comparison of structural parameters between (*S*)-thalidomide (**I**) and (*RS*)-thalidomide (**II**) crystals is listed in Table 4.2.

While the (*RS*)-thalidomide crystal consists of (*R*)- and (*S*)-thalidomide molecules in symmetrical conformations, the (*S*)-thalidomide crystal consists of two conformational isomers of (*S*)-thalidomide. To distinguish these four thalidomide molecules, namely (*R*)- and (*S*)-thalidomide molecules in the (*RS*)-thalidomide crystal and two conformational isomeric molecules of (*S*)-thalidomide in the (*S*)-thalidomide crystal, they are hereafter designated as $\mathbf{R_{RS}}$, $\mathbf{S_{RS}}$, **S1**, and **S2**, respectively. The conformation of $\mathbf{S_{RS}}$ with atomic numbering of non-hydrogen atoms is shown in Figure 4.5. In comparison of the conformational difference among three (*S*)-thalidomide molecules, $\mathbf{S_{RS}}$, **S1**, and **S2**, the dihedral angles between the mean plane composed of non-hydrogen atoms in the phthalimide ring and that in the glutarimide ring are 81.72° for $\mathbf{S_{RS}}$, 84.81° for **S1**, and 82.18° for **S2**, respectively. The packing structures of (*S*)- and (*RS*)-thalidomide crystal along *a*, *b*, and *c* axes are shown in Figures 4.6, 4.7, and 4.8, respectively. The bond lengths and angles of the three (*S*)-thalidomide molecules are listed in Table 4.3 and Table 4.4, respectively.

Table 4.2 Comparison of structural parameters between **I** and **II**.

	I	**II**
	(*S*)-thalidomide	(*RS*)-thalidomide
Crystal system	monoclinic	monoclinic
Space group	$P2_1$	$P2_1/n$
a (Å)	8.40187 (15)	8.3156(3)
b (Å)	10.02372 (18)	9.9732(4)
c (Å)	14.4814 (7)	14.5740(5)
β (°)	103.4938 (8)	102.762(2)
V (Å^3)	1185.93 (7)	1178.81(7)
Z	4	4
D (g cm^{-3})	1.446	1.455

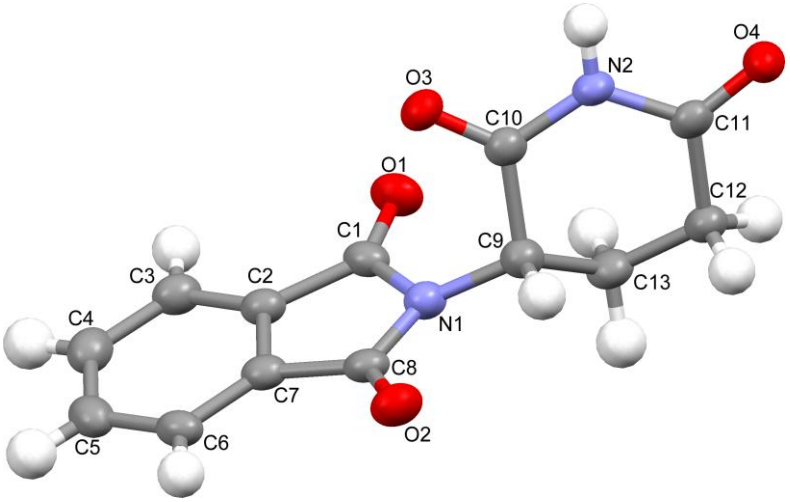

Figure 4.5 The configuration of $\mathbf{S_{RS}}$ drawn with thermal ellipsoids at 50% probability level. Color code: C: gray, N: blue, O: red, H: white.

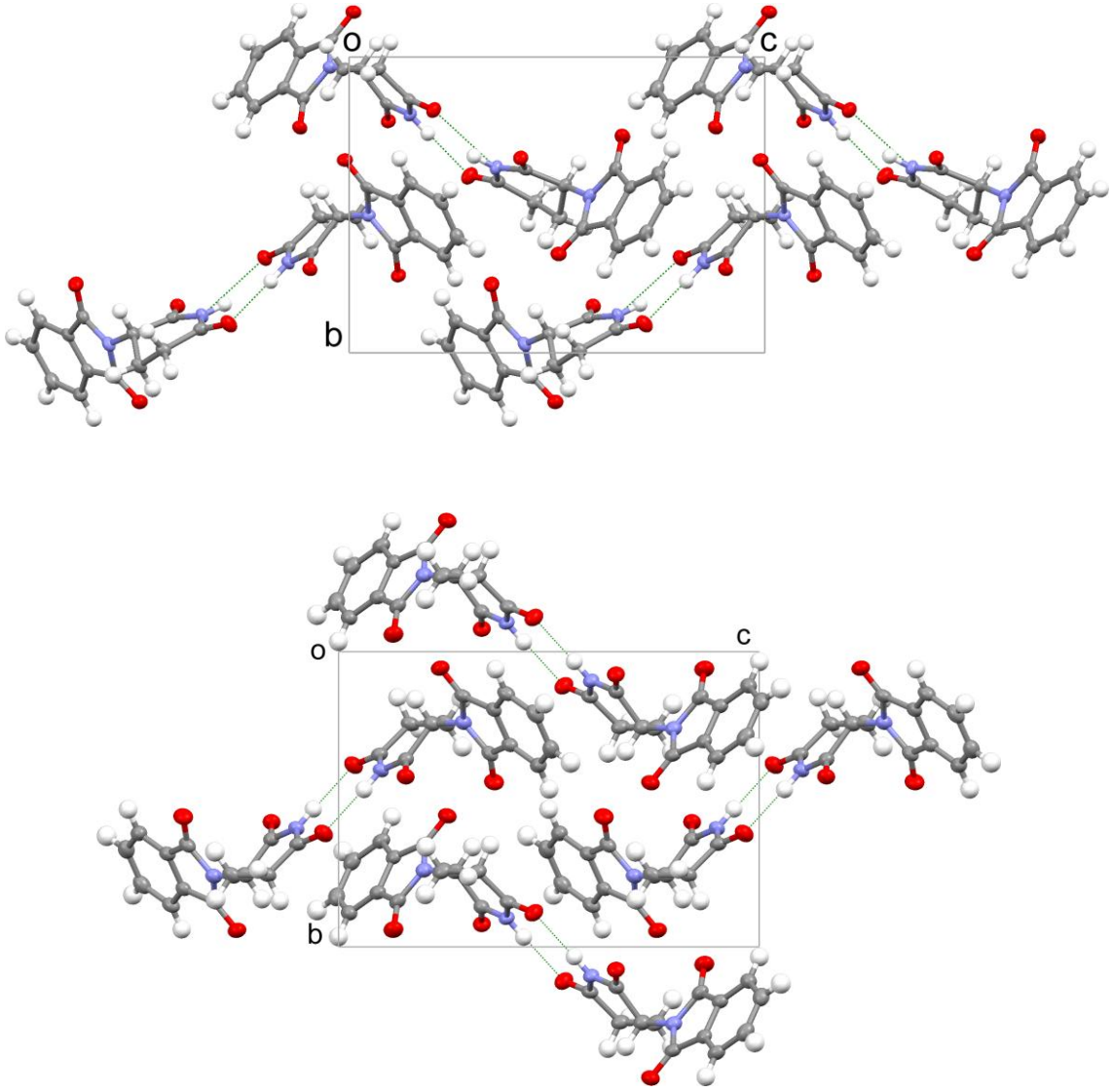

Figure 4.6 The packing structures of the (upper) (*S*)- and (lower) (*RS*)-thalidomide crystals along *a* axis.

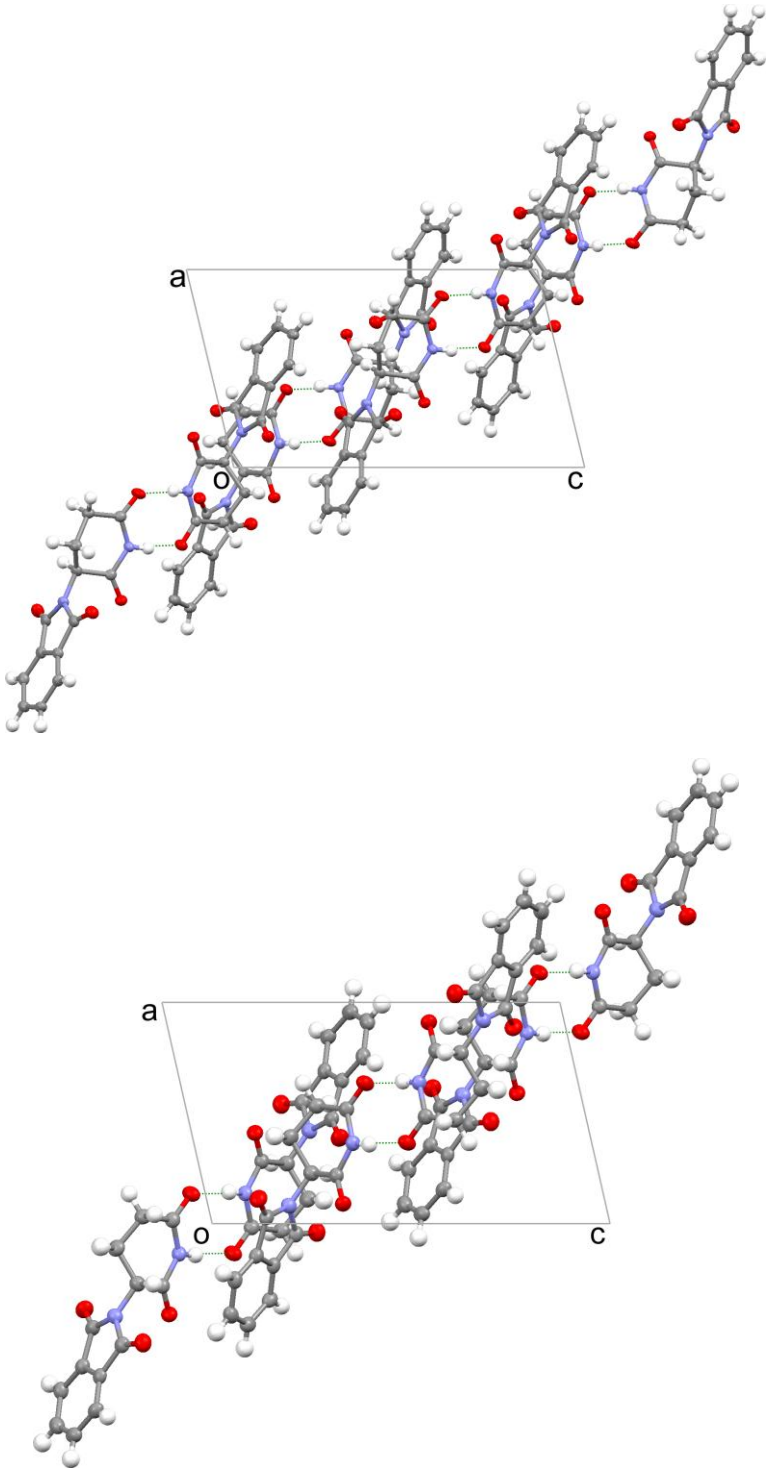

Figure 4.7 The packing structures of the (upper) (*S*)- and (lower) (*RS*)-thalidomide crystals along *b* axis.

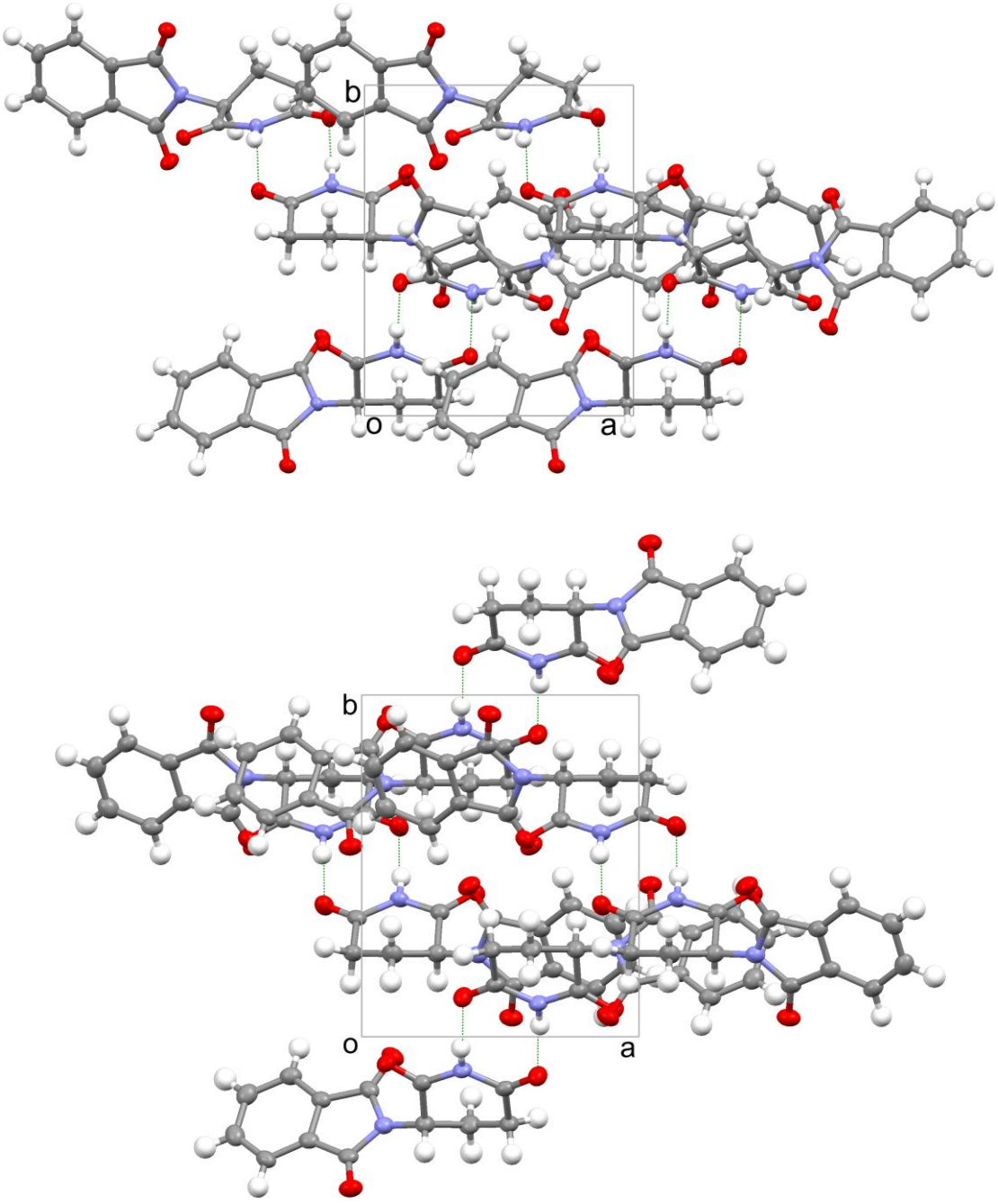

Figure 4.8 The packing structures of the (upper) (*S*)- and (lower) (*RS*)-thalidomide crystals along *c* axis.

Table 4.3 Comparison of bond lengths among **S1**, **S2**, and $\mathbf{S_{RS}}$ molecules. Values in the parentheses represent standard deviations.

Bond	Length		
	S1 (Å)	**S2** (Å)	$\mathbf{S_{RS}}$ (Å)
O1-C1	1.205(2)	1.205(2)	1.215(2)
O2-C8	1.218(3)	1.214(2)	1.212(2)
N1-C1	1.413(3)	1.409(2)	1.395(2)
N1-C8	1.400(2)	1.411(3)	1.403(2)
C1-C2	1.492(2)	1.494(2)	1.487(2)
C2-C3	1.379(3)	1.371(3)	1.372(2)
C2-C7	1.385(3)	1.386(3)	1.392(3)
C3-C4	1.392(3)	1.398(3)	1.395(2)
C4-C5	1.395(3)	1.393(3)	1.387(3)
C5-C6	1.393(3)	1.393(3)	1.394(2)
C6-C7	1.380(3)	1.393(3)	1.375(2)
C7-C8	1.480(3)	1.482(2)	1.486(2)
N1-C9	1.453(2)	1.450(2)	1.452(2)
O3-C10	1.210(2)	1.213(2)	1.216(2)
O4-C11	1.223(2)	1.223(2)	1.226(2)
N2-C10	1.379(2)	1.390(2)	1.378(2)
N2-C11	1.382(3)	1.377(2)	1.378(2)
C9-C10	1.521(3)	1.514(3)	1.516(3)
C9-C13	1.518(3)	1.528(3)	1.516(3)
C11-C12	1.501(3)	1.502(3)	1.500(3)
C12-C13	1.524(3)	1.522(2)	1.508(2)

Table 4.4 Comparison of bond angles among **S1**, **S2**, and $\mathbf{S_{RS}}$ molecules. Values in the parentheses represent standard deviations.

Bond	Angle		
	S1 (°)	**S2** (°)	$\mathbf{S_{RS}}$ (°)
C1-N1-C8	111.26(17)	111.66(16)	111.25(14)
C1-N1-C9	125.14(18)	123.98(18)	124.33(14)
C8-N1-C9	121.0(2)	122.09(18)	121.61(15)
O1-C1-N1	125.2(2)	124.17(18)	124.56(16)
O1-C1-C2	129.5(2)	130.2(2)	128.69(16)
N1-C1-C2	105.35(19)	105.64(19)	106.75(15)
C1-C2-C3	130.0(2)	130.7(2)	131.21(17)
C1-C2-C7	108.2(2)	107.77(18)	107.4(15)
C3-C2-C7	121.82(19)	121.5(2)	121.39(17)
C2-C3-C4	116.7(2)	117.4(2)	117.35(18)
C3-C4-C5	121.7(2)	121.4(2)	121.13(17)
C4-C5-C6	120.8(2)	120.9(2)	121.25(18)
C5-C6-C7	117.1(2)	116.9(2)	117.03(18)
C2-C7-C6	121.8(2)	121.9(2)	121.85(16)
C2-C7-C8	108.55(18)	109.33(19)	108.52(15)
C6-C7-C8	129.6(2)	128.8(2)	129.61(17)
O2-C8-N1	124.13(19)	124.54(18)	124.66(16)
O2-C8-C7	129.8(2)	130.3(2)	129.48(17)
N1-C8-C7	106.0(2)	105.20(19)	105.85(15)
N1-C9-C10	109.57(19)	108.92(18)	108.51(14)
N1-C9-C13	115.0(2)	114.35(18)	114.88(18)
C10-C9-C13	111.46(18)	111.00(19)	111.12(15)
O3-C10-N2	121.8(2)	120.5(2)	120.77(16)
O3-C10-C9	122.80(18)	124.15(18)	123.46(15)
N2-C10-C9	115.30(19)	115.32(19)	115.7(15)
C10-N2-C11	127.2(2)	126.59(19)	126.35(15)
O4-C11-N2	119.5(2)	119.6(2)	119.46(17)
O4-C11-C12	123.3(2)	122.7(2)	122.94(17)
N2-C11-C12	117.22(18)	117.65(17)	117.59(15)
C11-C12-C13	113.9(2)	113.9(2)	114.56(15)
C9-C13-C12	108.9(2)	108.52(19)	109.41(18)

On one hand, pairs of $\mathbf{R_{RS}}$ and $\mathbf{S_{RS}}$ molecules form heterochiral dimers in the (*RS*)-thalidomide crystal. On the other hand, pairs of **S1** and **S2** molecules form homochiral dimers in the (*S*)-thalidomide crystal. Both the heterochiral dimer and the homochiral dimer are formed with two intermolecular hydrogen bonds. These hydrogen bonds link the glutarimide moieties of each molecule in a ring shape. The center of the hydrogen-bonded ring in heterochiral dimer is the symmetry center of the (*RS*)-thalidomide crystal. Therefore, the dihedral angle between the mean plane composed of N2, C11 and O4 in $\mathbf{S_{RS}}$ and the corresponding plane in $\mathbf{R_{RS}}$ is 0° as shown in Figure 4.9(A). In contrast, the dihedral angle between the mean plane composed of N2, C11 and O4 in **S1** and that composed of N2', C11' and O4' in **S2** ,where the primed numbers represent atoms of **S2**, is not 0° but 14.52° because **S1** and **S2** are asymmetric as shown in Figure 4.9(B).

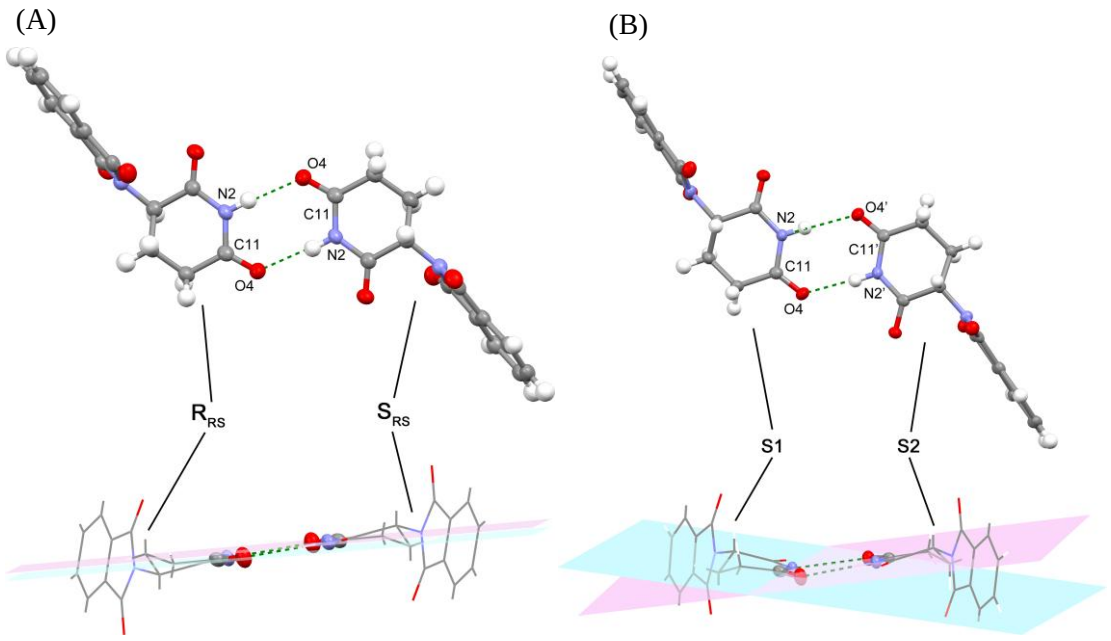

Figure 4.9 Top and side views of hydrogen-bonded rings in (A) heterochiral dimer and (B) homochiral dimer. Blue and pink planes represent each mean plane, and only constituent atoms of the mean plane are drawn with thermal ellipsoids in side view. Green broken lines represent hydrogen bonds. Color code: C: gray, N: blue, O: red, H: white.

4.4 Evaluation of the structural stabilities with energy calculations

4.4.1 Introduction

The structural stability of the molecular crystal such as thalidomide crystals is closely related with intermolecular interaction in the crystal. The intermolecular interactions in thalidomide crystals originate from hydrogen bonds and Van der Waals Force. The hydrogen bonds are thought to main intermolecular interaction because hydrogen bond is much stronger than Van der Waals Force. Therefore, it is reasonable expectation that the differences in melting point between enantiomeric and racemic thalidomides are caused by the difference in structural stabilities between hydrogen-bonded rings in homochiral dimers and those in heterochiral dimers. On this hypothesis, this study evaluated the stabilities of hydrogen-bonded rings with calculation of the hydrogen bond energies.

4.4.2 Experimental method

Single-point energy of a molecule is the sum of the electron energy and the nuclear repulsion energy, and is obtainable from the density functional theory (DFT) calculation with a combination of a functional and a basis set [12]. This study calculated the single-point energies of monomers and dimers from the atomic coordinates in the crystal structures of (*S*)-thalidomide (**I**) and (*RS*)-thalidomide (**II**) using Gaussian® 03 program [13] based on DFT. The calculations were performed employing 12 practically used combinations of 3 functionals, B3LYP, B3PW91, and O3LYP, with 4 basis sets, 6-31+G(d,p), 6-311++G(d,p), cc-pVDZ, and TZVP, respectively.

This study estimated the hydrogen bond energy in the homochiral dimer (ΔE_{homo}) by subtracting the sum of the single-point energies of each monomer, which contains no contribution of inter-monomer interaction, from the single-point energy of the dimer, which contains the contribution of inter-monomer interaction, as follows:

$$\Delta E_{homo} = E_{SS} - \left(E_{S1} + E_{S2}\right), \tag{4.1}$$

where E_{SS}, E_{S1}, and E_{S2} represent the single point energies of homochiral dimer, **S1**, and **S2**, respectively. Similarly, the hydrogen bond energy in the heterochiral dimer (ΔE_{hetero}) was estimated as follows:

$$\Delta E_{hetero} = E_{RS} - (E_R + E_S), \quad (4.2)$$

where E_{RS}, E_R, and E_S represent the single point energies of heterochiral dimer, $\mathbf{R_{RS}}$, and $\mathbf{S_{RS}}$, respectively.

These calculations assume the thalidomide monomer or dimer as alone in a vacuum, *i.e.* no neighboring molecules. Therefore, intermolecular interactions in crystalline state are not strictly reflected in these calculations. Moreover, to discuss the case in solution state, effect of solvents should additionally be included in calculation. Nevertheless, energy calculations for these dimer structures based on the crystal structures is significant for comparison between enantiomeric and racemic crystals composed with homochiral and heterochiral dimers, respectively.

4.4.3 Results

As shown in Table. 4.5, the hydrogen bond energies in heterochiral dimer are about 10% lower than that in homochiral dimer on all combinations of the functional and the basis set. This result suggests that the heterochiral dimer in the (*RS*)-thalidomide crystal is more stable than the homochiral dimer in (*S*)-thalidomide crystal. This is consistent with the differences of physicochemical properties that racemic thalidomide exhibits higher melting point than the enantiomeric thalidomide.

Table 4.5 Results of calculation in each combination of functionals and basis sets. ΔE_{homo} and ΔE_{hetero} represent estimated hydrogen bond energy in homochiral and heterochiral dimers, respectively.

Functional	Basis set	ΔE_{homo} (kcal mol^{-1})	ΔE_{hetero} (kcal mol^{-1})	ΔE_{homo}-ΔE_{hetero} (kcal mol^{-1})	ΔE_{hetero} / ΔE_{homo}
B3LYP	6-31+G(d,p)	-5.692864075	-6.448119450	0.755255374	1.132667031
B3LYP	6-311++G(d,p)	-5.885150557	-6.650696459	0.765545902	1.130080938
B3LYP	cc-pVDZ	-8.950256935	-9.913402611	0.963145676	1.107610953
B3LYP	TZVP	-5.903374060	-6.853759788	0.950385728	1.160990261
B3PW91	6-31+G(d,p)	-4.675627878	-5.450517397	0.774889519	1.165729510
B3PW91	6-311++G(d,p)	-4.954715866	-5.726484152	0.771768286	1.155764388
B3PW91	cc-pVDZ	-7.395916073	-8.356241552	0.960325479	1.129845373
B3PW91	TZVP	-4.800420692	-5.698508523	0.898087831	1.187085235
O3LYP	6-31+G(d,p)	-3.165314795	-3.852607125	0.687292330	1.217132378
O3LYP	6-311++G(d,p)	-3.159772631	-3.869748175	0.709975544	1.224691972
O3LYP	cc-pVDZ	-6.391051226	-7.224241397	0.833190171	1.130368251
O3LYP	TZVP	-3.286703998	-4.109936849	0.823232851	1.250473682

4.5 Conclusion

In this chapter, this study focuses on comparison of crystal structures between (*S*)- and (*RS*)-thalidomides. The crystals obtained with three different methods were determined as the isomorphic with previously known α-form. Although the crystal structure of (*RS*)-thalidomide have been investigated, special attention on the heterochiral dimer formation in the crystal have not been paid. On the basis of the crystal structure of (*S*)-thalidomide determination in chapter 3, comparison of crystal structures between (*S*)- and (*RS*)-thalidomides reveals the main difference between (*S*)- and (*RS*)-thalidomide crystals is in the dimer structures: homochiral dimers in the (*S*)-thalidomide crystal and heterochiral dimers in the (*RS*)-thalidomide crystal. The comparison of these dimer structures suggested that the symmetric heterochiral dimers are more stable than the asymmetric homochiral dimers. The theoretical calculation based on the crystal structures revealed that the intermolecular energy of the heterochiral dimer is lower than that of the homochiral dimer. These results indicate that the known differences of physicochemical properties between racemic thalidomide and enantiomeric thalidomide originate from the stability difference of hydrogen-bonded rings between heterochiral dimers and homochiral dimers.

4.6 References

[1] S. Fabro, R. L. Smith, and R. T. Williams, "Toxicity and Teratogenicity of Optical Isomers of Thalidomide", *Nature,* 215 (1967), pp. 296, DOI: 10.1038/215296a0.

[2] T. Eriksson, S. Björkman, and P. Höglund, "Clinical pharmacology of thalidomide", *Eur. J. Clin. Pharmacol.,* 57 (2001), pp. 365-376, DOI: 10.1007/s002280100320.

[3] T. Eriksson, S. Björkman, B. Roth, Å. Fyge, and P. Höglund, "Stereospecific determination, chiral inversion in vitro and pharmacokinetics in humans of the enantiomers of thalidomide", *Chirality,* 7 (1995), pp. 44-52, DOI: 10.1002/chir.530070109.

[4] Y. Hashimoto, "Structural development of biological response modifiers based on thalidomide", *Bioorg. Med. Chem.,* 10 (2002), pp. 461-479, DOI: 10.1016/S0968-0896(01)00308-X.

[5] M. E. Franks, G. R. Macpherson, and W. D. Figg, "Thalidomide", *The Lancet,* 363 (2004), pp. 1802-1811, DOI: 10.1016/S0140-6736(04)16308-3.

[6] M. Melchert and A. List, "The thalidomide saga", *Int. J. Biochem. Cell Biol.,* 39 (2007), pp. 1489-1499, DOI: 10.1016/j.biocel.2007.01.022.

[7] T. D. Stephens, C. J. W. Bunde, and B. J. Fillmore, "Mechanism of action in thalidomide teratogenesis", *Biochemical Pharmacology,* 59 (2000), pp. 1489-1499, DOI: 10.1016/S0006-2952(99)00388-3.

[8] S. Tseng, G. Pak, K. Washenik, M. K. Pomeranz, and J. L. Shupack, "Rediscovering thalidomide: A review of its mechanism of action, side effects, and potential uses", *J. Am. Acad. Dermatol.,* 35 (1996), pp. 969-979, DOI: 10.1016/S0190-9622(96)90122-X.

[9] F. H. Allen and J. Trotter, "Crystal and molecular structure of thalidomide, N-(α-glutarimido)-phthalimide", *J. Chem. Soc. B,* (1971), pp. 1073-1079, DOI: 10.1039/j29710001073.

[10] J. C. Reepmeyer, M. O. Rhodes, D. C. Cox, and J. V. Silverton, "Characterization and crystal structure of two polymorphic forms of racemic thalidomide", *J. Chem. Soc., Perkin Trans. 2,* (1994), pp. 2063-2067, DOI: 10.1039/p29940002063.

[11] G. M. Sheldrick, "A short history of SHELX", *Acta Crystallogr. A,* 64 (2008), pp. 112-122, DOI: 10.1107/S0108767307043930.

[12] J. B. Foresman, A. Frisch, and K. Tasaki, "*Exploring chemistry with electronic structure methods"*, Gaussan, Inc., Pittsburgh, (1998).

[13] M. J. Frisch, G. W. Trucks, H. B. Schlegel, G. E. Scuseria, M. A. Robb, J. R. Cheeseman, J. A. Montgomery, Jr., T. Vreven, K. N. Kudin, J. C. Burant, J. M. Millam, S. S. Iyengar, J. Tomasi, V. Barone, B. Mennucci, M. Cossi, G. Scalmani, N. Rega, G. A. Petersson, H. Nakatsuji, M. Hada, M. Ehara, K. Toyota, R. Fukuda, J. Hasegawa, M. Ishida, T. Nakajima, Y. Honda, O. Kitao, H. Nakai, M. Klene, X. Li, J. E. Knox, H. P. Hratchian, J. B. Cross, C. Adamo, J. Jaramillo, R. Gomperts, R. E. Stratmann, O. Yazyev, A. J. Austin, R. Cammi, C. Pomelli, J. W. Ochterski, P. Y. Ayala, K. Morokuma, G. A. Voth, P. Salvador, J. J. Dannenberg, V. G. Zakrzewski, S. Dapprich, A. D. Daniels, M. C. Strain, O. Farkas, D. K. Malick, A. D. Rabuck, K. Raghavachari, J. B. Foresman, J. V. Ortiz, Q. Cui, A. G. Baboul, S. Clifford, J. Cioslowski, B. B. Stefanov, G. Liu, A. Liashenko, P. Piskorz, I. Komaromi, R. L. Martin, D. J. Fox, T. Keith, M. A. Al-Laham, C. Y. Peng, A. Nanayakkara, M. Challacombe, P. M. W. Gill, B. Johnson, W. Chen, M. W. Wong, C. Gonzalez, and J. A. Pople, *Gaussian 03 Revision C.02, Gaussian, Inc., Wallingford, CT*, (2004),

5. Overall conclusion

5.1 Overall conclusion

This study focused on the crystal structures of thalidomide. The principal results of this study are summarized in Table 5.1. Methods for crystallization of thalidomide were evaluated with consideration of possible multiple forms, *i.e.* polymorphs or solvates. The different crystallization methods produced crystals with different habits. Crystal structures and absolute configurations were determined except for the case of crystals obtained with solvent evaporation technique from chloroform solution of (*S*)-thalidomide.

In the case of (*S*)-thalidomide, crystallization from high polar methanol-water solution, in which hydrogen bonds are not generally formed, produces unsolvated crystal, whereas crystallization from nonpolar chloroform solution, in which thalidomide molecules exist in dynamic equilibrium of three isomeric dimers, produces solvated crystal. Both unsolvated and solvated crystals are composed of two conformational isomers of (*S*)-thalidomide. The unsolvated crystals are formed with hydrogen bonded dimers consisting of pairs of these isomers, whereas the solvated crystals are formed with infinite hydrogen bonded chains consisting of alternately arranging conformational isomers (Figure 5.1). The clathrate structure in solvated crystals and non-stoichiometric inclusion of solvent molecules imply the capability for replacing solvent molecules at channel spaces with maintaining the host lattice of (*S*)-thalidomide. This property of solvated crystal will be expected for pharmaceutical application.

In the case of (*RS*)-thalidomide, the corresponding three methods produced only unsolvated (*RS*)-thalidomide crystals. These crystals were determined as the isomorphic with previously known α-form. The comparison of homochiral dimers in (*S*)-thalidomide crystal and heterochiral dimers in (*RS*)-thalidomide crystal suggested that the symmetric heterochiral dimers are more stable than the asymmetric homochiral dimers. The theoretical calculation based on the crystal structures revealed that the intermolecular energy of the heterochiral dimer is lower than that of the homochiral dimer. These results indicate that the known differences of physicochemical properties

between racemic thalidomide and enantiomeric thalidomide originate from the stability difference of hydrogen-bonded rings between heterochiral dimers and homochiral dimers.

Table 5.1 Comparison of solvate formation between (*S*)- and (*RS*)-thalidomide crystals obtained with three different methods.

Solvent	Technique	Solute	
		(*S*)-thalidomide	(*RS*)-thalidomide
methanol-water	solvent evaporation	unsolvate (**I**)	unsolvate (**II**)
chloroform	solvent evaporation	solvate (**III**)	unsolvate (**IV**)
chloroform-diethyl ether	vapor diffusion	solvate (**V**) / unsolvate (**VI**)	unsolvate (**VII**)

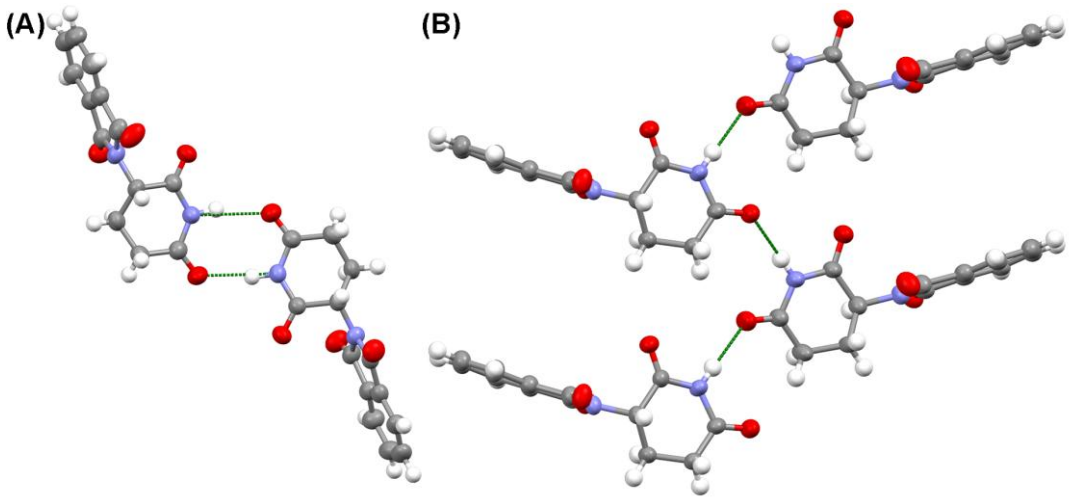

Figure 5.1 The structures of (A) hydrogen bonded dimer in unsolvated crystal of (*S*)-thalidomide and (B) hydrogen bonded chain in solvated crystal of (*S*)-thalidomide. Green broken lines represent hydrogen bonds. Color code: C: gray, N: blue, O: red, H: white, Cl: green.

The primary significance of this study is on the idea of comparison between an enantiomer and the racemate. Crystal structures of enantiomeric and racemic compounds are essentially different. However, almost no study concerning crystal of chiral compounds has focused on this idea.

Although the crystal structure of (*RS*)-thalidomide have been investigated, special attention on the heterochiral dimer formation in the crystal have not been paid. In this study, determination of the crystal structure of (*S*)-thalidomide revealed not only the homochiral dimer structure in the crystal but also the main difference between (*S*)- and (*RS*)-thalidomide crystals being in the dimer structures.

Furthermore, focusing on the result of **III** and **IV**, crystallization with solvent evaporation technique from chloroform solution demonstrated contrasting behavior at solvate formation: solvate of (*S*)-thalidomide and unsolvate of (*RS*)-thalidomide. This contrasting behavior should be significant, particularly for pharmaceutical compounds due to recent trends in the chiral drug development.

5.2 Future works

The exothermic peak without weight increase around 250 °C in TG-DTA on **I** indicated that the possible polymorphic transformation of (*S*)-thalidomide (Figure 5.2(A)). The previously study reported that β-(*RS*)-thalidomide is obtainable with melt of α-(*RS*)-thalidomide. Therefore, the result of TG-DTA suggests that (*S*)-thalidomide possibly transformed to the polymorph corresponding to β-(*RS*)-thalidomide. This possibility should be investigated for instance using X-ray diffractometry-differential scanning calorimetry. Moreover, the cause of the excess weight reduction around 150 °C in TG-DTA on **VI** should also be investigated (Figure 5.2(B)). This result is strange because **VI** is determined as the unsolvated crystal with single crystal X-ray diffractometry.

As to the solvated (*S*)-thalidomide crystals, the capability for replacing solvent molecules at channel spaces with maintaining the host lattice of the clathrate structure should be investigated. Achieving this property of solvated crystal will be expected for pharmaceutical application, particularly with water because only hydrates may be of practical use as drugs.

Although solvated (*RS*)-thalidomide crystals were not obtained in this study, the possibility for obtaining solvated (*RS*)-thalidomide crystals should exist. Finding

crystallization methods for solvated (*RS*)-thalidomide and applying the methods for crystallization of (*S*)-thalidomide will provide interesting results, especially in terms of comparison with the results of this study.

Furthermore, as the contrasting solvate formation of **III** and **IV**, contrasting behavior at polymorphs or solvates formation between an enantiomer and the racemate of other chiral compounds, particularly for pharmaceutical compounds, are of great interest.

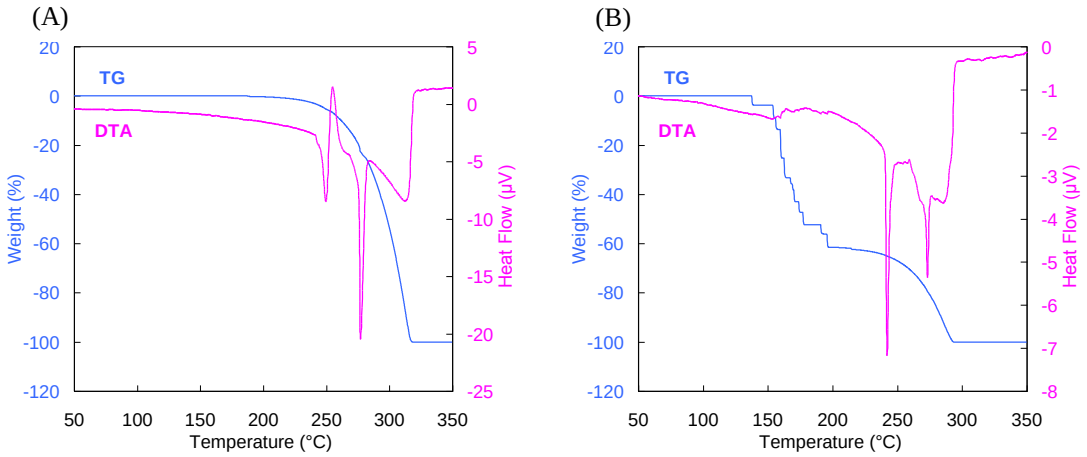

Figure 5.2 TG-DTA curves of unsolvated (*S*)-thalidomide crystals (A) obtained with solvent evaporation technique from methanol-water solution (**I**) and (B) obtained with vapor diffusion technique from chloroform solution (**VI**).

Acknowledgement

First, I am deeply indebted to my supervisor, Professor Dr. Toru Asahi for his professional education, spirited encouragement, and considerable support. The life in the Asahi laboratory was full with quite unique experience.

I am really grateful to referees of my thesis, Professor Dr. Kentaro Semba and Professor Dr. Naoya Takeda for their constructive advice and insightful comment.

I warmly thank collaborators of our research, Dr. Masahito Tanaka, Dr. Motoo Shiro, Professor Dr. Norio Shibata, and Professor Dr. Tetsuya Osaka for their technical advice and experimental support.

I express sincere gratitude to Professor emeritus Dr. Yoshiaki Shinoda, Professor Dr. Dwight W. Stevenson, and Professor Dr. J. C. Mathes, Professor Dr. Taeko Kintoku, Professor Tomoko Motohashi for their practical advice and valuable classes. The conference at the University of Michigan, remarkably improving our alumni's art of technical communication, is my precious memories.

I specially thank to Professor Dr. Naoya Sawamura, Professor Dr. Takahiro Shinada, Professor Dr. Hideko Koshima, Ms. Izumi Maeda, staffs at office of Global COE and TWIns, colleagues in our laboratory, and my friends for their warm encouragement and continuing support.

Finally, I greatly appreciate my parents, Norihiko Suzuki and Masayo Suzuki supporting my student life.

December, 2010

Toshiya Suzuki

Achievements

1. Articles

"Evaluation of stability difference between asymmetric homochiral dimer in (S)-thalidomide crystal and symmetric heterochiral dimer in (RS)-thalidomide crystal ", *Phase Transitions*, 83, (2010), pp. 223-234
Toshiya Suzuki, Masahito Tanaka, Motoo Shiro, Norio Shibata, Tetsuya Osaka, Toru Asahi.

2. Presentations

- **International Symposia**

“Chiroptical analysis of thalidomide and its hydrolytic products in solution”, 8th Joint Symposium between the University of Bonn and Waseda University, Tokyo, Oct. (2010)
Yoshiyuki Ogino, Toshiya Suzuki, Masahito Tanaka, Toru Asahi.

“Homochiral dimer in (S)-thalidomide crystal and heterochiral dimer in (RS)-thalidomide crystal”, 22nd International Symposium on Chirality, Sapporo, Jul. (2010)
Toshiya Suzuki, Masahito Tanaka, Motoo Shiro, Norio Shibata, Tetsuya Osaka, Toru Asahi.

“Spectroscopic investigation of collagen sheets with very high preferred orientation”, 22nd International Symposium on Chirality, Sapporo, Jul. (2010)
Toru Asahi, Toshiya Suzuki, Yoshiyuki Ogino, Yuji Tanaka, Masayuki Yamato, Naoya Sawamura.

“Temperature and pH dependence of thalidomide hydrolysis by chiroptical spectroscopy”, 22nd International Symposium on Chirality, Sapporo, Jul. (2010)
Yoshiyuki Ogino, Toshiya Suzuki, Masahito Tanaka, Toru Asahi.

“Determination of absolute structure and optical rotator dispersion of γ-glycine”, 22nd International Symposium on Chirality, Sapporo, Jul. (2010)
Kazuhiko Ishikawa, Toshiya Suzuki, Masahito Tanaka, Tsuneomi Kawasaki, Kenso Soai, Motoo Shiro, Toru Asahi.

"Asymmetric homochiral dimer in (S)-thalidomide crystal and symmetric heterochiral dimer in (RS)-thalidomide crystal", The 4th Global COE International Symposium on 'Practical Chemical Wisdom', Tokyo, Jan. (2010)
Toshiya Suzuki, Masahito Tanaka, Motoo Shiro, Norio Shibata, Tetsuya Osaka, Toru Asahi.

"Evaluation of stability difference between enantiomeric and racemic thalidomide crystals with X-ray structural analysis and energy calculation", 7th Joint Symposium between Waseda University and the University of Bonn, Bonn, Jan. (2010)
Toshiya Suzuki, Masahito Tanaka, Norio Shibata, Tetsuya Osaka, Toru Asahi.

"Measurements of chiroptical properties in condensed matters using the Generalized High Accuracy Universal Polarimeter", The 1st International Symposium on Biomedical Science and Engineering, Tokyo, Jul. (2009)
Toru Asahi, Toshiya Suzuki.

"Comparison of chiroptical properties between solid and solution states", 21st International Symposium on Chirality, Colorado, Jul. (2009)
Toshiya Suzuki, Tetsuya Osaka, Toru Asahi.

"Improvement of the Generalized High Accuracy Universal Polarimeter, G-HAUP", Waseda-Korea Universities' Joint Symposium on 'Practical Chemical Wisdom', Tokyo, Feb. (2009)
Toshiya Suzuki, Toru Asahi.

"General evaluation method of systematic errors in the Generalized High Accuracy Universal Polarimeter, G-HAUP", The 3rd Global COE International Symposium on 'Practical Chemical Wisdom', Tokyo, Jan. (2009)
Toshiya Suzuki, Toru Asahi.

"Novel evaluation method of systematic errors in the Generalized High Accuracy Universal Polarimeter, G-HAUP", 20th International Symposium on Chirality, Geneva, Jul. (2008)
Toshiya Suzuki, Toru Asahi.

"Deposition of crystalline films of amino acid using a vacuum evaporation method", 19th International Symposium on Chirality, San Diego, Jul. (2007)
Toshiya Suzuki, Toru Asahi, Masahito Tanaka, Kuniaki Tatsuta, Tetsuya Osaka.

"Anisotropic chiral films of isoleucine deposited with vacuum evaporation", 18th International Symposium on Chirality, Busan, Jun. (2006)
Toru Asahi, Toshiya Suzuki, Masahito Tanaka, Tetsuya Osaka, Hiroyuki Nishide, Kuniaki Tatsuta.

- **Internal symposia**

“キラルおよびラセミ結晶中のサリドマイド分子の二量体構造”, 第 4 回分子科学討論会, 大阪, 2010 年 9 月
石川和彦，鈴木俊哉，田中真人，城始勇，柴田哲男，朝日透.

“Evaluation of dimer structures in enantiomeric and racemic thalidomide crystals”, Symposium on Molecular Chirality 2010, 札幌, 2010 年 7 月
鈴木俊哉，田中真人，城始勇，柴田哲男，逢坂哲彌，朝日透.

“Chiroptical spectroscopic research on pH and temperature dependence of thalidomide hydrolysis”, Symposium on Molecular Chirality 2010, 札幌, 2010 年 7 月
荻野禎之，鈴木俊哉，田中真人，朝日透.

“Crystal structure and optical activity of γ-glycine crystal”, Symposium on Molecular Chirality 2010, 札幌, 2010 年 7 月
石川和彦，鈴木俊哉，田中真人，川崎常臣，硲合憲三，城始勇，朝日透.

“Crystal structures of enantiomeric and racemic thalidomide”, 第 3 回東京女子医科大学・早稲田大学 TWIns ジョイントシンポジウム, 東京, 2010 年 1 月
朝日透，鈴木俊哉，田中真人，柴田哲男，逢坂哲彌.

“サリドマイド結晶における分子の立体配置 : 対掌体結晶におけるホモキラル二量体とラセミ結晶におけるヘテロキラル二量体”, The Symposium on Chiral Science & Technology: Mesochemistry & Chemical Wisdom, 東京, 2009 年 9 月
鈴木俊哉，柴田哲男，田中真人，逢坂哲彌，朝日透.

“一般型高精度万能旋光計による異方性固体物質のキラル光学特性の測定”, モレキュラー・キラリティー2009, 大阪, 2009 年 5 月
鈴木俊哉，朝日透.

“アミノ酸結晶性膜作製法の開発”, モレキュラー・キラリティー2007, 東京, 2007 年 5 月
鈴木俊哉，田中真人，朝日透，竜田邦明，逢坂哲彌.

“アミノ酸結晶性膜の作製及びキラル光学的研究”, 第54回応用物理学関係連合講演会, 神奈川, 2007 年 3 月
鈴木俊哉，籠宮功，中村尚倫，田中真人，朝日透，竜田邦明，逢坂哲彌.

“Generalized High Accuracy Universal Polarimeterのナノ材料への応用”, 第15回有機結晶シンポジウム, 愛媛, 2006 年 11 月
朝日透，鈴木俊哉.

“アミノ酸単結晶薄膜のキラル光学特性の評価”, 第 53 回応用物理学関係連合講演会, 東京, 2006 年 3 月
鈴木俊哉，籠宮功，中村尚倫，田中真人，朝日透，竜田邦明，逢坂哲彌.

“アミノ酸薄膜のキラル光学的研究”, 第66回応用物理学会学術講演会, 徳島, 2005 年 9 月
鈴木俊哉，籠宮功，中村尚倫，田中真人，朝日透，竜田邦明，逢坂哲彌.

- **Workshops**

“G-HAUP を用いた有機/無機ハイブリッド層間化合物のキラル光学的研究”, 分子研研究会, 愛知, 2006 年 2 月
朝日透，中村尚倫，田中真人，籠宮功，鈴木俊哉.

3. Patents

“蒸着装置、蒸着方法、光学素子及びキラルセンサ”，PCT/JP2006/317644，朝日透，逢坂哲彌，田中真人，鈴木俊哉，2006 年 9 月.